INFORMATION TO USERS

This material was produced from a microfilm copy of the original document. While the most advanced technological means to photograph and reproduce this document have been used, the quality is heavily dependent upon the quality of the original submitted.

The following explanation of techniques is provided to help you understand markings or patterns which may appear on this reproduction.

1. The sign or "target" for pages apparently lacking from the document photographed is "Missing Page(s)". If it was possible to obtain the missing page(s) or section, they are spliced into the film along with adjacent pages. This may have necessitated cutting thru an image and duplicating adjacent pages to insure you complete continuity.

2. When an image on the film is obliterated with a large round black mark, it is an indication that the photographer suspected that the copy may have moved during exposure and thus cause a blurred image. You will find a good image of the page in the adjacent frame.

3. When a map, drawing or chart, etc., was part of the material being photographed the photographer followed a definite method in "sectioning" the material. It is customary to begin photoing at the upper left hand corner of a large sheet and to continue photoing from left to right in equal sections with a small overlap. If necessary, sectioning is continued again — beginning below the first row and continuing on until complete.

4. The majority of users indicate that the textual content is of greatest value, however, a somewhat higher quality reproduction could be made from "photographs" if essential to the understanding of the dissertation. Silver prints of "photographs" may be ordered at additional charge by writing the Order Department, giving the catalog number, title, author and specific pages you wish reproduced.

5. PLEASE NOTE: Some pages may have indistinct print. Filmed as received.

Xerox University Microfilms
300 North Zeeb Road
Ann Arbor, Michigan 48106

THE UNIVERSITY OF OKLAHOMA

GRADUATE COLLEGE

A STUDY OF HORIZONTAL BURNING RATES OF THIN MATERIALS

A DISSERTATION

SUBMITTED TO THE GRADUATE FACULTY

in partial fulfillment of the requirements for the

degree of

DOCTOR OF PHILOSOPHY

BY

CHARLES WENDELL ROOKS

Norman, Oklahoma

1973

A STUDY OF HORIZONTAL BURNING RATES OF THIN MATERIALS

APPROVED BY

C. M. Sliepcevich

Lyndon Welker

Curtis Wm Welty

William E. Martinsen

Harold R. Wesson

ABSTRACT

A study has been made on the horizontal burning rates of 87 thin materials, consisting of samples of nylon and vinyl automobile seat fabrics, heavy cotton cloth, standard Whatman laboratory filter paper, nylon automotive carpeting, and specially cut thin strips of balsa, ash, oak, and redgum. These horizontal burning rate tests were performed using a modified version (large cabinet) Federal Motor Vehicle Safety Standard 302 Horizontal Burning Rate Test. A mathematical model, which relates the horizontal burning process to the piloted ignition process, is proposed and tested; it is then used as the basis for an empirical model to describe the burning phenomenon as a function of piloted ignition data. The model is tested for validity against experimental data and found to predict burning rates within a factor of two, given the ignition curve and thermal and physical properties of a material.

Although this spread in predicted values of the horizontal burning rates seems large, it is approximately the same as the spread in experimental values. Hence, the model can predict burning rates almost as well as they can be measured.

ACKNOWLEDGMENTS

I would like to express my sincere gratitude to a number of persons who have contributed to this research effort.

Dr. C. M. Sliepcevich, George Lynn Cross Research Professor of Engineering, for his direction and support.

Dr. J. R. Welker, Associate Director of the Flame Dynamics Laboratory, for his helpful advice, comments, and assistance throughout the program.

Dr. A. W. Aldag, Assistant Professor of Chemical Engineering, and Dr. W. E. Martinsen, Assistant Professor of Materials Science for their contributions as members of my graduate committee.

Dr. H. R. Wesson for his informative and instructive discussions concerning this work, and for serving on my graduate committee.

Ms. B. T. Everidge for her assistance in the preparation of this manuscript.

I am very grateful to the National Science Foundation and University Engineers, Inc., for providing financial support.

I wish to express my deep gratitude to Dr. Ralph S. Hamilton, without whose skill in opthalmological surgery, I could not have reached this pinnacle in my life.

I wish to acknowledge my wife, Dana; her support and encouragement have been steadfast.

Finally, I wish to express my gratitude to my parents, Charles and Rose Marie; they have never faltered in their support of me, and their encouragement has been of extreme help many times when I have been discouraged.

TABLE OF CONTENTS

LIST OF TABLES

LIST OF ILLUSTRATIONS

CHAPTER I

INTRODUCTION

The rate at which a fire spreads over a given material has been of interest to the human race since fire was first discovered. Until recent times, very little has been known about the mechanisms of fire spread. It was not until the 1940's that scientists began to investigate experimentally how fires spread and how rapidly they spread. Most of the early work in the field of fire spread rates was done by the U.S. Forest Service in an attempt to predict how rapidly a fire would spread through a forest.

It was not until very recently that the general public became aware of the dangers inherent in wearing apparel made from flammable materials, mostly the new synthetic fibers. Since that time, new federal regulations regarding the maximum allowable burning rate for materials used for clothing, automobile interiors, furniture, draperies, carpeting, etc., have been passed or are being considered. Thus, it has become advantageous, especially for synthetic fiber manufacturers, to be able to estimate the burning rate of a given material without first manufacturing large quantities.

It is to this question that this dissertation addresses itself. It was felt that a model describing the fire spread phenomenon could be developed on the basis of piloted ignition data. The idea of treating the flame spread rate over a material as a series of ignitions is not new. It was first proposed by Fons in 1946 (7). A model which describes the burning rate has been obtained for a variety of thin materials, both synthetic and natural cloths and thin wooden strips, based on the ignition curve for the material and its physical and thermal properties.

It is felt the model developed herein is the first to correlate quite successfully burning rates of materials which have significant differences in their chemical composition.

A great number of tests for flammability of materials have been proposed and adopted by various private and governmental agencies. Trying to ascertain which one, or which combination, of these tests should be used to obtain burning rate data is quite difficult. The test chosen was that proposed by the Department of Transportation (Federal Motor Vehicle Safety Standard 302), which measures the horizontal burning rate of a material. It is certainly not as severe a test as some of those proposed, such as the vertical tests where the flames move from the bottom of the sample to the top, but it does indicate relative burning rates of materials. It also has the advantage of spreading the data over a larger range than the vertical tests.

An important point to keep in mind, and which will be demonstrated in the next section, is that no single test nor any combination of tests can, nor should be expected to, simulate to any degree of accuracy, the behavior of a material in a real fire. Unless materials are tested in a large scale test apparatus, approaching room size, their behavior based on bench scale tests may not be related to their behavior in a large scale fire in any easily discernible way.

This dissertation then attempts to show that the horizontal burning rate of a material, as obtained from a modification (larger cabinet) of the Department of Transportation FMVSS 302 Horizontal Burning Rate Test (hereinafter designated MFMVSS 302) is related to the material's ignition characteristics in a fundamental way. However, care should be exercised in extrapolating the equations developed herein for materials with significantly different properties.

CHAPTER II

LITERATURE REVIEW

Fire research has grown from its infancy in the 1930's and 1940's to a sophisticated science in the 1970's. And yet, very little is really known about the detailed processes which occur when a material is ignited and is consumed by fire. Extensive research into the phenomena of ignition and flame propagation exists, and more data are becoming available each year. Hilado (17) has conveniently divided the burning process into five stages. It is instructive to examine these stages separately.

The first stage consists of heating the material; heat being supplied from an external source. This process progressively raises the temperature of the material. The external supply of heat might be direct flame exposure (radiation and convection), heat transferred from hot gases (conduction and convection), or heat transferred from a hot solid mass (conduction). The rate of temperature rise is a function of the heat flux (the temperature differential between the flame and the material), the specific heat of the material, the thermal conductivity of the material, and the latent heat of fusion and vaporization.

Stage two begins when the material reaches its decomposition temperature and begins to decompose. Most substances yield a number of decomposition products as they pyrolyze. These products include combustible gases (those that burn in the presence of air), noncombustible gases (water vapor and CO_2 being most common), liquids (usually partially decomposed material), solids (carbonaceous char), and entrained solid particles which appear as smoke.

The third stage, as outlined by Hilado, is ignition. In this stage, sufficient oxygen or oxidizing agent is present and sufficiently well mixed with the combustible gases to obtain ignition. Ignition is usually brought about by an external flame source or spark, although most materials will also exhibit a self-ignition temperature, which is the temperature at which reactions within the material become self-sustaining to the point of igniting.

Stage four is the actual combustion of the material. Combustion of a unit of mass liberates a given quantity of heat. This heat of combustion then raises the temperature of the gaseous products of combustion, thus increasing heat transfer to the solid material by convection. Expansion of the heated gases increases convective heat transfer, and the heated entrained solid particles tend to increase heat transfer by radiation. This stage represents full-scale or fully developed burning. The most important characteristic at this point is the heat of combustion of the material.

Finally, stage five consists of flame propagation and ultimate consumption of the material. In order to obtain propagation, the heat generated by combustion of the material minus the heat lost to the surroundings, must be sufficient to bring an adjacent unit mass to the combustion stage.

If all five of the above mentioned stages were amenable to a precise and tractable mathematical description, then an accurate, comprehensive model of the burning process could be set forth. Unfortunately, none of these stages is well enough understood to predict theoretically the material behavior corresponding to the events which are known to occur in each stage. In the heating stage, equations can be developed to describe the process, but often these equations cannot be solved. The decomposition stage is the one about which the least is known. The reactions and mechanisms appear to be many and complex in nature and no truly successful approach has been developed to delineate them. Much work has been done in the area of ignition, which is perhaps one of the better understood phenomena leading to the burning of substances. Extensive data are available on ignition behavior of a wide range of substances using radiative sources from 0.5 cal/cm^2-sec to 3.0 cal/cm^2-sec although some data extend to 20 to 30 cal/cm^2-sec. Some of these data can be found in references 21, 25, 31, 32, 33, 34, and 39.

The data have been correlated empirically, based on theory, because it is beyond the realm of present technology

to predict theoretically ignition behavior a priori. The combustion stage has not been fully understood either, because it is intimately related to the heating and decomposition stages. The same applies to the propagation stage.

A central problem, which seems to reappear in trying to analyze these stages, is the inability to define accurate and significant boundary conditions. In many cases, no means of measuring the desired variables exist. This problem leads all of those involved in fire research into the predicament of having to make simplifying assumptions or estimating those variables which cannot be measured. Since the problems of heat transfer and kinetics involved in the overall process are of such a complex nature, it is quite possible that some, perhaps many, important variables have not even been discovered!

Since one of the basic assumptions being made in this thesis is that the burning rate of a material is related to the material's ignition behavior, it is instructive to examine the ignition process in some detail. A review of the burning phenomena and the various tests used to obtain flammability data will then follow.

Ignition of Cellulosic and Synthetic Materials

Brown (4) has concluded that a unique series of events occurs as a combustible solid is gradually heated in the presence of air. A very slow reaction takes place as the material absorbs energy at low temperatures. The reaction

between the material and the oxygen in the surrounding air increases appreciably at higher temperatures. This normally exothermic decomposition reaction produces heat which raises the temperature of the absorbing material, thus increasing the reaction rate. Energy losses to the surroundings by radiation, conduction, and convection oppose the increase in reaction rate. At some characteristic temperature, the rate of reaction becomes rapid enough to overcome the heat losses, and the temperature rises faster than it would due to external heating alone. Thus, the reaction accelerates itself and very rapid heating follows. If favorable conditions still exist, this process continues until glowing or flaming ignition occurs.

However, Brown's concept of the ignition process, as observed in a "fire" situation (i.e., external heating), has been proven incorrect by later work. It appears from the discussion Brown gives, that he conceptualizes ignition as occurring in the solid itself. He discusses the exothermic combustion process which liberates heat which raises the temperature of the solid. He does not mention the endothermic process which must occur in order to cause decomposition of the solid into volatile fragments which escape into the gas phase (4). Brown missed the point that combustion occurs in the gas phase, not in the solid phase. Therefore, there are two processes occurring; an endothermic decomposition reaction (the breakdown of the solid into fragments), and an

exothermic gas phase oxidation reaction. The exothermic process is this gas phase oxidation reaction, which usually occurs at some finite distance from the solid surface. If the heat contributed to the solid by this gas phase oxidation reaction and the energy absorbed from external sources does not equal or exceed the endothermic decomposition reactions in the solid, the solid will self-extinguish.

As an organic solid decomposes upon heating, it undergoes molecular rearrangement while simultaneously yielding molecular fragments in gaseous form. These fragments mix with the surrounding air. If this process is carried out at a sufficiently high rate, flaming ignition occurs. There are two extremes for thermal decomposition of solids. For very low thermal heating rates, the specimen may char completely without flaming. This charring without ignition occurs because the rate of evolution of combustible gases is so low that after mixing with air their concentration is below the flammable limits. For very high incident energy fluxes, the specimen may undergo no discernible charring up to the time of ignition. The specimen then decomposes rapidly, and almost completely, to volatile substances, leaving only a trace of solid residue, by a process termed "flash pyrolysis."

An ignition cabinet was designed, built and tested at the University of Oklahoma by Koohyar (21). This cabinet has been used to compile an extensive file of ignition data on cellulosic and synthetic materials, both thick and thin

samples. The test consists of exposing a specimen, about 100 square centimeters in area, to a monitored radiant flux from either a benzene flame or quartz-tungsten lamps until the specimen is ignited or completely pyrolyzed. A small pilot flame above the sample ignites the combustible gases vaporizing from the surface, hence the term "piloted ignition." The elapsed time between exposure and ignition is recorded as the ignition time. The benzene flame radiation data were chosen for use in relating ignition data to the burning process because the spectral properties of benzene flames are more nearly akin to those of the flames of the burning specimen. The range of incident irradiance was 0.5 cal/cm^2-sec to about 3 cal/cm^2-sec. A more complete description of the experimental apparatus and the types of data obtainable have been given by Koohyar (21), Wesson (39), and Rangaprasad (25).

Wesson (39) has developed a correlational scheme for piloted ignition which has been successfully used to correlate ignition data from woods. The same functional form used for woods was applied to synthetic woven cloths, cotton cloths, paper, and plastics with reasonable success. He assumed a one-dimensional model for heat conduction through an inert, opaque, infinite slab exposed to a constant heat flux on one face with no heat loss on the opposite face. He used the resulting analytical solution to obtain the functional form of the parameters for correlating the data. His derivation is repeated here.

The differential equation for one-dimensional heat conduction through an inert, opaque, infinite slab is given by:

$$\kappa \frac{\partial^2 \Delta T}{\partial x^2} = \frac{\partial \Delta T}{\partial t} \qquad \text{(II-1)}$$

The initial condition for all values of x is $\Delta T = 0$, with boundary conditions:

$$t > 0 \quad x = L \quad H_i = - k \frac{\partial \Delta T}{\partial x} \qquad \text{(II-2)}$$

$$t > 0 \quad x = 0 \quad \frac{\partial \Delta T}{\partial x} = 0 \qquad \text{(II-3)}$$

assuming that all the incident irradiance is absorbed.

The solution to Equation II-1 with the stipulated initial and boundary conditions is:

$$\Delta T_s = \frac{2 H_i t^{1/2}}{(k \rho c_p)^{1/2}} \sum_{n=0}^{\infty} \left\{ \text{ierfc} \frac{2nL}{2(\kappa t)^{1/2}} + \text{ierfc} \frac{(2n+1)L}{2(\kappa t)^{1/2}} \right\} \qquad \text{(II-4)}$$

where

$$\text{ierfc} \frac{2nL}{2(\kappa t)^{1/2}} = \frac{1}{\sqrt{\pi}} e^{-\left[\frac{2nL}{2(\kappa t)^{1/2}}\right]^2} - \frac{2nL}{2(\kappa t)^{1/2}} \text{erfc} \frac{2nL}{2(\kappa t)^{1/2}} \qquad \text{(II-5)}$$

Equation II-4 may be written in functional form as:

$$H_i \sqrt{t} = f\{\Delta T_s, (k \rho c_p)^{1/2}, \text{erf} \frac{L}{2\sqrt{\kappa t}}\} \qquad \text{(II-6)}$$

where erf $L/2\sqrt{\kappa t}$ is used for convenience in place of ierfc $L/2\sqrt{\kappa t}$.

If the specific heat, c_p, is assumed constant and the thermal conductivity, k, is dependent on the density, ρ, Equation II-6 becomes:

$$H_i\sqrt{t} = f\{\Delta T_s,\ \rho,\ \text{erf}\ \frac{L}{2\sqrt{\kappa t}}\} \qquad \text{(II-7)}$$

Since Wesson assumed that the surface temperature rise at ignition was relatively constant, Equation II-7 can be written in functional form as:

$$H_i t^a = A[\rho^b\ \text{erf}\ \frac{L}{2\sqrt{\kappa t}}]^c \qquad \text{(II-8)}$$

if the functional form of the equation is assumed to follow a power law distribution. The ignition time, t_i, and the sample thickness, L, are used in the power law expression. Equation II-8 can be rearranged to yield an expression for ignition time, where for emphasis, t is replaced by t_i,

$$t_i = B\left(\frac{\rho^b\ \text{erf}\ (\frac{1}{2\sqrt{F}})^c}{H_i}\right)^{1/a} \qquad \text{(II-9)}$$

where $F = \kappa t/L^2$ is the Fourier modulus.

Wesson then shows how Equation II-9 can be modified to use the initially absorbed irradiance, H_a, rather than the incident irradiance, H_i, which allowed him to collapse all of his ignition data for wood onto a single graph. The initially absorbed irradiance, H_a, is equal to the incident irradiance, H_i, times the integrated average absorbtance, $\bar{\alpha}$. The $\bar{\alpha}$ is a measure of the fraction of the incident irradiance initially absorbed by the specimen.

The resulting correlation obtained by applying the above technique to wood samples is given by:

$$t_i = 35 \left(\frac{\rho^{0.9} \left(\text{erf} \frac{1}{2\sqrt{F}}\right)^{1.2}}{(\bar{\alpha} H_i)^{2.8}} \right) \qquad \text{(II-10)}$$

The correlation obtained by applying this technique to woven nylon and vinyl seat fabrics, woven cotton cloth, paper, and nylon carpeting for automobiles is given by (36):

$$t_i = 21 \left(\frac{\rho^{0.2} \left(\text{erf} \frac{1}{2\sqrt{F}}\right)^{0.5}}{(\bar{\alpha} H_i)^{2.0}} \right) \qquad \text{(II-11)}$$

where ρ is in gm/cm^3, H_i is in cal/cm^2-sec, and t_i is in sec. These correlations were subsequently used in the analysis of burning rate data on these materials.

Flame Propagation

Once the ignition behavior of a material is understood, it is instructive to examine its burning characteristics via some sort of experimental flame propagation test. A major problem arises at this point, however. In order for a flame propagation test to be practical and economical, it must be relatively small scale, i.e., a bench-type laboratory experiment; but, to obtain data that might be useful in predicting 'real' fire spread rates over a material, it is necessary to perform large-scale experiments. The question then arises: Does there exist a small-scale test or combination of small-scale tests which can be used as a basis for determining the

flammability characteristics of thin materials? There are a large number of burning rate tests in existence, each general type designed to test particular characteristics of the material. Those presented here concern the determination of burning rates of automobile interior materials.

Goldsmith (13) has tabulated the various flammability tests that are applicable to automobile interior materials and his tabulation is reproduced in Appendix B. An examination of Appendix B reveals that most of the tests are small-scale tests with the most significant difference between the bench-type tests being the sample orientation and the time of exposure to the ignition source. Sample orientation is a critical factor in determining burning rates.

If a specimen is burned vertically upward, the evolving gases and the flames preheat the material ahead of the advancing flame front, hence increasing the burning rate. If the specimen is burned vertically downward, the flame preheats the sample by radiation only and the hot gases travel opposite to the advancing flame front. The latter is perhaps the least severe of all burning test types. A horizontal burning test is more severe than vertical downward flame propagation, but less severe than vertical upward burning. It has been found by Goldsmith (13) and Sliepcevich, et al. (36) that a vertical test method is impractical because the flame front cannot be accurately defined, making the measurement of the rate of travel of the front virtually impossible. A vertical

method also tends to cluster the burning rate data in a narrow range. For these reasons, a horizontal test method was chosen by Goldsmith and by Sliepcevich. This test procedure is described in the next chapter; it basically consists of an earlier version (larger cabinet) of a horizontal burning test for automobile interior materials which was proposed by the Department of Transportation. Subsequently, the cabinet was reduced in size to correspond to SAE J369, "Flammability of Automotive Interior Trim," and the Automobile Manufacturers Association Method S 121. The only difference between SAE J369 and the current FMVSS 302 is the orientation of the face of the material, that is, the side that would be normally exposed in use. In FMVSS 302 this side would face up during the test and in SAE J369, it would face down. These tests procedures are also similar to Method FSS 453, "Flight Resistant Material."

Both the larger and smaller cabinet versions of the FMVSS 302 test are less severe than Method 5906 Federal Specification CCC-T191b because the specimen is only exposed to the igniting flame for 15 seconds in the former, whereas, in the latter it is exposed continuously. As stated previously, a horizontal test provides a greater spread in the data, thus allowing for some qualitative estimates in the differences in flammability of materials. Since much of the flammability data used in this study were obtained under contract with the Department of Transportation, the FMVSS 302 test, and in particular the modified (larger cabinet version) MFMVSS 302 test, was adopted for present purposes.

Horizontal Burning

A majority of the experimental and theoretical work in the area of fire spread has dealt with the spreading of a fire through a forest. Fons (1946) was the first to suggest the important parameters that control the rate of spread of fire through porous fuel arrays. He found that the rate of spread within a given fuel bed remains constant if the fuel size, bed configuration, and environment are homogeneous. He postulated that a fire propagates through the fuel as a series of ignitions.

Fons (9) has conducted extensive studies on flame propagation through wood cribs. The technique developed involved moving the crib into the flame so that the flame remained stationary. Measurements were made on radiation fluxes from the flame, gas velocities, temperatures, and combustion products. A correlation for burning time for line fires was developed as a function of dimensionless groups. His correlation is given by:

$$\left(\frac{\theta_r^{\alpha}}{d_o}\right)\left(\frac{L}{D}\right) = f\left[\left(\frac{k_g}{hd_o}\right)^{1.5}\left(\frac{\rho_f}{\rho_g}\right)M_f^{0.15}\left(\frac{h_b}{w_b}\right)^{0.1}\left(\frac{h_b}{\lambda}\right)^{0.65}\right] \quad \text{(II-12)}$$

where $\lambda = V_g d_o / 4V_f$. In Equation II-12, θ_r = burning time, L/D is the ratio of the flame height to the flame depth in the crib, d_o is the initial fuel thickness, k_g/hd_o is the reciprocal of the Nusselt number, ρ_f and ρ_g are the fuel and gas densities respectively, h_b and w_b are the height and width

of the fuel bed, V_f and V_g are the volume of fuel and gas in the crib, and α is the thermal diffusivity of the fuel. Equation II-12 correlates the data of Fons very well. This equation gives the scale effects of the fuel and fuel bed variables on burning time, propagating rate, and burning rate for laboratory crib fires. Fons expressed the propagation rate, R, by:

$$R = \frac{1.57}{HW} (L)^{3/2} \qquad \text{(II-13)}$$

where H is the heat of combustion, W is the weight of fuel burned per unit area, and L is the flame height. Equations II-12 and II-13 can be used to make qualitative estimates of R for forest fires. However, in order to make quantitative estimates, extensive data on the properties of the fuel, the configuration of the bed and the transport coefficients must be known as is readily evident from Equation II-12.

Frandsen (10) has developed a model for fire spread through a fuel bed based on an energy flux conservation basis. His model is based on the steady-state solution of the energy equation:

$$\frac{\partial I_x}{\partial x} + \frac{\partial I_y}{\partial y} + \frac{\partial I_z}{\partial z} = - \frac{\partial \bar{Q}}{\partial t} \qquad \text{(II-14)}$$

where I is the heat flux, $\bar{Q} = \rho_{be} Q$ is the net heat absorbed per unit volume, ρ_{be} is the effective bulk density, and Q is the net heat absorbed per unit mass. The boundary conditions are:

$$I = 0 \qquad \bar{Q} = 0 \qquad x = -\infty$$

$$I = I_{ig} \qquad \bar{Q} = \bar{Q}_{ig} \qquad x = 0$$

where I_{ig} and $\bar{Q}_{ig}$ are the values of I and $\bar{Q}$ at ignition. With these boundary conditions and the assumption that the fuel bed is wide enough to achieve a straight line fire front, i.e., $\partial I_y/\partial y = 0$, Frandsen solves Equation II-14 to obtain

$$-R\,\bar{Q}_{ig} = I_{x_{ig}} + \int_{-\infty}^{0} \left(\frac{\partial I_z}{\partial z}\right)_{z_c} dx \qquad \text{(II-15)}$$

He then terms the right hand side of Equation II-15 the propagating heat flux,

$$I_p = I_{x_{ig}} + \int_{-\infty}^{0} \left(\frac{\partial I_z}{\partial z}\right)_{z_c} dx \qquad \text{(II-16)}$$

so that in simplified form the rate of propagation, R, is given by:

$$-R = I_p/\bar{Q}_{ig} \qquad \text{(II-17)}$$

where I_p, $I_{x_{ig}}$, and $\bar{Q}_{ig}$ are restricted to the same plane as $(\partial I_z/\partial z)_{z_c}$. The detailed steps used by Frandsen to derive Equation II-15 are questionable from the standpoint of mathematical rigor; nevertheless, Equation II-16 appears plausible in view of the assumptions made. Frandsen does not present any experimental validation of his model, and it appears to be somewhat difficult to use.

Frandsen, Rothermel and Philpot (30) have extended the work done by Frandsen, and have empirically defined a number of the quantities in Frandsen's work. They define $\overline{Q}_{ig}$, the volumetric heat of preignition, as:

$$\overline{Q}_{ig} = \varepsilon \rho_b Q_{ig} \qquad \text{(II-18)}$$

where ε is the effective heating number, the fraction of fuel in the unit volume that is effectively involved in the ignition process; ρ_b is the bulk density; and Q_{ig} is the heat of preignition. Frandsen has shown that ε is given by:

$$\varepsilon = e^{-45.3/\sigma} \qquad \text{(II-19)}$$

where σ is the particle surface-area-to-volume ratio. Frandsen has also developed an expression for the heat of preignition, Q_{ig}, as:

$$Q_{ig} = 139 + 620\ M \text{ cal/gm} \qquad \text{(II-20)}$$

where M is the moisture content of the fuel.

The propagating intensity, I_p, is the effective flow of energy that propagates the fire. It has its source in the combustion zone through the reaction intensity, a term derived from the mass loss rate of the fuel. The reaction intensity is given by:

$$I_R = -hdw/dt \qquad \text{(II-21)}$$

where h is the heat content of the fuel, w is the fuel loading, mass/area, and t is time. Frandsen and Rothermel (12) present a method for obtaining dw/dt. Rothermel shows that the reaction intensity, I_R, is related to the propagating flux, I_p, through a packing ratio, β. This relationship is presented graphically, since there exists a different curve for each fuel type.

They then account for wind effects and slope effects by:

$$I_p = (I_p)_o \ (1 + \phi_w + \phi_s) \qquad \text{(II-22)}$$

where

$$(I_p)_o = R \varepsilon \rho_b Q_{ig} \qquad \text{(II-23)}$$

and R is the spread rate, ϕ_w is wind coefficient and ϕ_s is the slope coefficient. Thus the flame spread rate is given by:

$$R = I_o(1 + \phi_w + \phi_s)/\varepsilon\rho_b Q_{ig} \qquad \text{(II-24)}$$

where I_o is given by Equation II-23, the no wind case.

Although this model takes into account the effects of moisture, wind and changes in terrain in predicting the fire spread rate, R, it requires an extensive knowledge of the potential fuel. A rate, R, must be determined for no wind, no slope conditions, presumably using small-scale model fires, and extensive data must be obtained for reaction intensities versus packing ratio for the full range of fuels for which the model is to apply. These limitations seem to be acute in the case of applying this model to thin homogeneous materials

such as those considered here. However, the model seems to be quite acceptable for forest fires.

Neither of the above models appears to be applicable to the problem of predicting horizontal burning rates of thin materials. Fons, Frandsen, and Rothermel all considered forest-type fuel beds which are several inches to a foot or more in thickness. On the other hand, most automotive interior materials are only a few millimeters thick. Therefore, the thickness of the material is a major difference between the work performed by the Forest Service and that presented in this dissertation. Another major difference is the type of fuel bed and the manner in which the fuel bed, or sample, is situated in the test apparatus. Their tests were performed on cribs or open arrays of forest fines (e.g., pine needles), whereas the interest in the present case is with relatively homogeneous woven fabrics and wooden slabs. Therefore, since the correlations presented above are based on empirical relations for many of the variables involved, it is not readily apparent how the results of Fons or those of Frandsen and Rothermel could be extrapolated to encompass the present case.

Two extensive studies of the flammability characteristics of vehicle interior materials have appeared recently. The first was by Goldsmith (13) at Illinois Institute of Technology. He experimentally determined the horizontal burning characteristics for a number of automotive interior

materials including seat fabrics, seat cushion material, headliners, door panels, etc. However, he did not attempt to correlate the data obtained from these tests. The second study was performed at the University of Oklahoma Research Institute by Sliepcevich, et al. (36). They obtained burning rate data for automobile interior materials as well as piloted ignition data for those materials used as seat fabrics.

Sliepcevich, et al., not only studied the horizontal burning as prescribed by the MFMVSS 302 horizontal burning rate test, but they also studied the effects of wind, moisture content, fabric orientation, and angle of inclination on the burning rate of automotive seat fabrics. All of these variables can have a substantial effect on the burning rates measured in the MFMVSS 302 apparatus. Moisture content had little effect on synthetic fabrics, such as nylons and vinyls, found in automobiles, but it had a pronounced effect on the burning rate of cellulosic materials. It was found that the horizontal burning rate of a vinyl fabric with a heavy cotton backing exhibited a decrease from 4.3 inches/minute at zero percent relative humidity to 2.8 inches/minute at 100 percent relative humidity. Hence, a material's backing can exhibit a controlling influence on the burning rate as determined by the MFMVSS test method.

The orientation of the fibers in the fabric also affects horizontal burning rate. The correlation to be presented later assumes a lengthwise normal burning direction,

i.e., parallel to the decorative pattern or backing fabric. However, some samples reported by Sliepcevich have burning rates that differ considerably from the lengthwise normal rates, if they are burned using a different orientation of the fibers. In some cases, this difference arises simply because of the "ease of burning" along the fibers as opposed to burning across the fibers. In other cases this variation could be due to different fibers being present, such as a rayon for the fill and nylon for the warp, thus achieving a composite woven material which could quite easily exhibit two different burning rates depending on direction.

As stated earlier, as a material is inclined toward the vertical, its burning rate will increase rapidly. Sliepcevich shows that an approximate relationship exists between the horizontal burning rate and an inclined burning rate using the MFMVSS 302 apparatus, modified so that the clamp assembly can be rotated. This approximate relation is given by:

$$R_\theta = (9 \sin \theta + 1) R_o \qquad \text{(II-25)}$$

where R_θ is the burning rate at angle θ measured above the horizontal plane; R_o is the burning rate of the material in the horizontal burning test.

Sliepcevich, et al., present a correlation of their data for fabric burning rates obtained from the MFMVSS 302 test. This correlation is based on the suggestion Fons made in 1946, that the propagation rate is a series of ignitions.

The derivation given by Sliepcevich will be repeated here in some detail.

The ignition measurements, mentioned previously, provide a functional relationship between the absorbed radiant heat flux H_a ($= \bar{\alpha} H_i$), and the ignition time, t_i. Figure II-1 shows this relationship for a typical fabric sample, vinyl sample V-7. An energy balance can be written for an ignition sample as:

$$(H_a t_i) A_y = c_p \, (\bar{T}_{ig} - T_o) \, \rho (\delta A_y) \qquad \text{(II-26)}$$

where H_a = absorbed energy flux, cal/cm^2-sec

t_i = ignition time, sec

A_y = area of the sample face exposed to the flux, cm^2

c_p = specific heat of the original sample, cal/gm-°C

$\bar{T}_{ig}$ = average temperature of the sample at ignition, °C

T_o = ambient temperature, °C

δ = thickness of the sample, cm

ρ = initial bulk density, gm/cm^3

Rearranging Equation II-26, a defining equation for an average ignition temperature, $\bar{T}_{ig}$, is obtained:

$$\bar{T}_{ig} = \frac{H_a t_i}{\rho \delta c_p} + T_o \qquad \text{(II-27)}$$

Since δ, ρ, c_p and T_o are assumed to be constant, it can be seen that $\bar{T}_{ig}$ depends on the product $(H_a t_i)$. Furthermore, as shown in Figure II-2, $(H_a t_i)$ is a strong function of t_i;

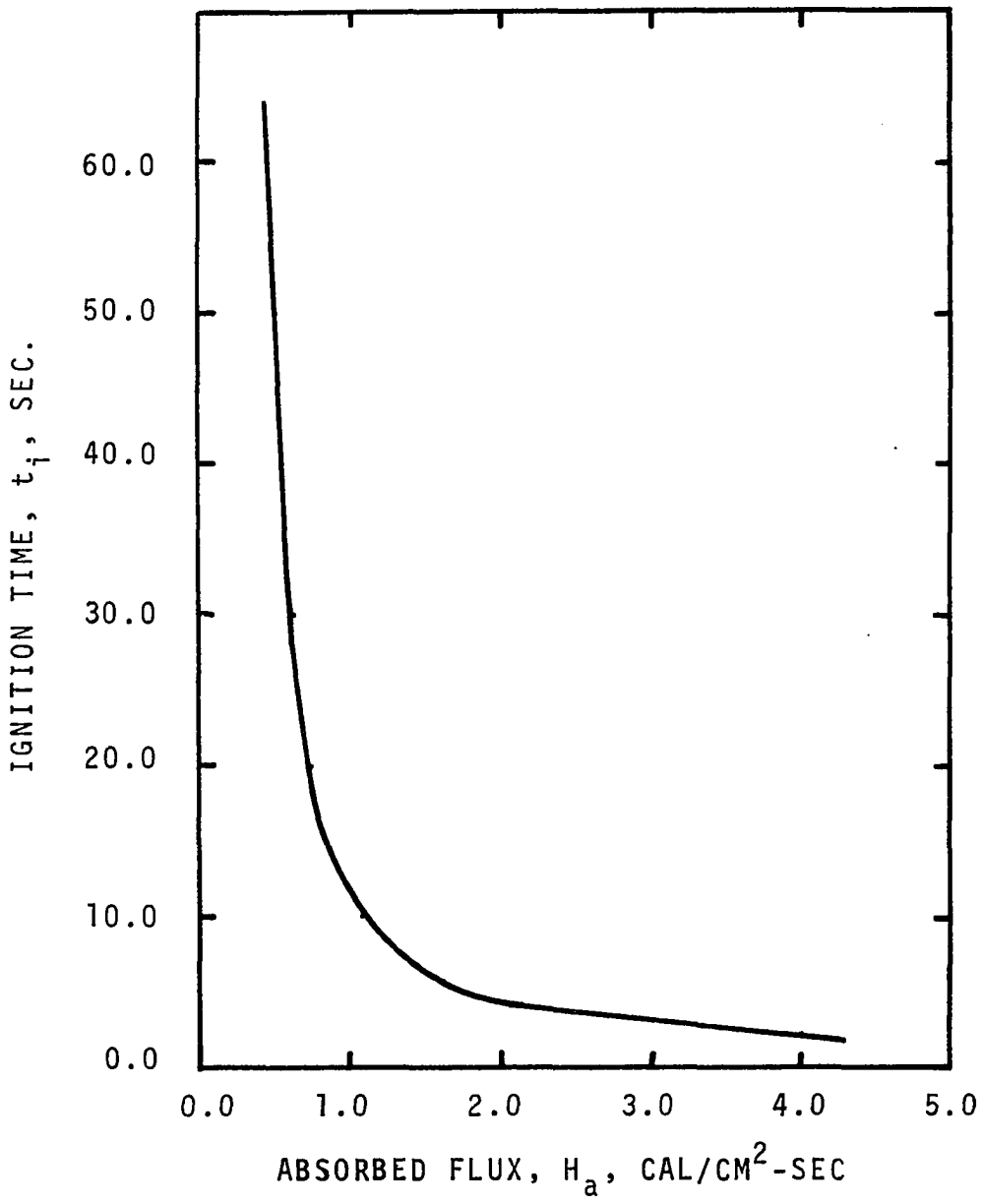

Figure II-1. The Variation of the Absorbed Flux with Ignition for Vinyl, V-7.

therefore, the average ignition temperature, $\overline{T}_{ig}$, cannot be a unique characteristic or a property of a material since it depends on the heating rate. It is emphasized that the value obtained from Equation II-27 represents an integrated average temperature for the sample and is not to be regarded as the local, surface temperature. Thus, $\overline{T}_{ig}$, as defined here can be quite different from the customary ignition temperatures reported in the literature; the latter refer to a somewhat arbitrary temperature of the exposed (but not in direct flame contact) surface at the instant that ignition occurs.

As can be seen from Figure II-2, $(H_a t_i)$, and consequently (according to Equation II-27) $\overline{T}_{ig}$ increases with increasing ignition times. However, the magnitude of the increase shown in this figure is misleading since the absorbed energy, H_a, does not account for heat losses from the ignition sample during preheating to the ignition point. Following the procedure used by Wesson (39), the heat losses were roughly estimated to be on the order of 0.25 cal/cm^2-sec (due to reradiation and convection from the exposed face and radiation and convection from the rear face). Deducting these losses from H_a, to obtain a value for the retained energy, H_R, values for $(H_R t_i)$ were computed. By replacing $H_a t_i$ in Equation II-27 with $H_R t_i$, new values of $\overline{T}_{ig}$ were computed. These results are shown in the dashed lines of Figure II-2. These values are more realistic; in fact, a more accurate form of Equation II-27 requires $H_R t_i$ in place of $H_a t_i$. Unfortunately, data which would provide

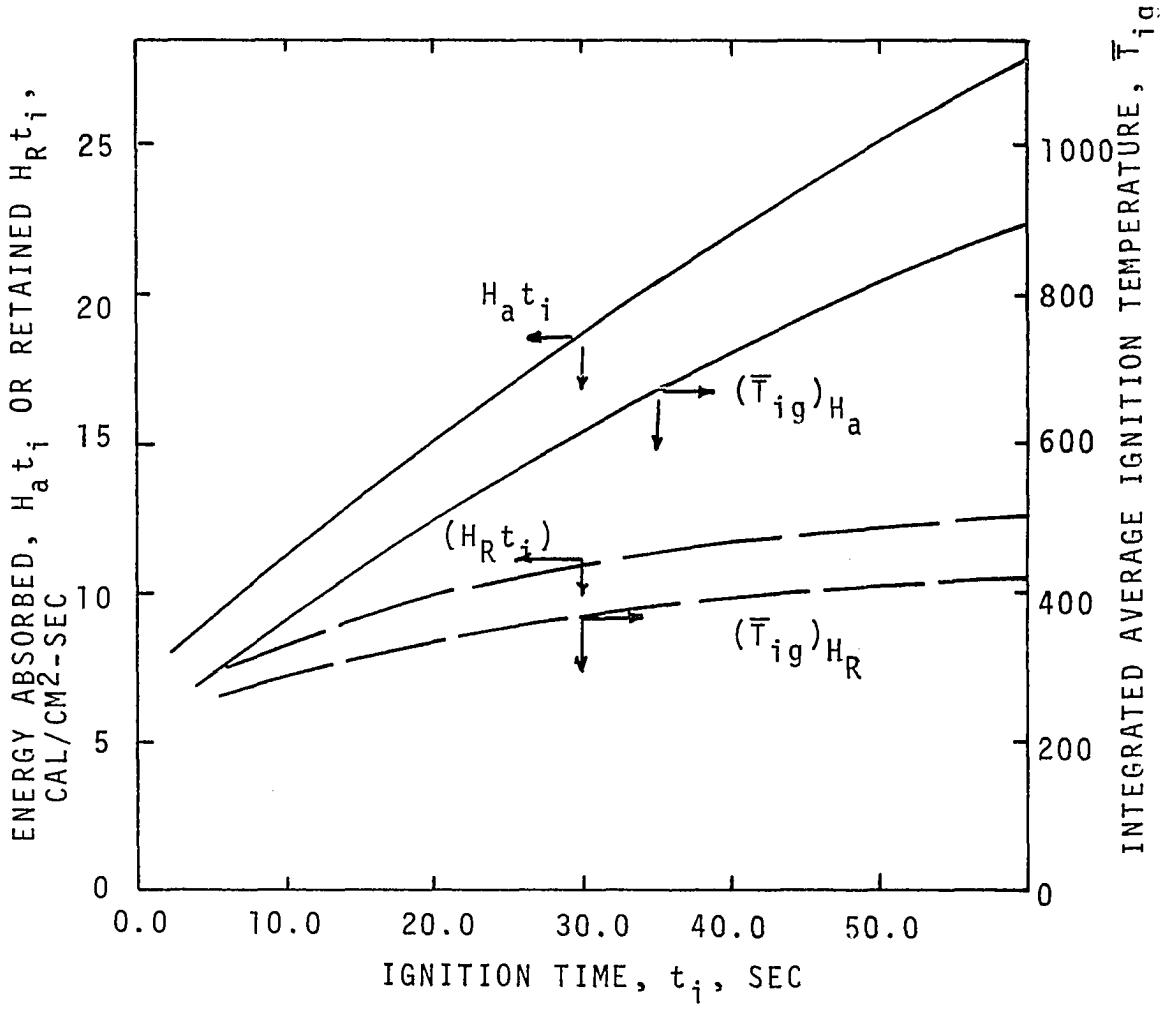

Figure II-2. The Variation of Energy Absorbed Per Unit Area and Average Temperature at Ignition with Time for Vinyl, V-7.

a more reliable estimate of heat losses as a function of irradiation fluxes are not available. Nevertheless, the $\overline{T}_{ig}$'s based on H_R appear to be in reasonably close agreement with the temperatures observed for maximum rates of weight loss in thermal gravimetric analyses; the latter have been used to predict ignition characteristics with some degree of success.

Wesson (39) demonstrated the applicability of transient, one-dimensional, heat conduction through an infinite, solid slab of an inert, opaque material to the analysis of the ignition process. Since the burning process is visualized as a series of successive ignitions (9), it seems reasonable, as a first approximation, to utilize a similar approach for the burning or flame propagation process.

Before proceeding with the mathematical development, it is important to emphasize that unlike the ignition test which gives absolute values for ignitability, the burning rate test generates numbers which are grossly dependent upon the test apparatus and procedure (36). Therefore, it can be anticipated that any burning rate model will contain at least a calibration constant for the particular apparatus and procedure since, in reality, a burning rate is defined by the apparatus and procedure.

In the MFMVSS 302 horizontal burning test, it was observed that the sample, Figure II-3a, ahead of the flame front is preheated on both sides, Figure II-3b. The heat fluxes in the vertical direction on the top surface, $\dot{q}_y$, and

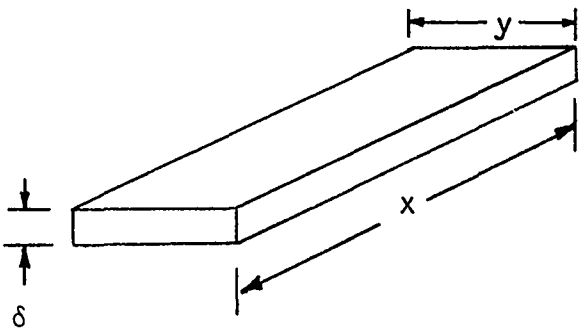

a. Test Sample.

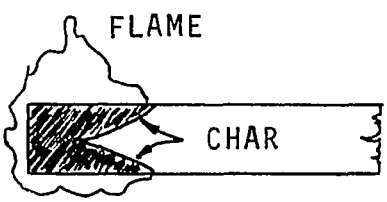

b. Burning Sample.

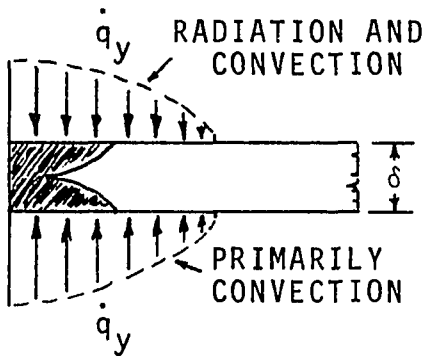

c. Vertical Heat Fluxes.

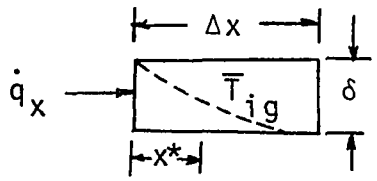

d. Individual Element at Incipient Ignition When $x = 0$, $T = T_F$ and $x = x^*$, $T = T_{ig}$. Vertical Fluxes Reduced to Single Horizontal Flux.

Figure II-3. Schematic of Flame Propagation.

on the bottom surface, $\dot{q}_y'$, are not necessarily equal, as pictured in Figure II-3c. For the sake of simplification, without due regard for mathematical rigor or physical reality, it will be assumed that the vertical fluxes can be replaced by an "equivalent" horizontal flux, $\dot{q}_x$, which results in a temperature gradient in the horizontal direction as illustrated by the dashed curve in Figure II-3d. Consequently, the horizontal burning process can be reduced to a one-dimensional model by the further assumption of invariance of the temperature across the y- and z-planes for a given value of x.

Consider an element $(\Delta x)_1$ of the sample which is initially at a uniform temperature, T_o, throughout as shown in Figure II-4a. If the specimen is exposed to direct contact with a flame on its left face, it is assumed that the temperature at this surface jumps immediately to $T_s = T_F$ which is the flame (optical pyrometer) temperature. A temperature gradient is likewise established, and the length of the element, $(\Delta x)_1$, is selected such that its temperature at the opposite face is essentially equal to the ambient temperature, T_o. To facilitate visualization, the temperature gradient is shown as a dashed, straight line in Figure II-4b. Since the temperature gradient is linear, the temperature at the midpoint of the element represents the "average" temperature in this element, $\overline{T}_{ig}$, and the penetration distance is $(\Delta x)_1/2 = x^*$, as shown in Figure II-4b. Note that the assumption of a linear temperature gradient does not introduce any additional

a. Initial Temperature Uniform Throughout at T_o.

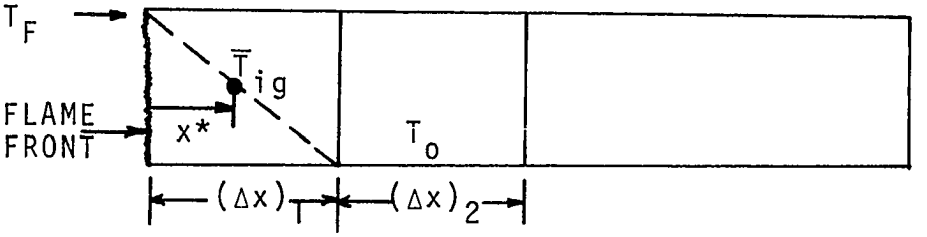

b. Temperature Distribution at Instant of Ignition on Left Face.

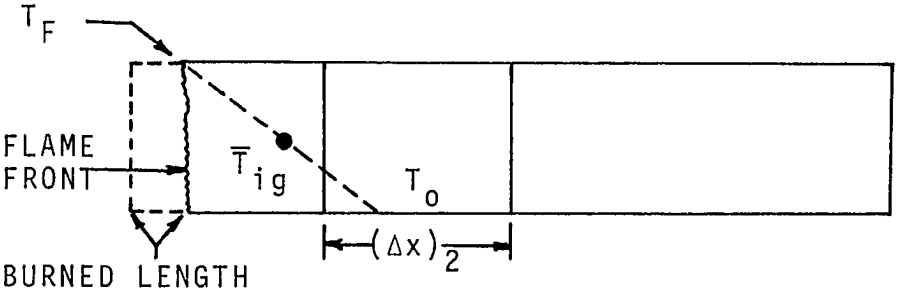

c. Temperature Distribution After Burning Has Penetrated 1/4 of the Distance into Element $(\Delta x)_1$.

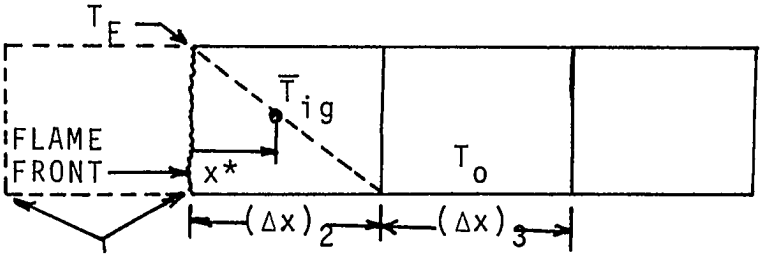

d. Temperature Distribution at the Instant of Completed Burning of First Element $(\Delta x)_1$ and Simultaneous Ignition of Left Face of Second Element $(\Delta x)_2$.

Figure II-4. Idealized Schematic of Quasi-Steady State Propagation of Horizontal Burning.

restrictions in this analysis since the assumption of a non-linear gradient would simply shift the $\overline{T}_{ig}$ away from the mid-point of the element.

As the sample proceeds to burn, the flame front moves to the right; consequently the temperature gradient advances. For example, Figure II-4c shows the temperature gradient and horizontal displacement of $\overline{T}_{ig}$ at the time when the flame front has advanced 1/4 of the way through $(\Delta x)_1$. As a result of this propagation, the adjacent element, $(\Delta x)_2$, undergoes preheating, and by the time the flame front has completely traversed element $(\Delta x)_1$, element $(\Delta x)_2$ is fully preheated to the ignition point as shown in Figure II-4d. As the flame front advances through element $(\Delta x)_2$, element $(\Delta x)_3$ undergoes preheating, etc. Thus, the burning process consists of successive periods of preheating followed by ignition, element by element. The criterion for ignition is given by Equation II-27 which proposes that when the "average" temperature in the element reaches $\overline{T}_{ig}$, the element will ignite. The rate at which $\overline{T}_{ig}$ advances through the element is therefore a measure of the rate at which successive ignitions occur, which in turn is equal to the burning rate, R_o. Thus,

$$R_o = x^*/t^* \qquad \text{(II-28)}$$

where x^* = penetration distance

$t^* = t_i$ = elapsed time to advance $\overline{T}_{ig}$ a distance x^*

Note that if the temperature gradient were linear, R_o would be also equal to $\Delta x/2t^*$ since the time required to burn an element which is $2x^*$ (or Δx) in length is $2t^*$. As stated before, there is no loss in generality introduced by visualizing a linear gradient.

An energy balance for one-dimensional transient heat conduction through a semi-infinite, inert and opaque solid is then formulated. It is assumed that the heat capacity, c_p, thermal conductivity, k, and density, ρ, are temperature and position independent. The energy balance yields:

$$\kappa \frac{\partial^2 T}{\partial x^2} = \frac{\partial T}{\partial t} \qquad \text{(II-29)}$$

where κ is the thermal diffusivity $(k/\rho c_p)$. The boundary conditions are:

Initial condition: $t = 0,\ T = T_o$ all x (II-30a)

Boundary conditions: $t > 0,\ T = T_s,\ x = 0$ (II-30b)

$t > 0,\ T = T_o,\ x = \infty$ (II-30c)

The solution of Equation II-29 with the initial and boundary conditions II-30 is given by:

$$\frac{T - T_o}{T_s - T_o} = 1 - \text{erf}\ \frac{x}{2\sqrt{\kappa t}} \qquad \text{(II-31)}$$

For the problem as formulated here, $t = t^*$, $x = x^*$, $T = \overline{T}_{ig}$, $T_s = T_F$, so that:

$$\frac{\overline{T}_{ig} - T_o}{T_F - T_o} = 1 - \text{erf}\ \frac{x^*}{2\sqrt{\kappa t^*}} \qquad \text{(II-32)}$$

The value for x* in terms of R_o and t* from Equation II-28 is then substituted into II-32, yielding:

$$\frac{\overline{T}_{ig} - T_o}{T_F - T_o} = 1 - \text{erf} \frac{R_o\sqrt{t^*}}{2\sqrt{\kappa}} \qquad \text{(II-33)}$$

Since it is clear from Equation II-27 that for each absorbed flux, H_a, there is a corresponding ignition time, t_i, and the burning process is assumed to be a series of ignitions, then there is a unique ignition time, $t = t^*$, and a flux, $H_a = H_a^*$ corresponding to the burning rate $R_o = x^*/t^*$. Therefore, Equation II-27 becomes:

$$\overline{T}_{ig} - T_o = \frac{H_a^* t^*}{\delta\rho\, c_p} \qquad \text{(II-34)}$$

Combining Equations II-33 and II-34:

$$\frac{H_a^*\, t^*}{(T_F - T_o)\, \delta\rho c_p} = 1 - \text{erf} \frac{R_o\sqrt{t^*}}{2\sqrt{\kappa}} \qquad \text{(II-35)}$$

Equation II-35 gives a relationship among the burning rate, characteristic ignition time, and the heat flux required to sustain propagation.

Calculations showed that t* was very small, on the order of tenths of a second, and the O.U.R.I. ignition test cannot be used to obtain accurate data at very short times (i.e., less than 2 seconds). Extrapolating the ignition data to these limits is not reliable. Therefore, some other means had to be devised for obtaining the relationship between H_a^* and t*. Had $(H_a^* t^*)$ been a constant, this problem would not

have arisen, because $\overline{T}_{ig}$ could have then been calculated from Equation II-27 directly. It was found that for short ignition times and for thin materials the error function in Equation II-11 approaches a value of one. Since ρ is raised to the 0.2 power, its value is fairly constant for the fabrics considered in this study; hence, it was deduced that:

$$\sqrt{t_i} \simeq \text{constant}/H_a \qquad \text{(II-36)}$$

As $H_a \to \infty$, $\sqrt{t} \to 0$. Thus a plot of $\sqrt{t}$ versus $1/H_a$ using the actual ignition data was made for each of the materials considered. A typical example of these plots is given in Figure II-5. These plots were forced to be straight lines passing through the origin, so that a relationship between t* and H_a* was obtained as:

$$\text{slope} = s^* = H_a\sqrt{t_i} = H_a^*\sqrt{t^*} \qquad \text{(II-37)}$$

When Equation II-37 is substituted into II-35 the result is:

$$\frac{s^*\sqrt{t^*}}{957\ w_o c_p} = 1 - \text{erf}\ \frac{R_o\sqrt{t^*}}{2\sqrt{\kappa}} \qquad \text{(II-38)}$$

where $w_o = \delta\rho$, $T_F = 982°C$, and $T_o = 25°C$. The value of 982°C = T_F was used because it corresponds to T_F = 1800°F, approximately the temperature of a benzene flame as measured by an optical pyrometer.

Trial and error calculations were made on Equation II-38 to find values of t* using the experimental values of R_o. It was found that:

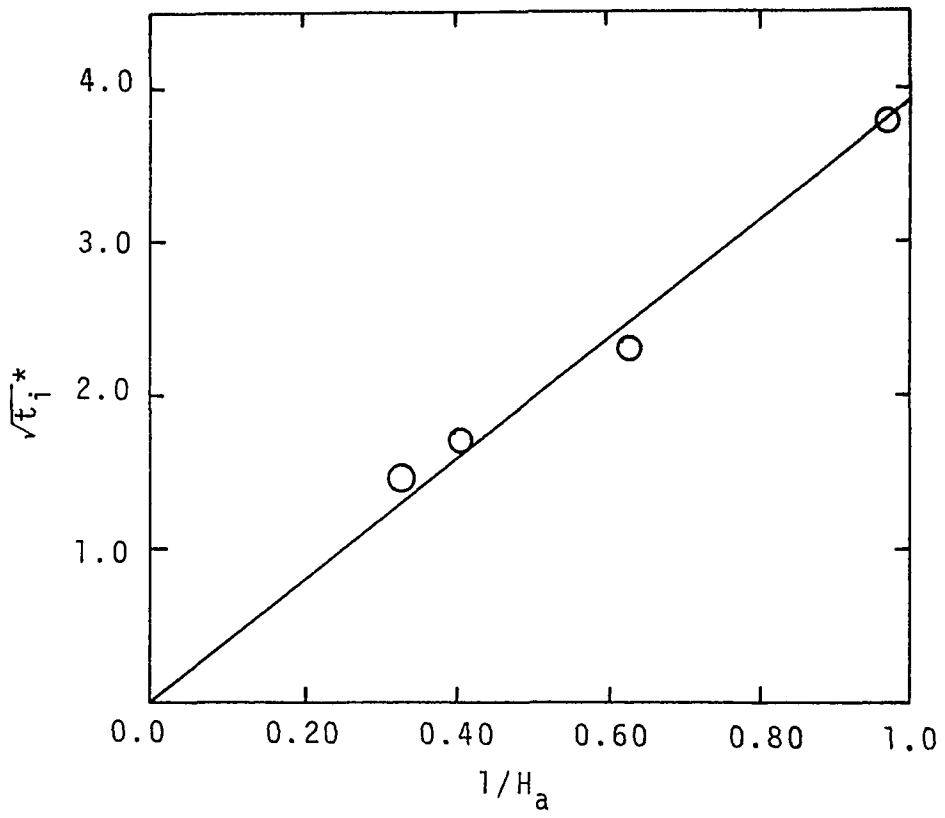

Figure II-5. Line Obtained for Vinyl, V-7, Resulting from Plotting $\sqrt{t_i}^*$ versus $1/H_a$, from Which the Slope, s*, is Calculated.

$$R_o\sqrt{t^*} = C_F \qquad \text{(II-39)}$$

for each class of materials considered, i.e., a unique value was found for nylon fabrics, another for vinyl fabrics, etc.

The C_F, the calibration factor, appears to be unique for a particular material in a specific burning rate experimental apparatus, such as the MFMVSS 302 test apparatus used for this study. Thus, the characteristic ignition time for the burning process is

$$\sqrt{t^*} = C_F/R_o \qquad \text{(II-39a)}$$

If Equation II-39a is substituted on the left-hand side of Equation II-38, and Equation II-39 is substituted on the right-hand side of Equation II-38, after rearranging, the result is:

$$R_o = \left(\frac{C_F}{957\, c_p \left(1 - \operatorname{erf} \frac{C_F}{2\sqrt{\kappa}}\right)} \right) \frac{s^*}{w_o} \qquad \text{(II-40)}$$

or

$$R_o = C^* \left[s^*/w_o\right] \qquad \text{(II-41)}$$

where C* is the bracketed term in Equation II-40.

Equation II-41 has the following specialized form for the materials considered by Sliepcevich, et al.:

Vinyls: R_o (cm/sec) = $(2.91 \times 10^{-3})\ s^*/w_o$ (II-41a)

Nylons: R_o (cm/sec) = $(5.65 \times 10^{-4})\ s^*/w_o$ (II-41b)

Nylon carpets: R_o (cm/sec) = $(3.35 \times 10^{-4})\ s^*/w_o$ (II-41c)

Cottons: R_o (cm/sec) = $(1.84 \times 10^{-3})\ s^*/w_o$ (II-41d)

Filter papers: R_o (cm/sec) = $(1.56 \times 10^{-3})\ s^*/w_o$ (II-41e)

A plot of calculated R_o versus experimental R_o is presented by Sliepcevich. The correlation coefficient of the resulting least squares fit was 0.955 and the standard error of estimate was 0.033 cm/sec, and the equation of the line is R_o (calc) = 0.991 x R_o(exp).

The correlation presented by Sliepcevich, et al., appears to be the first formulation which directly combines the ignition data and burning rate data. It seems obvious that these two phenomena should be related, which was first suggested by Fons in 1946.

The model which is presented above has several advantages over those of Fons, Frandsen and Rothermel when applied to homogeneous substances that are reasonably thin. This model was developed specifically for thin homogeneous materials. It incorporates the ignition behavior into the mathematical formulation through the use of the slope, s*, of the ignition curve at short times, t_i. It is not dependent on the flame height, depth, or width as is Fons' model. It is not necessary to know values of the heat of combustion of a specimen nor its heat of preignition as in the model of Frandsen and Rothermel. A detailed knowledge of the kinetics of decomposition, which so many working in this field have tried to incorporate into their models, is unnecessary. These are some of the distinct advantages offered by the Sliepcevich model.

However, there are certain assumptions made in arriving at Equation II-38 that should be examined. In Equation II-26, the terms for the heat of vaporization and pyrolysis have been omitted. This assumption is probably valid, since the heating rates in a flame are high compared to the heats of decomposition.

Another assumption which is open to question is the use of a one-dimensional model in which heat is propagated through the specimen only by conduction in the horizontal plane. Referring to Figure II-3c which depicts the visual observations on the horizontal burning process, it is clear that heat is transferred from the flame to the surfaces of the specimen by radiation and convection in the vertical plane. The observation of the char zones clearly indicates that the temperature in the vertical plane of the specimen is not uniform across the thickness, δ. In fact, by employing baffles, maintained about 1/8 inch ahead of the flame front, it was possible to reduce the burning rate virtually to zero. Therefore, from the standpoint of physical reality, a two-dimensional model would be more appropriate, which will be presented in Chapter IV.

Another criticism of the one-dimensional model is that a different constant must be empirically determined for each class of materials indicated by Equation II-41.

CHAPTER III

EXPERIMENTAL PROCEDURE

As noted previously, the burning rate test used in this study was the FMVSS 302 horizontal burning rate test (6). The only deviations from this procedure were that the cabinet used to house the burning rate apparatus was much larger than the FMVSS 302 test specifies (36), and all tests were run at laboratory conditions of temperature and humidity since the laboratory did not have facilities to maintain a 70°F temperature and a 50 percent relative humidity.

The apparatus consists of a large cabinet, 45 inches wide, 20 inches deep, and 41 inches high, with a full front window as shown in Figure III-1. Combustion gases exhaust through a 3-3/4 inch hole in the center of the cabinet roof, and fresh air enters through a rectangular 3 inch opening which extends across the bottom of the front. The sample holder consists of two steel U-shaped clamps 4 inches wide and 14 inches long. These clamps then fit into a frame which elevates the clamps about 8 inches above the floor of the cabinet, as shown in Figure III-2. The top steel clamp has etched marks at one inch intervals. The ignition source is

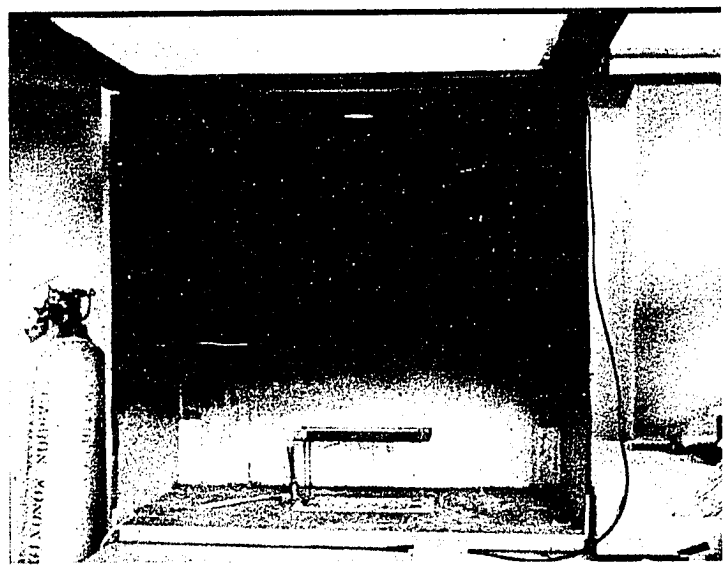

Figure III-1. Horizontal Burning Rate Apparatus.

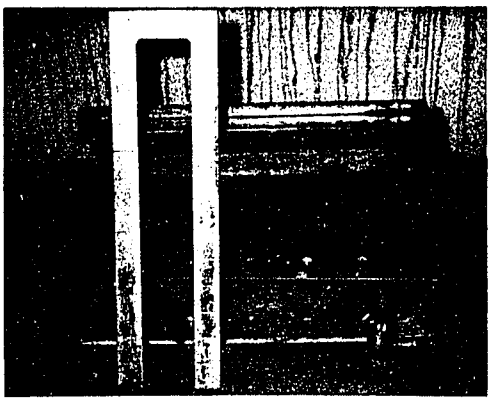

Figure III-2A. Sample Holder and U-Shaped Clamp Assembly.

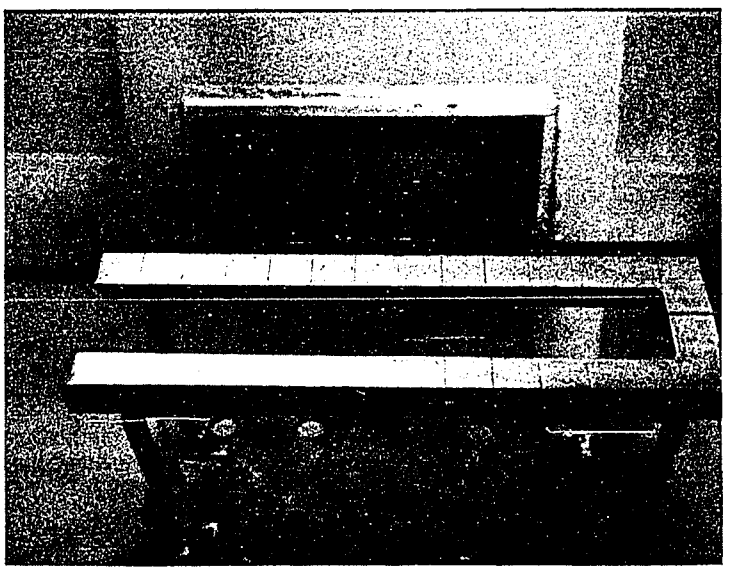

Figure III-2B. Sample Holder with U-Shaped Clamp Showing Indicating Marks.

a Bunsen burner which is supplied with any fuel which has a flame temperature equivalent to natural gas.

The samples to be tested were cut into strips 4 inches wide and 14 inches long. The fabric samples were then conditioned at 70°F and 50 percent relative humidity for at least 24 hours prior to testing. The wood samples were oven-dried for a minimum of 48 hours. When it was desired to run a test, the sample holder frame was placed in the center of the cabinet, the burner was lighted (Matheson "B" gas was used, being 55 ± 1 percent hydrogen, 24 ± 1 percent methane, 18 ± 1 percent carbon monoxide, and 3 ± 1 percent ethane), and the flame adjusted, from the 3/8 inch inside diameter burner tube, to a 1-1/2 inch height. A sample was removed from the conditioning chamber and placed between the clamps in the frame holder, care being taken that minimal sample sagging occurred. The front door of the cabinet was lowered and locked. The flame from the Bunsen burner was then applied to the exposed end of the sample for 15 seconds. The burning length was 10 inches and timing of the flame propagation started at the 2 inch mark from the ignited end. This procedure nullified any effects which the burner flame might have on propagating the flame.

Three things could happen and are so reported:

1. The flame propagates the entire length of the sample (most common occurrence).
2. The flame propagates past the beginning timing mark, but not the full 10 inches.

3. The flame self-extinguishes before reaching the 2 inch timing mark.

In Case 1, the burning rate is reported for the sample in inches/minute. In Case 2, attempts to obtain a burning rate were not satisfactory since the flame often became stationary and then extinguished. The timing ended when flame extinguishment was obtained, a matter of 10 to 90 seconds after propagation ceased. In Case 3, the behavior was defined as self-extinguishing and no burning rate data were reported for such samples.

The samples used were seat fabrics (nylons and vinyls) from 1968, and later, model automobiles, cotton cloth, Whatman filter papers, nylon automobile carpeting, and wood samples cut to nominal 1/8 inch thicknesses. Table A-1 in Appendix A lists all samples used and gives a physical description of each.

Ignition data were obtained using the O.U.R.I. ignition test for the nylon, vinyl, and cotton cloths; the filter paper; and the nylon carpeting. Ignition data for the woods were extracted from Wesson's work on wood ignition (39), and these data were then corrected for thin materials. The description of the ignition test procedure and the results can be found elsewhere (21, 25, 39).

Several hundred burning rate tests were performed on 26 nylons, 14 vinyls, and 6 cotton fabrics, 7 filter papers and 7 nylon carpets and 6 each of 1/32, 1/16, and 3/32 inch

balsa wood, and 6 samples each of nominal 1/8 inch thick ash, oak, and redgum. Each test consisted of making from 3 to 30 runs on each type of sample. A sample is defined as a material with a unique color, weave (if applicable), density, weight per unit area, thickness, and a unique ignition curve. Only average burning rates for each material are reported.

The reproducibility of data in the horizontal burning rate test was found to be within 5 percent on the whole. However, some samples had a much higher variability, as great as 50 percent. The 5 percent variability can be attributed to the test procedure, apparatus and experimentalist. The larger variations appear to be due to surface finishes on the materials, decorative patterns, and non-uniformities in the sample. Table III-1 presents several examples of burning rate data, and shows the standard deviation of these selected data from their mean. The data in the table represent the complete range of variability encountered in this study.

Property data were obtained for each sample. The weight per unit area (W_o) was obtained by weighing a 25 sq cm piece of dried material on an electro balance. The thickness (δ) was obtained by placing the sample between two round steel discs having a thickness of 0.051 cm each. The total thickness of discs and material was then measured using a dial micrometer and the material thickness obtained by subtracting the sum of the discs' thickness from the total. This seemingly elaborate procedure was necessary in order that repeatability

TABLE III-1

EXAMPLES OF THE VARIABILITY OF BURNING RATE DATA

Material	Burning Rate, in/min			No. of Samples	Standard Deviation	
	Max	Min	Aver		in/min	% of Mean
1 sheet #1 Whatman Filter Paper (F-1)	9.26	7.94	8.53	30	0.40	4.6
2 sheets #1 Whatman Filter Paper (F-1)	6.32	4.32	5.20	30	0.51	9.0
Vinyl Fabric (V-4)	2.08	1.90	1.99	3	0.12	6.2
Vinyl Fabric (V-13)	4.33	2.40	3.67	30	1.29	35.0
Vinyl Fabric (V-15)	6.67	5.36	6.05	30	0.46	7.6
Cotton Fabric (CT-1)	3.52	2.54	3.02	30	0.28	9.4
Nylon Fabric (N-1)	1.61	1.37	1.52	3	0.19	12.3
Nylon Fabric (N-3)	2.26	1.70	1.93	3	0.41	21.3
Nylon Fabric (N-10)	1.18	1.08	1.12	3	0.07	6.5
Nylon Fabric (N-25)	2.76	2.33	2.55	30	0.11	4.3
Nylon Fabric (N-27)	9.33	1.36	3.43	30	1.70	50.0

in measurements could be obtained. Many of the fabrics were heavily patterned with ridges and indentations. The above procedure gave an average thickness although it is certain that for these types of fabrics the thicknesses are biased toward the high side. The density (ρ) is a bulk density obtained by dividing the weight per unit area by the thickness ($\rho = w_o/\delta$). Heat capacity was assumed constant for each type of material; values were obtained from Hilado's Flammability Handbook for Plastics and Lange's Handbook of Chemistry. The thermal conductivities of the fabrics, carpeting, and filter papers were obtained by plotting a straight line through the thermal conductivity point for air and a point at a given density as found in Lange's Handbook of Chemistry. These straight line approximations are shown in Figure III-3. For woods and filter papers, the equation for thermal conductivity suggested by McLean (22) was used:

$$k = 4.78 \times 10^{-4} \left(\frac{\rho}{\rho_w}\right) + 5.68 \times 10^{-5} \ \frac{cal}{cm\text{-}sec\text{-}^\circ C}$$

It should be noted that flame appeared both above and below the sample as it was burning. The open structure of the clamp supporting frame allowed free access of air to both sides of the sample during a test. As mentioned in Chapter II, the sample positioning can have a significant effect on the observed burning rate.

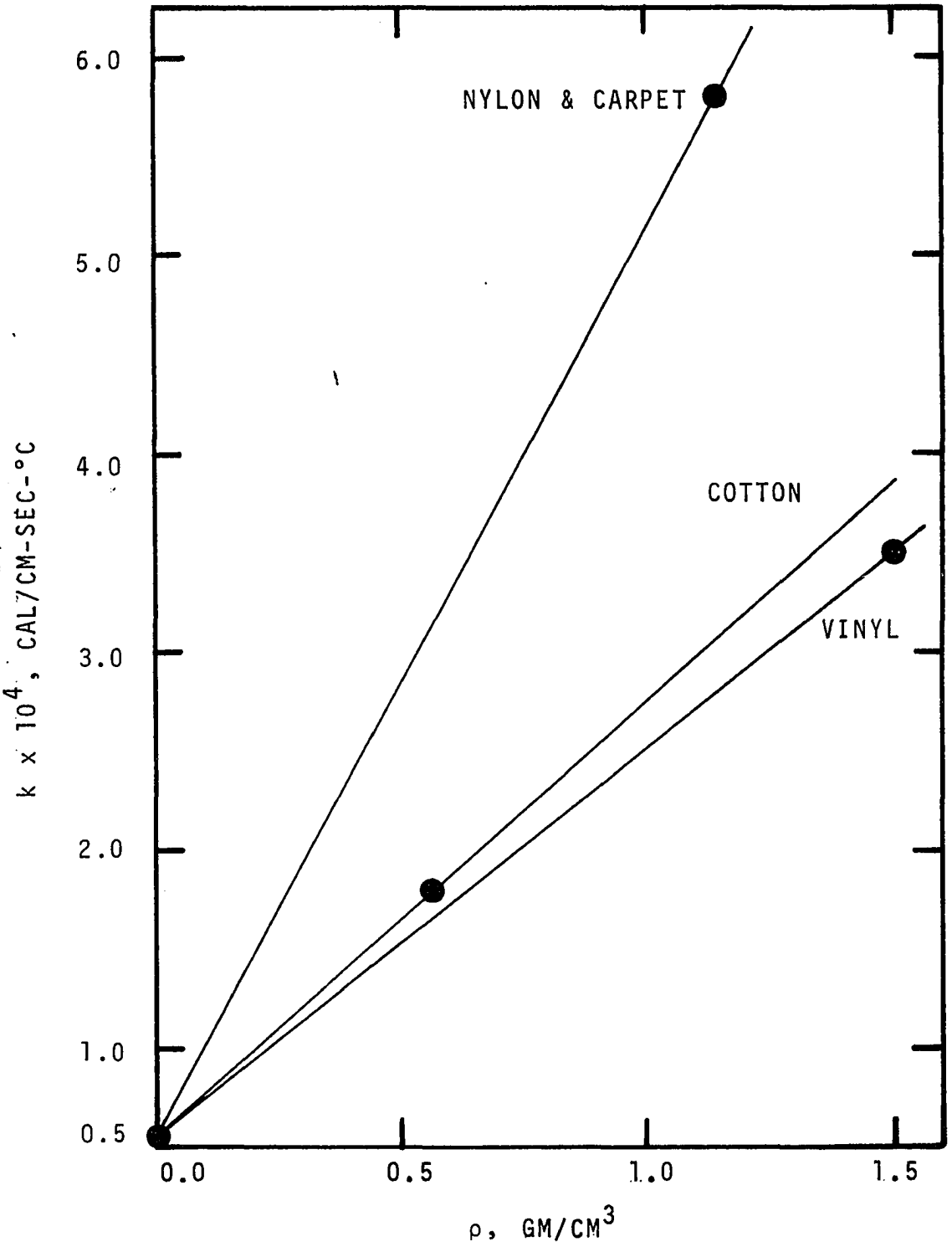

Figure III-3. Thermal Conductivity's Dependence on Density for Nylon, Nylon Carpeting, Vinyl, and Cotton Fabrics.

CHAPTER IV

RESULTS AND DISCUSSION

As indicated in Chapter II, the horizontal burning rate data obtained from the MFMVSS 302 test for nylon and vinyl seat fabrics, nylon automotive carpeting, woven cotton cloth, and filter paper, can be correlated with the ignition data for these materials. This correlation is based on the use of a one-dimensional heat conduction model for a semi-infinite inert and opaque slab with constant thermal and physical properties, as was given by:

$$\frac{s^*\sqrt{t^*}}{957\, w_o c_p} = 1 - \text{erf}\left(\frac{R_o\sqrt{t^*}}{2\sqrt{\kappa}}\right) \qquad \text{(II-38)}$$

where s^* is the slope defined by Equation II-37, t^* is the characteristic ignition time, w_o is the material weight per unit area, c_p is the heat capacity, R_o, is the horizontal burning rate, and κ is the thermal diffusivity.

It was felt that this model could be improved and extended to cover a wider range of materials, e.g., woods. One of the objectives of this work was to seek a method for predicting $R_o\sqrt{t^*}$ for other materials without having to perform extensive burning rate tests. Thus, if $R_o\sqrt{t^*}$ could be related

to some easily measured property, or properties, of the materials, it might also be possible to obtain a single correlation or model for all the materials used, rather than one equation for each class of materials (see Equations II-41).

In order to extend the work done by Sliepcevich, et al. to cover a wider range of materials, thin (nominal 1/8 inch thick) samples of ash, oak, and redgum and 1/32, 1/16 and 3/32 inch samples of balsa were subjected to the modified (MFMVSS) FMVSS 302 horizontal burning rate test. The data obtained from burning these thin wooden samples is presented in Table A-1, Appendix A.

Calculation of s* for Woods

Before the technique developed by Sliepcevich, et al., i.e., Equation II-38, could be applied, it was necessary to calculate the slope s* as defined by Equation II-37. Consequently, ignition data, H_a versus t_i, was required for each material and particularly at short ignition times on the order of a few seconds. Wesson (39) has obtained extensive data on the ignition of woods. His correlation for ignition time, t_i, as a function of initially absorbed flux, H_a, and density, ρ, was presented in Chapter II:

$$t_i = 35 \left[\frac{\rho^{0.9} \left(\operatorname{erf} \frac{\delta}{2\sqrt{\kappa t_i}} \right)^{1/2}}{(\bar{\alpha} H_i)^{2.8}} \right] \qquad \text{(II-10)}$$

where t_i is in sec, ρ is in gm/cm^3, H_i is in cal/cm^2-sec, δ, the sample thickness, is in cm, and κ is in cm^2/sec. The

error function term corrects for the effect of thickness on the ignition time.

His data were obtained for each of the woods studied, using both tungsten quartz lamps and benzene flames as irradiation sources. In the present work, the ignition data extracted from Wesson's study utilizes only the data for the benzene flame because the spectral distribution of radiant energy from benzene flames more nearly reproduces the spectral distribution of the flame of a burning specimen (36). His data were obtained using specimen thicknesses ranging from 0.318 cm to 2.54 cm. The data for woods extracted from Wesson's work corresponded to the thicknesses of balsa (δ = 1.97 cm), ash (δ = 2.54 cm), redgum (δ = 2.54 cm), and oak (δ = 2.54 cm). Since the wood samples used in the burning rate tests were approximately 0.32 cm, or less, in thickness, a correction had to be applied to Wesson's data in order for it to be used in predicting the slope, s*, for these thin samples.

The data of Wesson, for each material, was plotted as t_i versus $H_a/[\rho^{1/3}(\text{erf } 1/2\sqrt{F})^{3/4}]$. The error function term, which corrects for differences in thickness, was then obtained for each sample of wood used in this study. From plots of t_i versus $H_a/[\rho^{1/3}(\text{erf } 1/2\sqrt{F})^{3/4}]$, assuming an ignition time between one and 60 seconds, such that t_i, ρ, and erf $1/2\sqrt{F}$ were known, new values of H_a corresponding to the thin samples were obtained. The calculations resulting from this procedure along with the original data of Wesson and the plots referred to

above are presented in Table A-4 and A-5 and Figures A-1 through A-8 of Appendix A.

Once the H_a data had been corrected for thickness effects, the slope, s*, according to Equation II-37, for each of the wood samples considered in this study was calculated; these values are presented in Table A-2 of Appendix A. These slopes were then incorporated into Equation II-38, and values of $\sqrt{t^*}$ were calculated by trial and error (Table A-3, Appendix A). It was found that $R_o\sqrt{t^*}$ was also a constant for each type of wood used as had been previously found for each class of materials (synthetic and natural fibers) by Sliepcevich.

Extension of Sliepcevich Model

The desired extension of the one-dimensional model was to obtain a method of predicting values of $R_o\sqrt{t^*}$ from physical properties. Therefore, attempts were made to correlate the $R_o\sqrt{t^*}$ values with the density, ρ, of the material, and with the weight/area of the material, w_o. A computerized least squares fit was made on the data, obtaining $R_o\sqrt{t^*}$ as a function of ρ^a and separately as a function of w_o^b. A t-distribution test, which is explained in Appendix C, was performed simultaneously with the least squares fits. It indicated that $R_o\sqrt{t^*}$ correlated well with density, ρ, but very poorly with weight/area, w_o. The correlation of $R_o\sqrt{t^*}$ with density is, for all the wood samples:

$$R_o\sqrt{t^*} = 8.93 \times 10^{-2} \ (\rho)^{-0.099} \qquad \text{(IV-1)}$$

and for the fabrics (nylon and vinyl seat covers, cotton cloths, Whatman filter papers and nylon carpets):

$$R_o\sqrt{t^*} = 8.49 \times 10^{-2}(\rho)^{0.419} \qquad \text{(IV-2)}$$

where the units of R_o are cm/sec, t* are sec, and ρ are gm/cm^3.

By substituting Equation IV-1, or the average value for $R_o\sqrt{t^*}$ for all the woods, i.e., $(R_o\sqrt{t^*})_{aver} = 0.103$, into Equation II-38, and solving for $\sqrt{t^*}$, the following equation is obtained:

$$\sqrt{t^*}_{wood} = \frac{957\ w_o c_p}{s^*}\left[1 - \text{erf}\ \frac{0.103}{2\sqrt{\kappa}}\right] \qquad \text{(IV-3)}$$

and by substituting Equation IV-2 into Equation II-38, the resulting equation is:

$$\sqrt{t^*}_{fabrics} = \frac{957\ w_o c_p}{s^*}\left[1 - \text{erf}\ \frac{8.49 \times 10^{-2}(\rho)^{0.42}}{2\sqrt{\kappa}}\right] \qquad \text{(IV-4)}$$

where t* is in sec, w_o is in gm/cm^2, c_p is in cal/gm-°C, and s* is in $cal/cm^2\text{-}sec^{1/2}$. A single value of thermal diffusivity was used by Sliepcevich, et al. (36), $\kappa = 1.06 \times 10^{-3}$ cm^2/sec; thus Equation IV-4 can be simplified to:

$$\sqrt{t^*}_{fabrics} = \frac{957\ w_o c_p}{s^*}\left[1 - \text{erf}\ (1.31\ \rho^{0.42})\right] \qquad \text{(IV-5)}$$

Since Equations IV-3 and IV-5 depend only on thermal and physical properties and the slope based on ignition data, they could be used to predict values of $\sqrt{t^*}$ for a material. These $\sqrt{t^*}$ values could then be substituted into Equations IV-1 and IV-2, and R_o values could be obtained. This technique of calculating R_o was performed on three nylon samples and six balsa samples which were not included in the previous calculations of $R_o\sqrt{t^*}$. The results are shown in Table IV-1. It can be seen that the technique developed above predicts the burning rate for the woods considered very well and predicts the burning rates for the nylons within a factor of two.

The generalization of $R_o\sqrt{t^*}$ as a function of density, and the subsequent predicted results for R_o as shown in Table IV-1, account for most of the deficiencies in the development of Sliepcevich, et al., outlined in Chapter II. However, since the method of obtaining the values of $R_o\sqrt{t^*}$, which were used to obtain Equations IV-1 and IV-2, were based on a one-dimensional heat conduction model, and since a two-dimensional model would be more realistic, a different approach to the problem was sought. The new approach still has as its basis that the burning rate and the ignition process are related.

The Two-Dimensional Model

As stated previously, a two-dimensional model of the burning process appears to be more realistic than the one-dimensional model. On the other hand, a three-dimensional

TABLE IV-1

COMPARISON OF EXPERIMENTAL AND CALCULATED BURNING RATES

Sample	ρ g/cm^3	Slope s* cal/cm^2-sec$^{1/2}$	w_o gm/cm^2	R_o exper cm/sec	R calc by Eq IV-1 and IV-2 cm/sec	$\sqrt{t^*}$ sec$^{1/2}$
1/32" Balsa: $c_p = 0.34$; $\kappa = 1.765 \times 10^{-3}$						
B1/32-1	0.127	1.445	0.0129	0.6415	0.520	0.211
B1/32-2	0.127	1.430	0.0128	0.580	0.515	0.213
B1/32-3	0.134	1.47	0.0135	0.672	0.532	0.203
B1/32-4	0.1173	1.40	0.0117	0.632	0.625	0.177
B1/32-5	0.0994	1.33	0.0100	0.799	0.765	0.147
B1/32-6	0.1164	1.40	0.0117	0.730	0.636	0.174
Nylon: $c_p = 0.40$; $\kappa = 1.06 \times 10^{-3}$						
N-2	0.487	3.95	0.0321	0.0656	0.117	0.538
B-3	0.410	4.85	0.0353	0.0816	0.103	0.568
N-6	0.407	4.15	0.0373	0.0453	0.083	0.705

model would be even more preferable except for the mathematical complexities. If the flame front advances in a straight line, then a two-dimensional formulation should represent the phenomenon quite well. The burning process was mathematically formulated assuming an inert, opaque solid at steady-state, with a moving boundary, and heat conduction through the thickness of the sample, but not along its length (Refer to Figure IV-1).

The mathematical formulation, considering the above assumptions, becomes:

$$R_o \frac{\partial T}{\partial x} = \kappa \frac{\partial^2 T}{\partial y^2} \qquad \text{(IV-6)}$$

where R_o is the burning rate, T is the temperature, and κ is the thermal diffusivity. The boundary conditions for Equation IV-6 are assumed to be

$$\left.\frac{\partial T}{\partial y}\right|_{y=0} = 0 \qquad y = 0 \qquad \text{any } x \qquad \text{(IV-7a)}$$

$$T = T_{ig} \qquad y = \delta/2 \qquad x = 0 \qquad \text{(IV-7b)}$$

$$T = T_o \qquad \text{any } y \qquad x = \infty \qquad \text{(IV-7c)}$$

where T_{ig} is the ignition temperature, T_o is the ambient temperature, and δ is the thickness. Equation IV-6 can be written in dimensionless form by making the following substitutions:

$$\eta = \frac{y}{\sqrt{4x\kappa/R_o}} \qquad \text{(IV-8)}$$

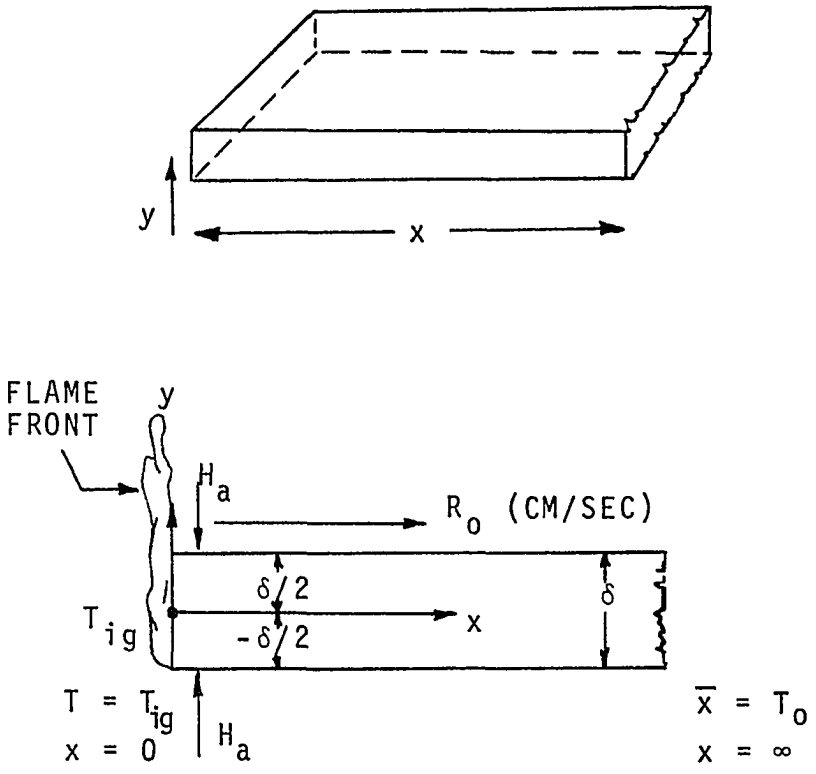

Figure IV-1. Schematic of Flame Propagation Model for Equation IV-6.

and:

$$\theta = \frac{T - T_{ig}}{T_o - T_{ig}} \qquad \text{(IV-9)}$$

Making these substitutions in Equation IV-6 yields:

$$\frac{d^2\theta}{d\eta^2} + 2\eta \frac{d\theta}{d\eta} = 0 \qquad \text{(IV-10)}$$

with boundary conditions:

$$\left.\frac{d\theta}{d\eta}\right|_{\eta=0} = 0 \qquad \eta = 0 \qquad \text{(IV-11a)}$$

$$\theta = 0 \qquad \eta = \infty \qquad \text{(IV-11b)}$$

$$\theta = 1 \qquad \eta = 0 \qquad \text{(IV-11c)}$$

Equation IV-10 with the boundary conditions given by Equations IV-11 has a solution of:

$$\theta = 1 - \text{erf}\ \eta \qquad \text{(IV-12)}$$

or, in terms of the original variables:

$$\frac{T - T_{ig}}{T_o - T_{ig}} = 1 - \text{erf}\ \frac{y}{\sqrt{4x\kappa/R_o}} \qquad \text{(IV-13)}$$

This equation gives the temperature distribution within the solid as a function of position and burning rate.

Since the heat being transferred into the solid at $y = \pm \delta/2$ is of interest if Equation IV-13 is to be related to the ignition process, it is desirable to calculate:

$$k \left.\frac{\partial T}{\partial y}\right|_{y=\delta/2} = H_a - h(T-T_o) - \sigma\varepsilon T^4 \qquad \text{(IV-14)}$$

where H_a is the heat flux being absorbed by the solid at its surface, h is the convective heat transfer coefficient, ε is the emissivity of the solid, σ is the Stefan-Boltzmann constant, and T is the temperature of the solid. The H_a above is assumed equal to the absorbed heat flux from the ignition test.

Since the values for h and ε were not known, Equation IV-14 was rewritten using a retained energy concept as:

$$H_R = H_a - h(T-T_o) - \sigma\varepsilon T^4 \qquad \text{(IV-15)}$$

where H_R is the retained energy in the sample. Therefore, Equation IV-14 becomes

$$k \left.\frac{\partial T}{\partial y}\right|_{y=\delta/2} = H_R \qquad \text{(IV-16)}$$

Equation IV-16 may be written as:

$$\left.\frac{\partial \theta}{\partial y}\right|_{y=\delta/2} = \frac{-H_R}{\Delta T_{ig} k} \qquad \text{(IV-17)}$$

Taking the desired derivatives of Equation IV-12, i.e., $\partial\theta/\partial y$, yields:

$$\frac{\partial \theta}{\partial y} = \frac{\partial \theta}{\partial \eta}\frac{\partial \eta}{\partial y} = \frac{-2}{\sqrt{\pi}} e^{-\eta^2} \frac{\partial \eta}{\partial y} \qquad \text{(IV-18)}$$

but from Equation IV-8

$$\frac{\partial \eta}{\partial y} = \frac{1}{(4\kappa x/R_o)^{1/2}} \qquad \text{(IV-19)}$$

Therefore, upon substituting Equation IV-19 into Equation IV-18, the result is

$$\frac{\partial\theta}{\partial y} = \frac{-2}{\sqrt{\pi}} e^{-y^2 R_o/4\kappa x} \left[\frac{1}{(4\kappa x/R_o)^{1/2}}\right] \qquad \text{(IV-20)}$$

Applying the boundary condition of Equation IV-17 to Equation IV-20, the result is

$$\frac{H_R}{k\Delta T_{ig}} = \frac{2}{\sqrt{\pi}} \left[\frac{1}{(4\kappa x/R_o)^{1/2}}\right] e^{-\delta^2 R_o/(16\kappa x)} \qquad \text{(IV-21)}$$

Equation IV-21 can be solved for the retained flux, H_R, at the surface $y = \delta/2$, as

$$H_R = \Delta T_{ig} \left[\frac{k\rho c_p R_o}{\pi x}\right]^{1/2} e^{-\delta^2 R_o/16\kappa x} \qquad \text{(IV-22)}$$

where ΔT_{ig} is the temperature rise at the surface at the instant of ignition in °C, δ is the thickness of the sample, cm, k is the thermal conductivity, cal/cm-sec-°C, ρ is the density, gm/cm^3, c_p is the heat capacity, cal/gm-°C, R_o is the horizontal burning rate, cm/sec, κ is the thermal diffusivity, cm^2/sec, and x and y are spatial coordinates, cm.

The retained flux at the surface, as a function of length along the sample, has been calculated according to Equation IV-22 for representative materials included in this study. Nine representative graphs of the retained flux, H_R, versus the length coordinate, x, are presented in Figure IV-2 through IV-10. The tabulated values of the properties of these nine samples are presented in Table IV-2. Table IV-3

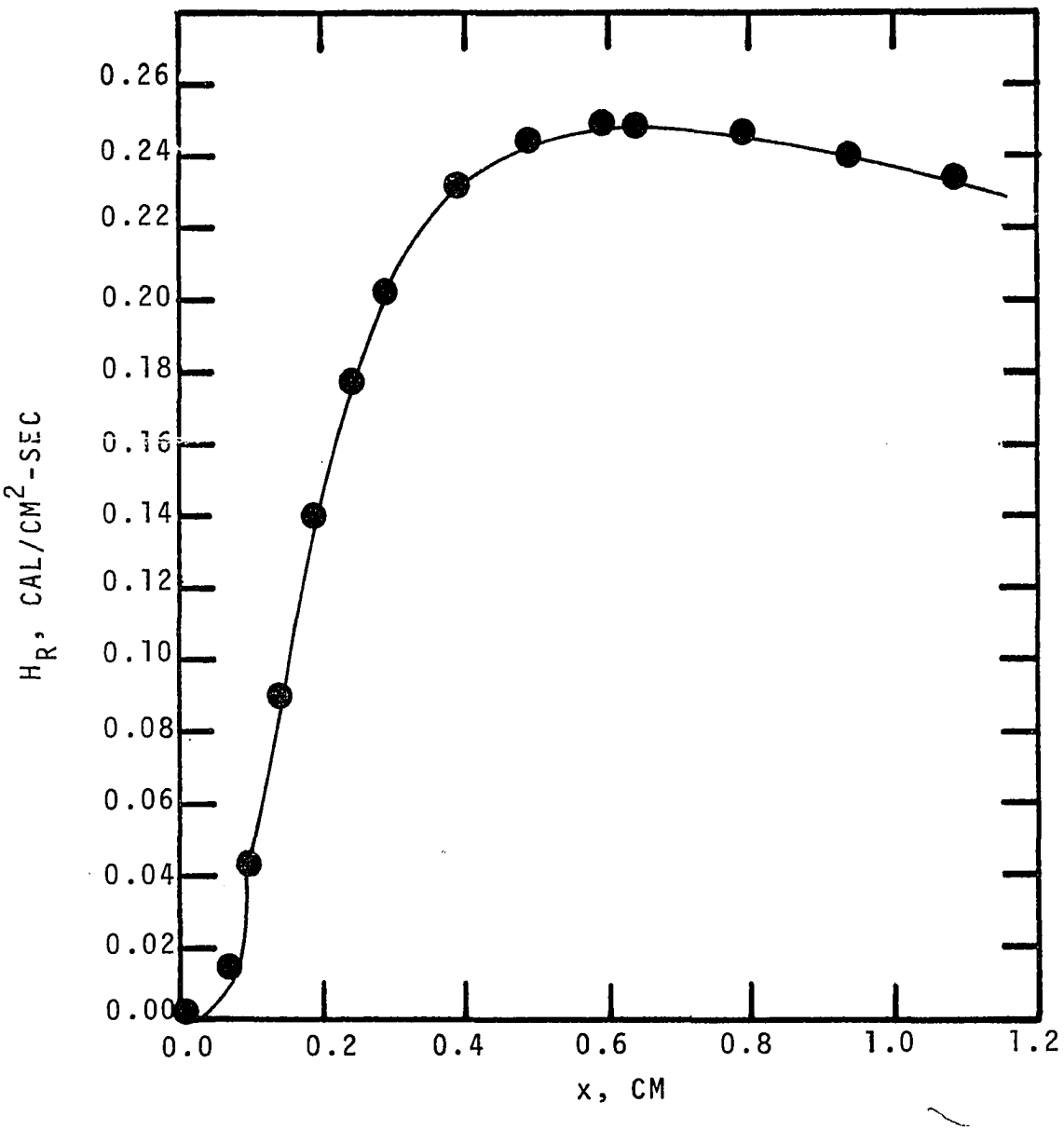

Figure IV-2. The Variation of the Retained Energy with Distance Along the Surface for Balsa, B3/32-11.

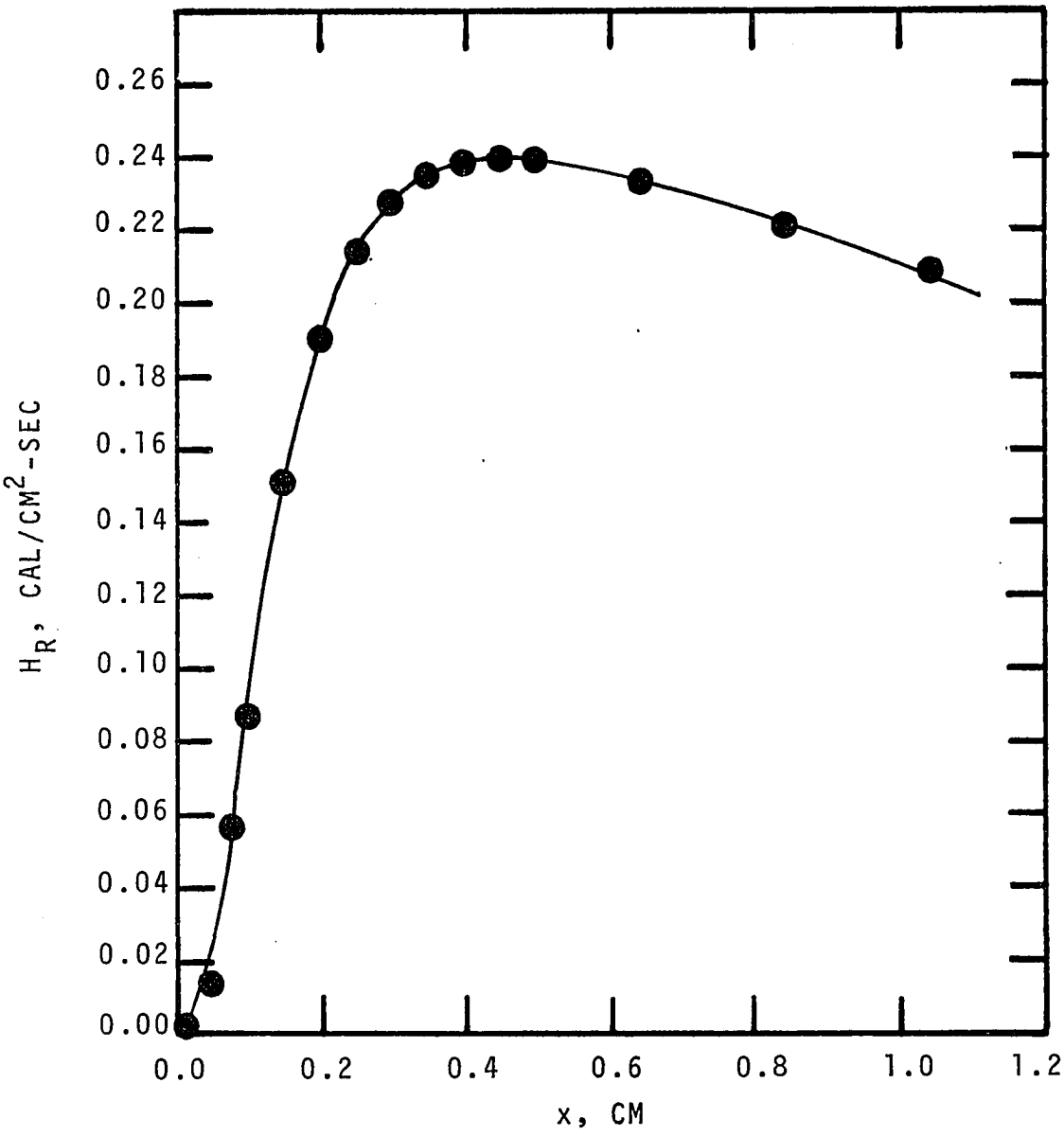

Figure IV-3. The Variation of the Retained Energy with Distance Along the Surface for Balsa, B1/16-4.

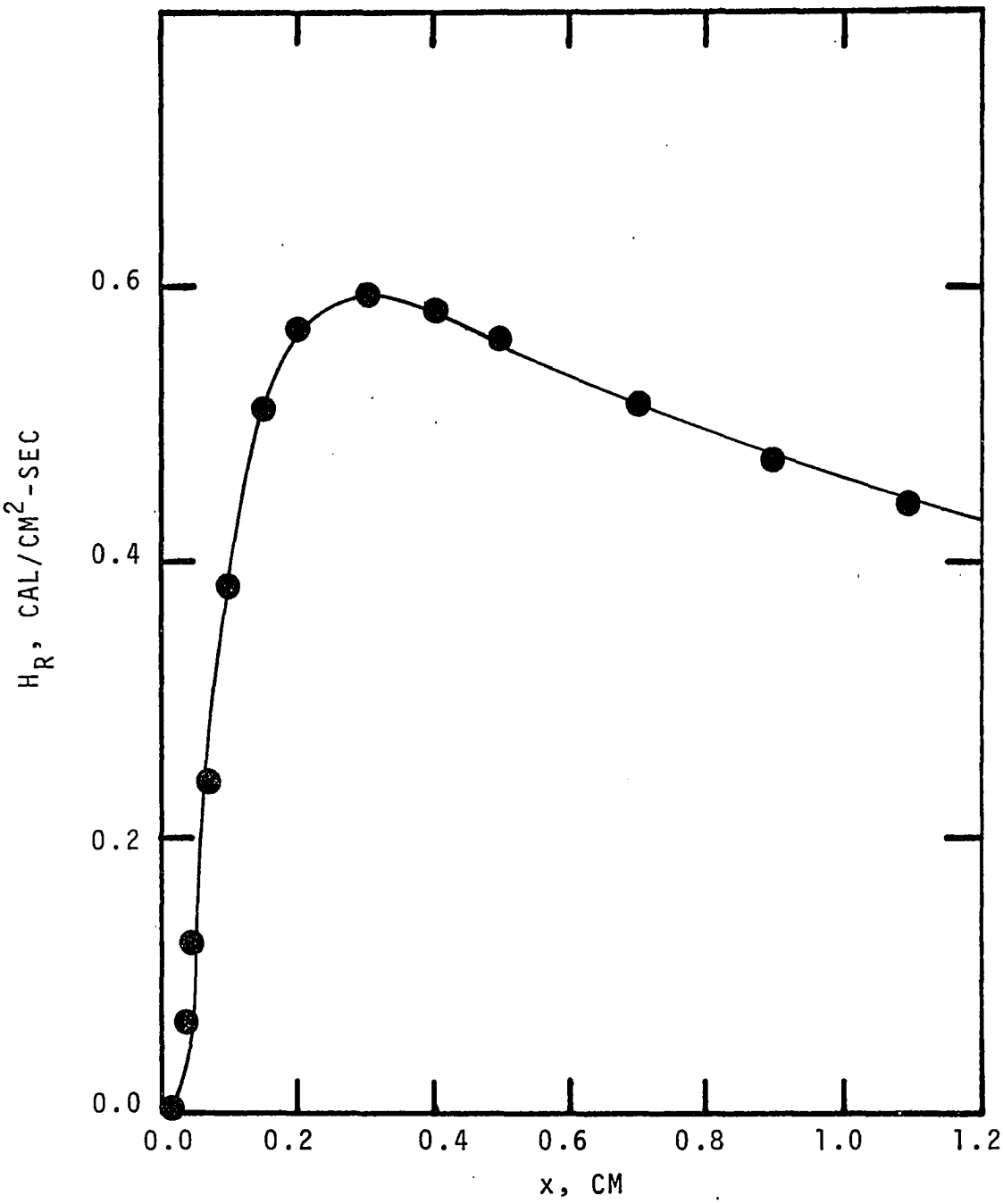

Figure IV-4. The Variation of the Retained Energy with Distance Along the Surface for Redgum, G-1.

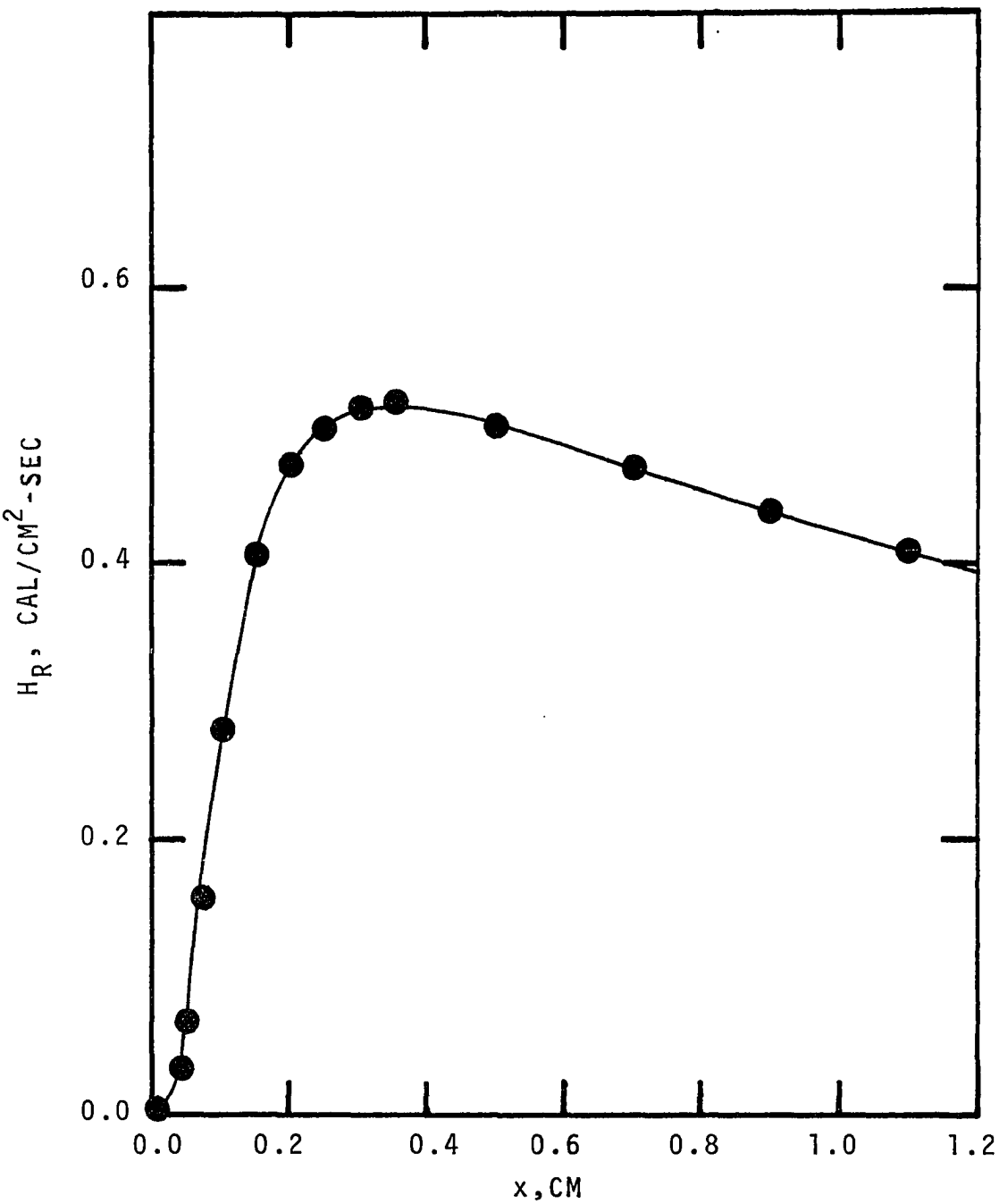

Figure IV-5. The Variation of the Retained Energy with Distance Along the Surface for Oak, O-2.

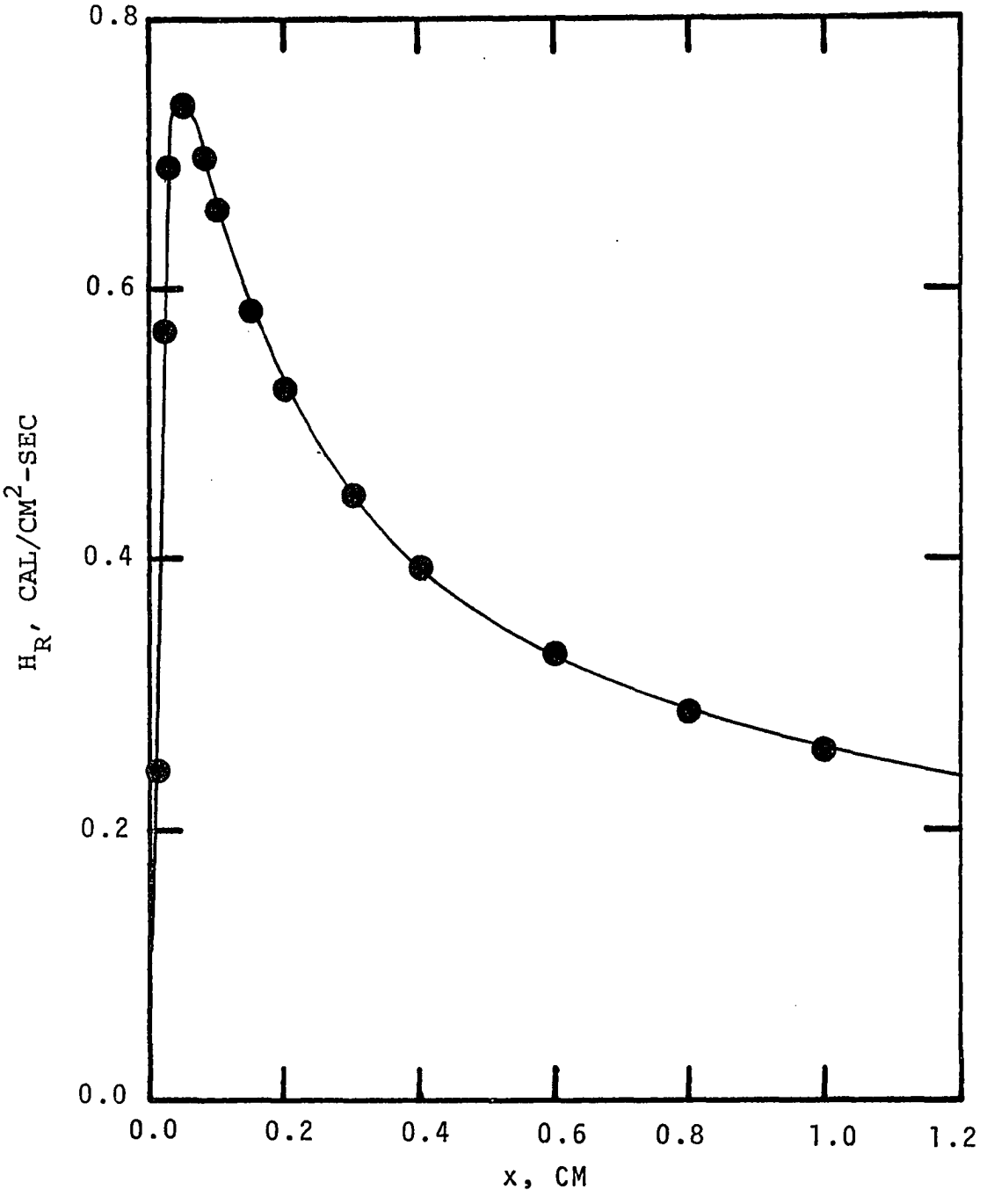

Figure IV-6. The Variation of the Retained Energy with Distance Along the Surface for Nylon Fabric, N-7.

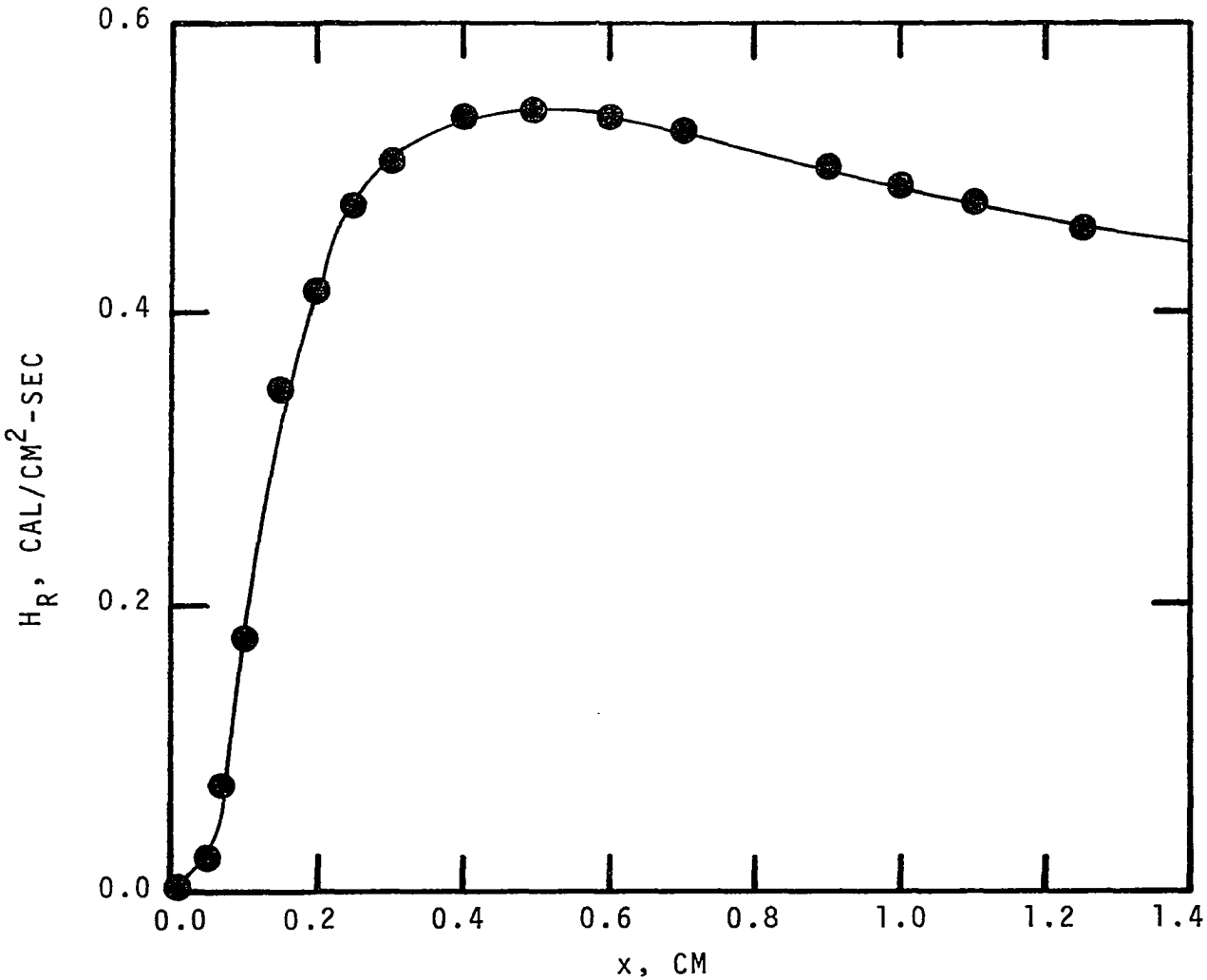

Figure IV-7. The Variation of the Retained Energy with Distance Along the Surface for Vinyl Fabric, V-5.

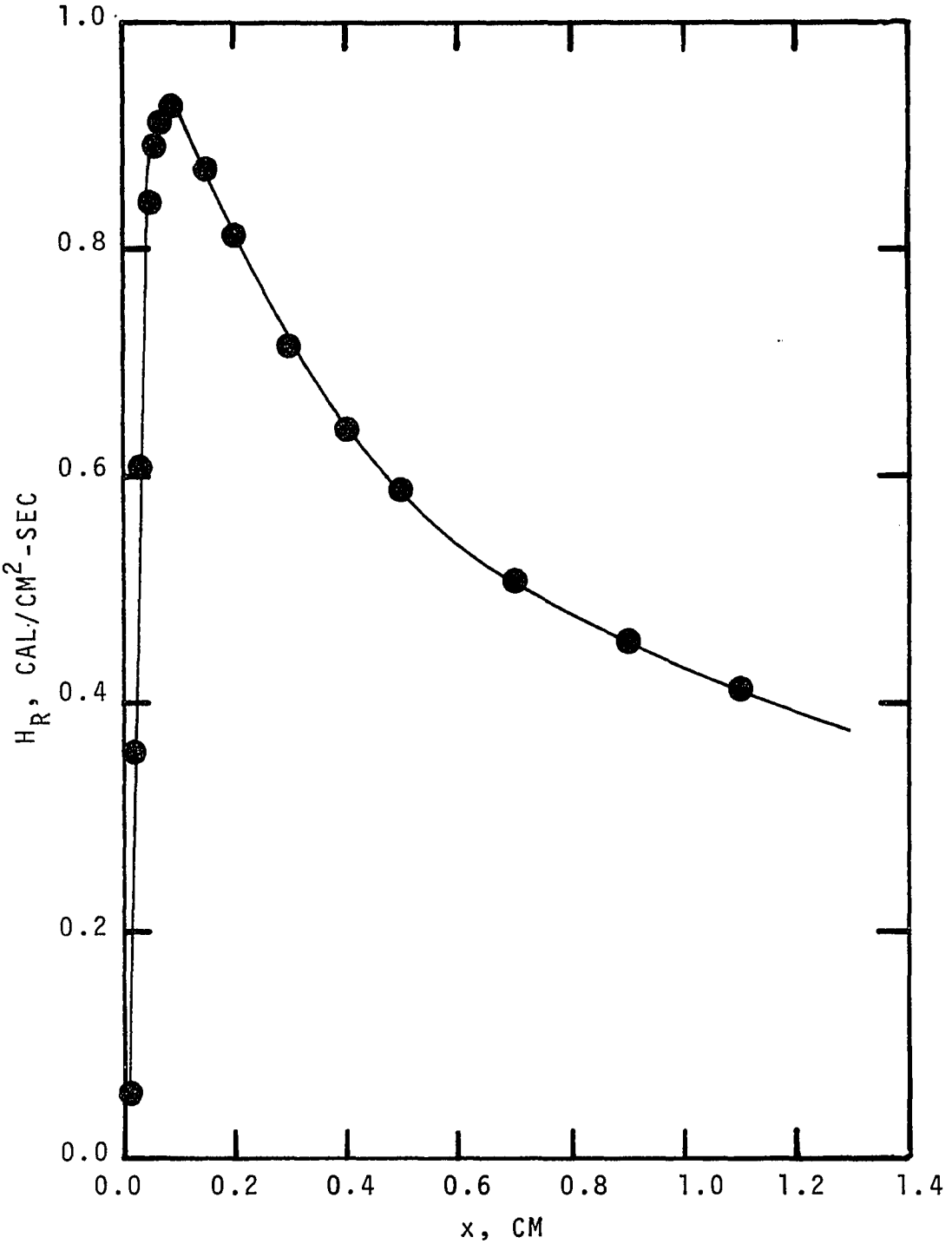

Figure IV-8. The Variation of the Retained Energy with Distance Along the Surface for Cotton Fabric, CT-1.

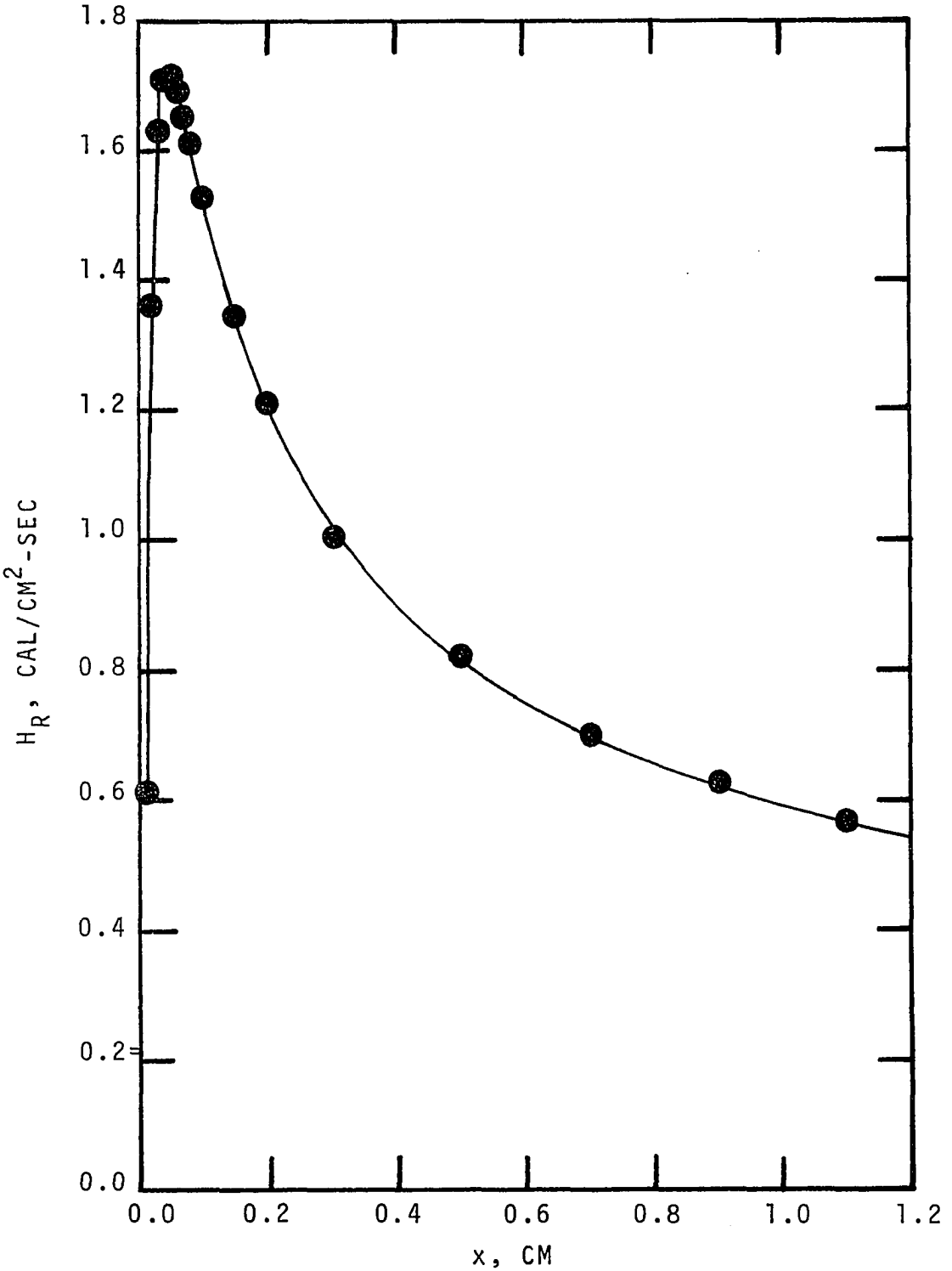

Figure IV-9. The Variation of the Retained Energy with Distance Along the Surface for Whatman Filter Paper, FP-2.

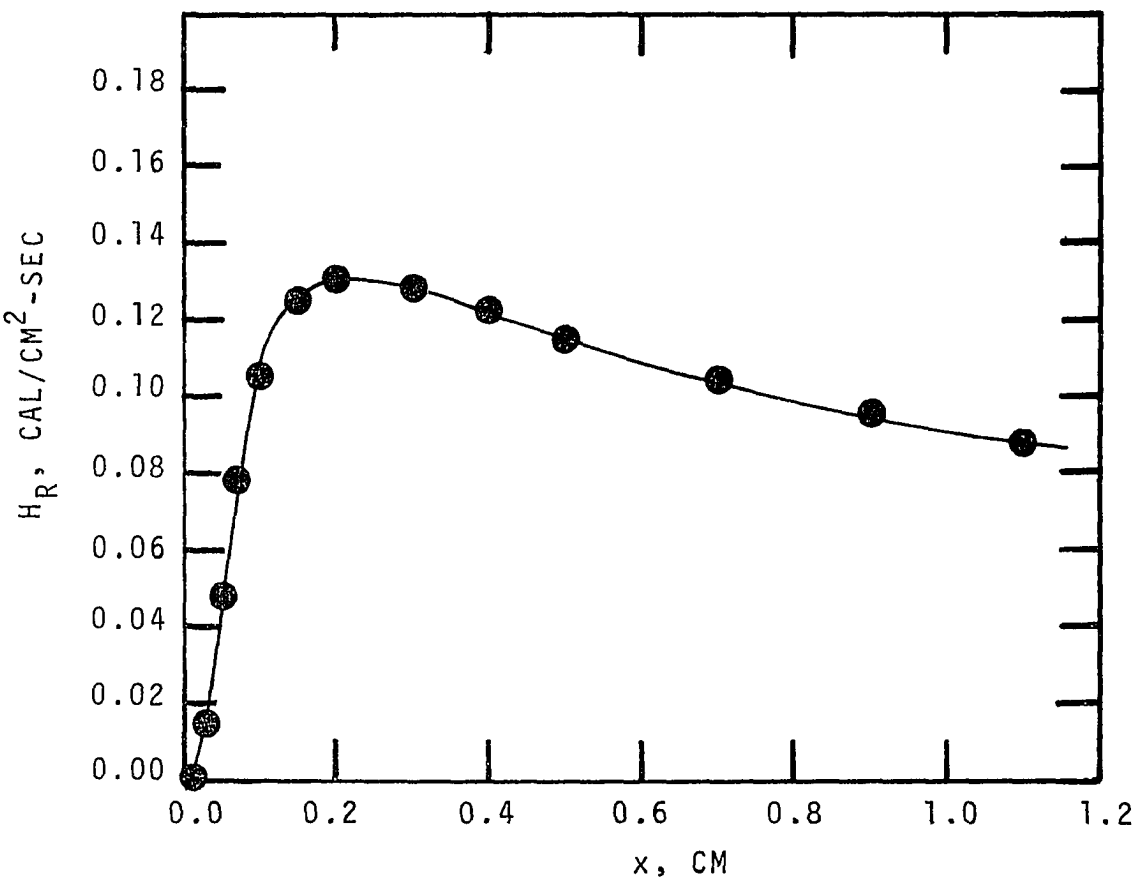

Figure IV-10. The Variation of the Retained Energy with Distance Along the Surface for Nylon Carpeting, C-1.

TABLE IV-2

VALUES USED TO CALCULATE H_R FOR FIGURES IV-2 THROUGH IV-10

Sample	v cm/sec	ρ gm/cc	δ cm	c_p cal/gm°C	$\kappa \times 10^3$ cm^2/sec	ΔT_{ig}* °C
Balsa 1/32-11	0.202	0.211	0.236	0.34	2.20	385
Balsa 1/16-4	0.428	0.0994	0.162	0.34	3.08	385
Gum-1	0.189	0.390	0.152	0.34	1.83	385
Oak-2	0.0629	0.711	0.270	0.34	1.64	365
Nylon-7	0.0457	0.356	0.113	0.40	1.53	395
Vinyl-5	0.181	0.780	0.119	0.40	0.667	320
Cotton-1	0.155	0.540	0.066	0.34	0.953	361
Filter paper-2	0.273	0.470	0.038	0.34	1.06	399
Nylon carpet-1	0.0224	0.174	0.394	0.40	1.94	395

*Taken from References 5, 25.

TABLE IV-3

SUMMARY OF PROPERTIES OF SAMPLES

Material	Range of Thickness δ, cm	Ignition Temp.* T_{ig}, °C	Average Thermal Diffusivity, κ cm^2/sec	Heat Capacity c_p, cal/gm-°C	Density Range ρ, gm/cm^3
Nylons	0.06-0.12	420	14.4×10^{-4}	0.40	0.36-0.61
Vinyls	0.05-0.14	345	6.65×10^{-4}	0.40	0.67-1.05
Cottons	0.036-0.066	386	9.43×10^{-4}	0.34	0.53-0.564
Filter papers	0.010-0.04	424	10.6×10^{-4}	0.34	0.46-0.735
Nylon carpet	0.32-0.47	420	18.25×10^{-4}	0.40	0.174-0.230
Balsa	0.147-0.24	410	24.3×10^{-4}	0.34	0.099-0.21
Redgum	0.15-0.21	410	18.5×10^{-4}	0.34	0.37-0.39
Ash	0.24-0.34	390	16.95×10^{-4}	0.34	0.57-0.60
Oak	0.24-0.28	390	16.5×10^{-4}	0.34	0.65-0.72

*References 5, 25.

presents a summary of the properties of all the materials used in calculating Equation IV-22.

In order to compute the retained energy, H_R, in Equation IV - 22, it is necessary to know ΔT_{ig}, the temperature rise to ignition, from an independent source. The values for the T_{ig} for the materials studied here were obtained based on thermogravimetric analysis by Brown (5) and Rangaprasad (25) by arbitrarily assuming that the ignition temperature, T_{ig}, would be equal to the temperature at which the rate of weight loss reached a maximum given a 20°C/min heating rate. The values for the T_{ig} were assumed to be the same within a given class of materials (e.g., all balsa materials were assigned the same T_{ig} value, 410°C). The values for the ΔT_{ig} (= T_{ig} - 25.0°C) are listed in Table IV-2.

From Figures IV-2 through IV-10, it can be seen that the retained heat flux, H_R, increases rapidly to a maximum value and then drops off exponentially as the distance, x, from the flame increases. At first glance, one might think that H_R should have its maximum at x = 0. However, this premise is incorrect. If Equation IV- 15 is closely examined, the behavior of Equation IV-22 as shown by Figures IV-2 through IV-10, becomes evident. In Equation IV -15, H_a, the absorbed flux, increases as the distance of the surface from the flame decreases; however, T, the temperature of the solid, also increases as distance to the flame decreases. Hence, the energy loss terms, $h(T - T_o)$ and εT^4, increase rapidly as the flame

is approached. The net result is that H_R, the retained energy, tends to zero as $x \to 0$. The peaks in Figures IV-2 through IV-10 occur as a result of a rapid decrease in the solid temperature, T, as x increases. The absorbed flux, H_a, decreases as x increases, but not nearly as rapidly as T decreases. In fact, from Equation IV-13, it can be seen that at $x = \delta^2 R_o/0.8\kappa$, corresponding to $\eta = 0.05$, the temperature, T, will be within 5 percent of the value of T_o. If $\delta \simeq 10^{-1}$ cm, $R_o \simeq 10^{-1}$ cm/sec and $\kappa \simeq 10^{-3}$ cm^2/sec, then x will be given by $x \simeq 1.0$ cm. At $T \simeq T_o$, the loss terms will be approximately zero; but with such a small change in x, i.e., $\Delta x \simeq 1.0$ cm, H_a will decrease negligibly and the resulting value of H_R will increase rapidly. Thus a peak will occur, after which the value of H_R will then decrease as x increases because H_a decreases.

The position of the peak depends on the physical and thermal properties. The very rapid peaking obtained with nylon-7, cotton-1, and filter paper-2 samples appears to be attributable to the combination of low thermal diffusivity, κ, small thickness, δ, and a relatively high ignition temperature which leads to a high ΔT_{ig}.

Equation IV-22 does not solve the problem of being unable to define a unique energy (either $H_a t_{ig}$ or $H_R t_{ig}$); for, although H_R can now be calculated independently of t_{ig}, it has become a function of position x, about which nothing is known in relation to the burning process. Hence, there has been a trade off of variables, x for t_{ig}, and another approach is needed.

As can be seen from Equation IV-22, it is necessary to know the burning rate, R_o, in order to calculate the retained energy, H_R, as a function of position. At the outset, it was stated that the purpose of this work was to understand the burning process better and to attempt to model that process. The assumptions made and the boundary conditions used in obtaining Equation IV-22 appear to be valid, but the equation does not allow prediction of burning rates from easily obtainable data. However, Equation IV-22 does suggest certain variables which are important to the burning process. These variables are density, ρ; heat capacity, c_p; thermal diffusivity, κ; thickness, δ; temperature rise to ignition, ΔT_{ig}; and retained energy, H_R, which is related to the absorbed flux, H_a, from the ignition test. A dimensional analysis using the Buckingham Pi method was performed on the variables using the slope, s*, instead of H_a. This method was used because data for the slope, s*, were available and the exact value of H_a required to propagate the flame was not known. Two dimensionless groups resulted from this analysis; see Appendix D. They are:

$$\Pi_1 = \frac{R_o \delta}{\kappa} \qquad \text{(IV-23)}$$

$$\Pi_2 = \frac{s^*}{\sqrt{\kappa}\rho c_p \Delta T_{ig}} \qquad \text{(IV-24)}$$

These groups were then combined into an equation as follows:

$$\frac{R_o \delta}{\kappa} = K \left[\frac{s^*}{\sqrt{\kappa}\rho c_p \Delta T_{ig}}\right]^a \qquad \text{(IV-25)}$$

where K is dimensionless constant. Equation IV-25 was then rewritten as:

$$R_o = K(s^*)^a \ (\kappa)^{-a/2} \ (\rho c_p)^{-a} \ (\Delta T_{ig})^{-a} \ \kappa \ \delta^{-1} \qquad \text{(IV-26)}$$

which can be reduced to:

$$R_o = K(s^*)^a \ (\kappa)^{1-(a/2)} \ (\rho c_p)^{-a} \ (\Delta T_{ig})^{-a} \ \delta^{-1} \qquad \text{(IV-27)}$$

Equation IV-27 suggests that R_o may be written in functional form as:

$$R_o = f[(s^*)^a \ (\kappa)^b \ (\rho c_p)^c \ (\delta)^d \ (\Delta T_{ig})^e] \qquad \text{(IV-28)}$$

However, the ignition temperature, as obtained from thermal gravimetric analysis (5, 25) of the samples showed that ΔT_{ig} was approximately a constant for the materials under consideration. Therefore, Equation IV-28 was reduced to:

$$R_o = f[(s^*)^a \ (\kappa)^b \ (\rho c_p)^c \ (\delta)^d] \qquad \text{(IV-29)}$$

and a product form of the equation was assumed such that:

$$R_o = Cs^{*a}\kappa^b(\rho c_p)^c\delta^d \qquad \text{(IV-30)}$$

where C is a constant. Equation IV-30 was then rewritten in logarithmic form as:

$$\ln R_o = \ln C + a \ln s^* + b \ln \kappa + c \ln (\rho c_p) + d \ln \delta \qquad \text{(IV-31)}$$

Equation IV-31 was used to perform a multi-regression analysis on the data for the 87 samples. The data used to perform the analysis are tabulated in Table A-2, Appendix A. A statistical analysis of the data was incorporated into the regression analysis computer program which checked the data for bad data points and which performed a t-test on each variable versus the burning rate, R_o. If the t value was less than 2, the variable under consideration was assumed negligible in correlating the data and was subsequently deleted from the analysis. The statistical tests used and the justification for them are presented in Appendix C.

The equations resulting from the regression analysis of the data, are, for all wood samples considered together:

$$R_o = (2.69 \times 10^{-6})(\rho c_p)^{-0.95} (s^*)^{-1.14} (\delta)^{-0.30} \times (\kappa)^{-1.55} \qquad \text{(IV-32a)}$$

for the nylon, vinyl, and cotton cloths, the filter papers and nylon carpeting:

$$R_o = (3.32 \times 10^{-9})(\rho c_p)^{-1.0} (s^*)^{0.096} (\delta)^{-0.825} \times (\kappa)^{-1.96} \qquad \text{(IV-32b)}$$

It was found that the wood data and the fabric, carpet and paper data gave good correlations with only the slope, s*. The exponents obtained for s* were about 2.5 for both the above sets of data. Therefore, it would seem possible to correlate burning rate data with ignition data alone. When

all the data (i.e., woods, fabrics, carpeting and paper) were collapsed into one correlation, the t-test described in Appendix C was applied to the correlating variables (ρc_p, δ, s*, and κ) and the value of t was found to be less than 2 for all the correlating variables except s*. Hence, the general correlation considering all 87 samples became:

$$R_o = 2.12\ (s^*)^{-2.44} \qquad \text{(IV-32c)}$$

The units in Equations IV-32 are cm/sec for R_o, gm/cm^3 for ρ, cal/gm-°C for c_p, cal/cm^2-sec$^{1/2}$ for s*, cm for δ, and cm^2/sec for κ. Equations IV-32 are plotted in Figures IV-11 through IV-13, as experimental R_o versus calculated R_o. The dashed lines on each figure are the 95 percent confidence limits. The correlation coefficient is also shown on each of these figures.

The above results would seem to substantiate the original assumption that was made at the outset; that the burning process could be related to the ignition process. Equations IV-32a and b do precisely this. It is instructive to examine Equations IV-32. Comparing Equations IV-32a and IV-32b, it can be seen that the power on the slope based on ignition data appears in Equation IV-32a as negative and in Equation IV-32b as positive, while all other variables maintain the same sign on the exponent in the two equations. This result is a consequence of the regression analysis technique used. No functional form other than that given by Equation

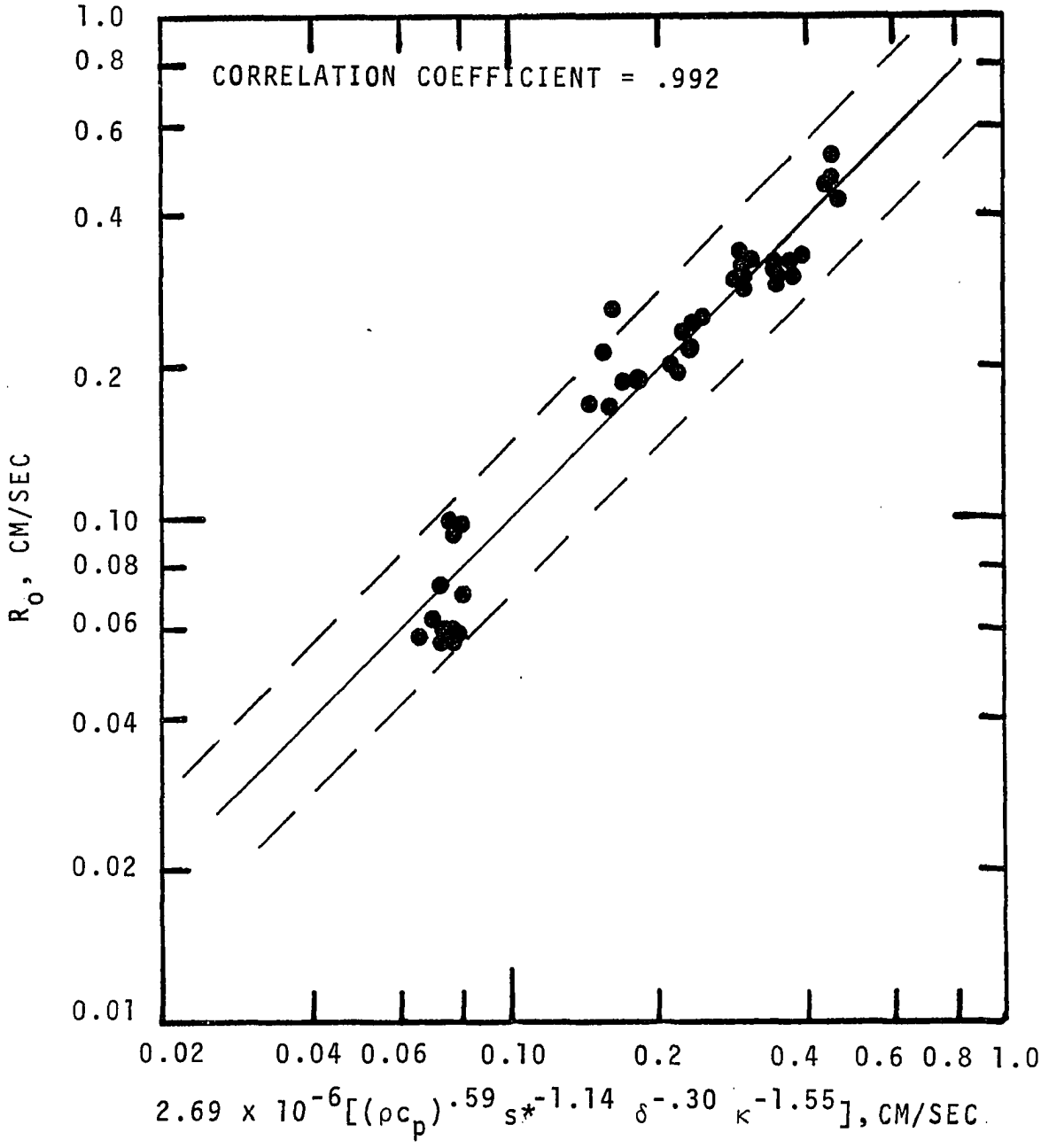

Figure IV-11. Comparison of Experimental Burning Rates with Burning Rates Calculated by Equation IV-32(a) for Woods.

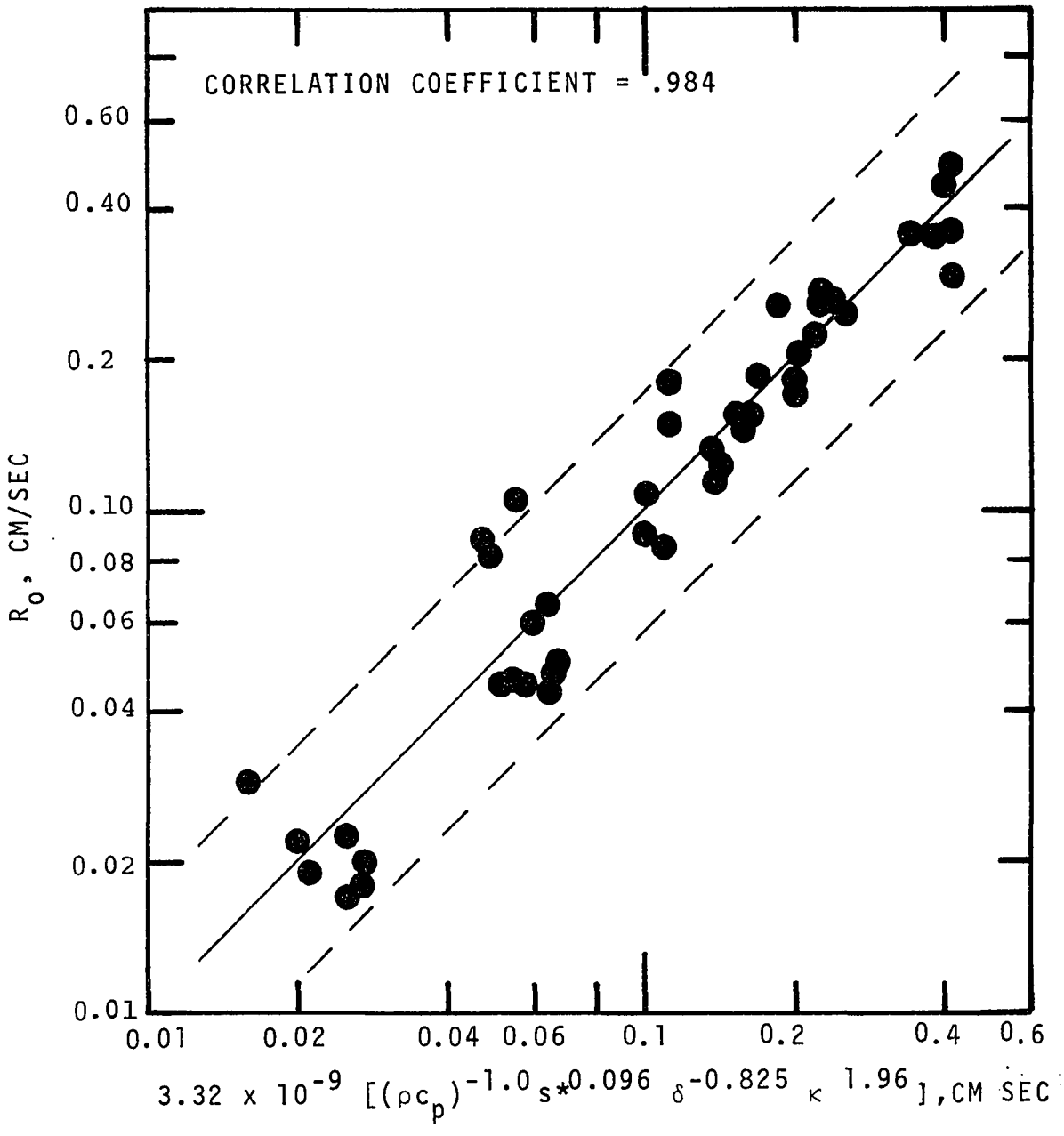

Figure IV-12. Comparison of Experimental Burning Rates with Burning Rates Calculated by Equation IV-32(b) for the Fabrics, Carpeting and Filter Papers.

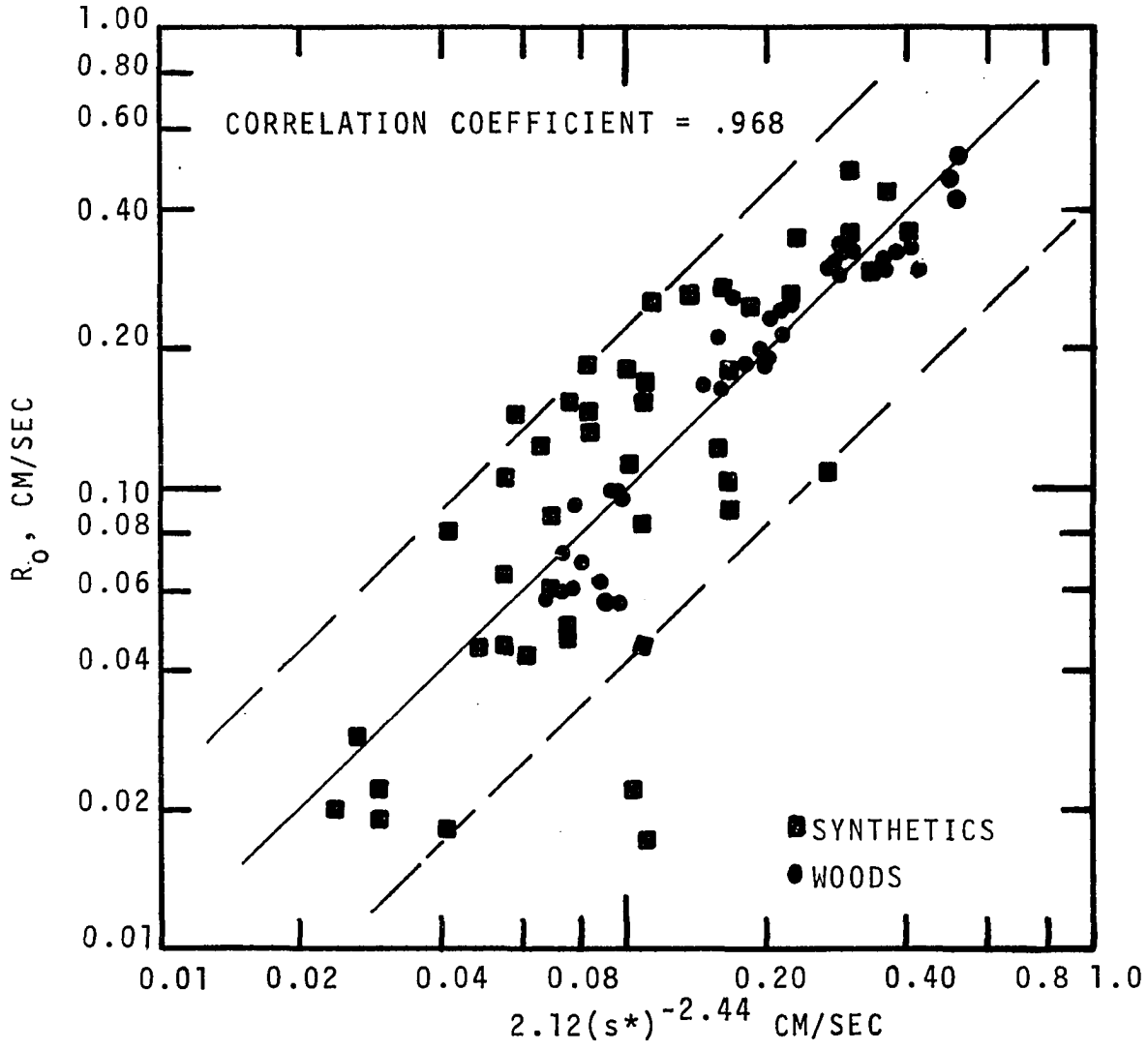

Figure IV-13. Comparison of Experimental Burning Rates with Burning Rates Calculated by Equation IV-32(c) for All Samples Considered Together.

IV-28 was assumed, so that the exponents that were calculated were not restricted in any way.

From Equation IV-32c, it is seen that for a generalized correlation including all the materials used in this study, that only the slope, s*, or $H_a\ t_i$ which derives from the ignition measurements, is an important correlating parameter. The basic premise of this work, then, has been demonstrated. The horizontal burning rate data for diverse thin materials obtained from burning samples in the MFMVSS 302 Horizontal Burning Rate test can be correlated using the ignition behavior of the material. These correlations can also be used to predict burning rates of new materials if ignition data are available.

As a final point, it is to be emphasized that the ignition data used throughout this study were obtained from one-sided ignitions. In reality, two-sided ignition (simultaneous irradiation from both sides) would probably be more applicable for burning rate correlations. Finally, it would be desirable to have retained energy, H_R, as a function of ignition time since the retained energy is more pertinent than the absorbed energy, H_a.

Other Correlation Attempts

Although previous attempts to correlate the horizontal burning rate against the material weight per unit area for each class of materials were quite unsatisfactory (36), it

might be instructive to demonstrate the adequacy of this correlation, here. Both the data obtained previously (36) and the data obtained in this study will be employed in the following relationship:

$$R_o = C\, w_o^{a} \qquad \text{(IV-33)}$$

The same regression technique that was used in obtaining Equations IV-32 was also employed in the calculation of the constant C and the power, a, on w_o for Equation IV-33. All the wood samples were used to obtain a correlation, Equation IV-34a; all fabrics (nylon, vinyl, cotton), nylon carpet and filter paper were used to obtain a second correlation, Equation IV-34b; and then all 87 samples were used to obtain a third correlation, Equation IV-34c. These equations are:

For woods:

$$R_o = (1.84 \times 10^{-2})\, w_o^{-0.80} \qquad \text{(IV-34a)}$$

For fabrics, etc.:

$$R_o = (7.81 \times 10^{-3})\, w_o^{-0.80} \qquad \text{(IV-34b)}$$

For all samples considered together:

$$R_o = (1.63 \times 10^{-2})\, w_o^{-0.70} \qquad \text{(IV-34c)}$$

The units in Equations IV-34 are cm/sec for R_o and gm/cm^2 for w_o.

Equations IV-34 are plotted in Figures IV-14 through IV-16 as experimental R_o versus calculated R_o. The dashed lines on each figure are the 95 percent confidence limits. The correlation coefficients are shown on the figures.

Comparison of Figures IV-11 through IV-13 with Figures IV-14 through IV-16 reveals that indeed the correlational technique employing the ignition data does correlate the data much better than simply using the material weight. Although, for woods, either correlation yields approximately equivalent results, Equation IV-32b predicts R_o much better than Equation IV-34b for the fabrics, carpets, and paper, and Equation IV-32c has a very marked improvement over Equation IV-34c in predicting burning rates over a very wide range of materials.

Equations IV-32a and IV-32b have been used to predict R_o from the values of s^*, ρc_p, κ, and δ for the six balsa samples and three nylon fabric samples listed in Table IV-1. The predicted values of R_o are listed in Column 6 and the experimental values in Column 7 of Table IV-4. It can be seen that agreement between the calculated value and the predicted value is quite close for woods and within a factor of two for the nylons. If one examines Figure IV-12, it can be seen that the confidence limits indicate that the burning rate can be predicted within a factor of two of the true value. Hence, the predicted values in Table IV-3 are well within these limits.

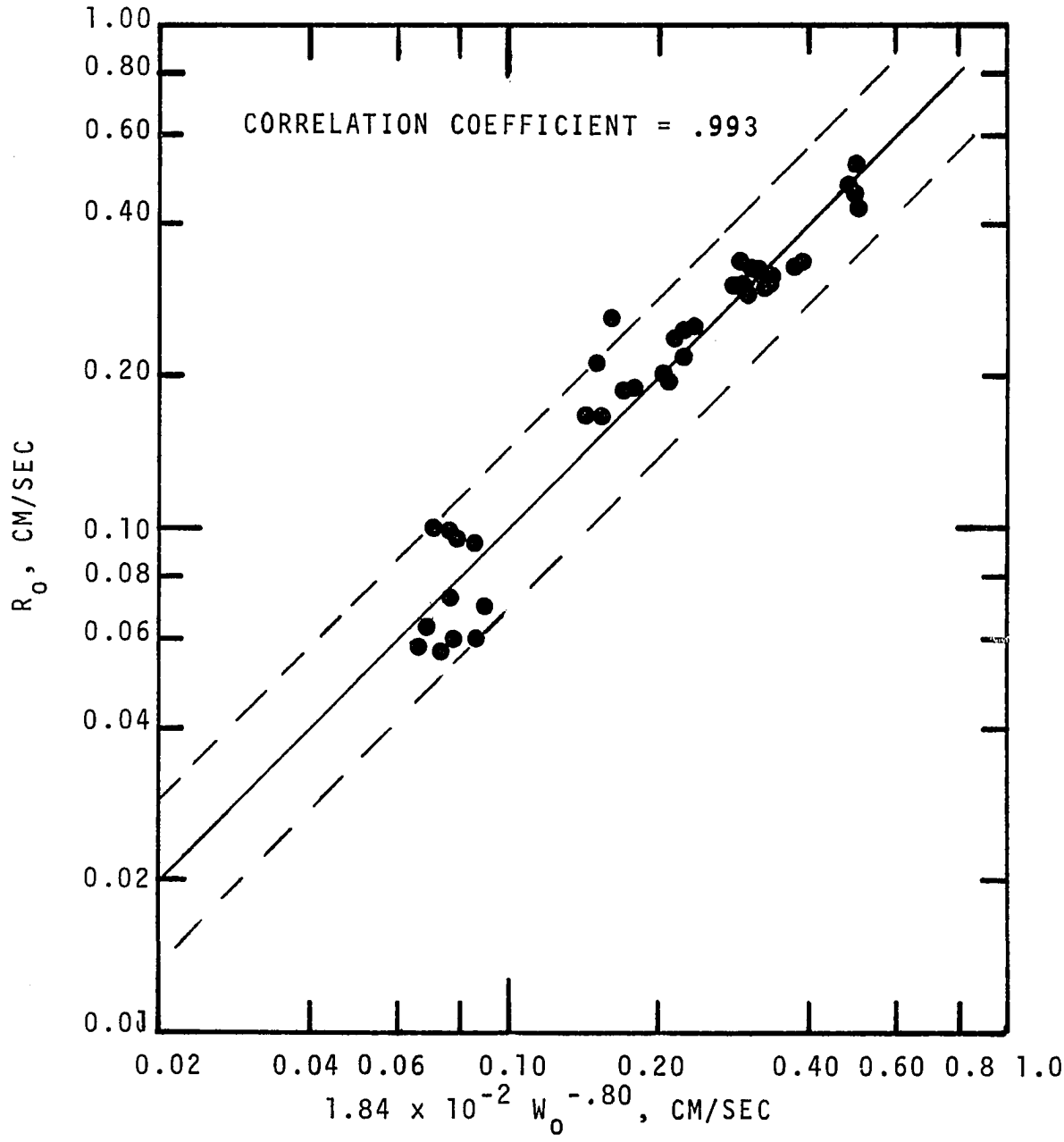

Figure IV-14. Comparison of Experimental Burning Rates with Burning Rates Calculated by Equation IV-34(a) for the Woods.

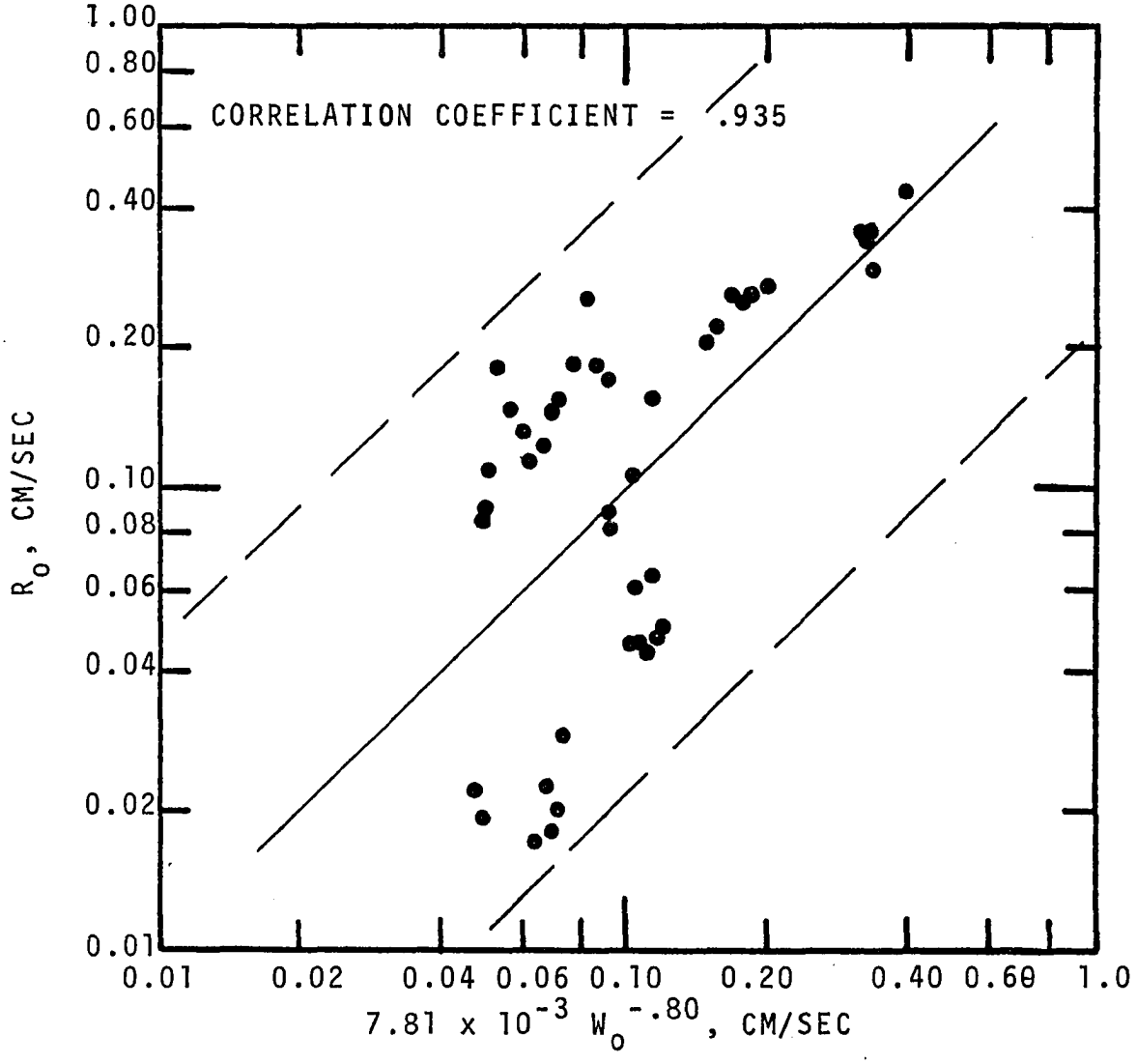

Figure IV-15. Comparison of Experimental Burning Rates with Burning Rates Calculated by Equation IV-34(b) for the Fabrics, Carpets and Filter Papers.

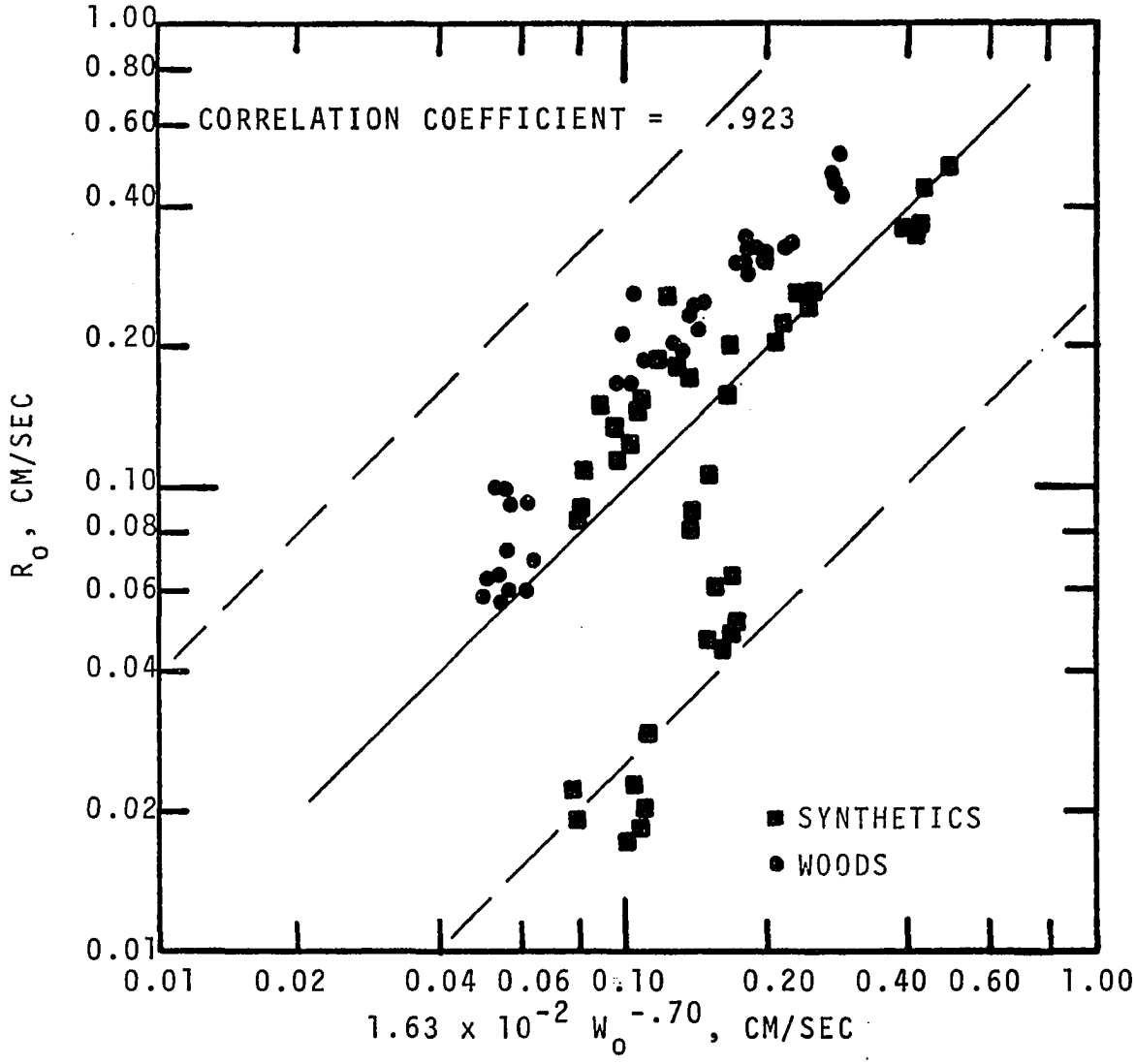

Figure IV-16. Comparison of Experimental Burning Rates with Burning Rates Calculated by Equation IV-34(c) for All the Samples Considered Together.

TABLE IV-4

COMPARISON OF EXPERIMENTAL AND CALCULATED BURNING RATES FOR SELECTED MATERIALS

Sample	ρc_p g/cm^3	Slope $cal/cm^2\text{-}sec^{1/2}$	$\kappa \times 10^3$ cm^2/sec	δ cm	R_o calc cm/sec by Eqs.IV-32(a,b)	R_o exper cm/sec
1/32" Balsa						
B1/32-1	0.0432	1.445	2.72	0.1016	0.647	0.642
B1/32-2	0.0432	1.430	2.72	0.1008	0.656	0.580
B1/32-3	0.0456	1.470	2.65	0.1006	0.628	0.672
B1/32-4	0.0398	1.400	2.83	0.1001	0.684	0.632
B1/32-5	0.0337	1.330	3.08	0.1006	0.741	0.799
B1/32-6	0.0396	1.400	2.68	0.1006	0.684	0.730
Nylon						
N-2	0.195	3.95	1.44	0.066	0.088	0.068
N-3	0.164	4.85	1.48	0.086	0.081	0.082
N-6	0.163	4.15	1.48	0.0915	0.076	0.0453

It would appear, therefore, that Equations IV-32a and IV-32b can be used to predict the horizontal burning rate for a thin material which is subjected to the MFMVSS 302 horizontal burning rate test from data on ignition, density, heat capacity, thermal diffusivity and thickness of the material. Care should be exercised in extrapolating these results beyond the range of values of physical and thermal properties used here.

CHAPTER V

SUMMARY

In recapitulation, the following points should be restated:

1. It has been successfully demonstrated that the horizontal burning rate of a thin material is related to the ignition characteristics of the material in a fundamental way.
2. It has been shown that Equations IV-32a - IV-32c can be used to predict the horizontal burning rate of a material within a factor of two for materials with physical and thermal properties within the range of values of those used in the development of the equations.
3. This study has demonstrated that the following variables (there may be others) affect the burning process: the product $H_a\sqrt{t^*}$ or s^*, which is derived from ignition data, the thermal diffusivity, the density, the heat capacity, the thickness, and the ignition temperature.
4. Caution should be exercised in applying Equations IV-32 to new situations. They were developed based on burning rate data obtained by use of the MFMVSS 302 horizontal burning rate test, and are <u>not</u> necessarily applicable to

other test procedures. However, the development leading up to Equations IV-32 should be applicable to results from other test methods; what is required is the determination of the appropriate calibration constant.

5. For some classes of materials, such as nylons and vinyls, the variation in the measured burning rates was no better than a factor of 2; in these cases, Equation IV-32 appears to be as reliable for predictions as the measured values.
6. The correlation of the burning rate in terms of ignition data could probably be improved by using retained energy, H_R, and two-sided ignition measurements, over the present technique of employing absorbed energy, H_a, based on one-sided ignitions.

NOMENCLATURE

A	area	cm^2
A,a	constant	dimensionless
B,b	constant	dimensionless
C,c	constant	dimensionless
C_F	calibration constant from Equation II-39	$cm/sec^{1/2}$
c_p	heat capacity	cal/gm-°C
D	flame depth	cm
d	constant	dimensionless
d_o	initial fuel thickness	cm
e	constant	dimensionless
e	exponential	dimensionless
erf	error function	dimensionless
erfc	complimentary error function	dimensionless
F	Froude number (Kt/L^2)	dimensionless
f	mathematical function	dimensionless
H, H_i	incident irradiance	cal/cm^2-sec
H	heat of combustion	cal/gm
H_a	absorbed energy flux ($\bar{\alpha}H_i$)	cal/cm^2-sec
H_R	retained energy	cal/cm^2-sec

h	heat content of fuel	cal/gm
h	surface heat transfer coefficient	cal/cm^2-sec-°C
h_b	height of fuel bed	cm
$\vec{I}$	heat flux vector	cal/cm^2-sec
I_x, I_y, I_z	spatial scalar heat fluxes	cal/cm^2-sec
I_{ig}	heat flux at ignition	cal/cm^2-sec
I_p	propagating heat flux	cal/cm^2-sec
ierfc	integral of the complimentary error function	dimensionless
k	thermal conductivity of solid	cal/cm-sec-°C
k_g	thermal conductivity of gas	cal/cm-sec-°C
L	flame height	cm
M	moisture content of wood	dimensionless
Q	net heat absorbed per unit mass	cal/gm
Q_{ig}	heat of preignition	cal/gm
$\bar{Q}$	volumetric heat flux per unit area	cal-cm^3/cm^2
$\bar{Q}_{ig}$	volumetric heat flux/area at ignition	cal-cm^3/cm^2
R	flame propagation rate	cm/sec
R_o	horizontal burning rate	cm/sec
s^*	slope of the $\sqrt{t^*}$ versus $1/H_a$ line ($t_i \leq 10$ sec)	cal/cm^2-sec$^{1/2}$
T	temperature	
T_F	flame temperature (assumed = 982°C)	°C

T_{ig}	arbitrary ignition temperature of solid as derived from thermal gravimetric analysis	°C
$\overline{T}_{ig}$	integrated average temperature of the sample at ignition	°C
T_o	ambient temperature (assumed = 25°C)	°C
T_S	surface temperature	°C
t	time	sec
t_i, t_{ig}	ignition time	sec
V_f, V_g	volume of fuel and gas respectively	cm^3
W	weight of fuel burned	gm
w	fuel loading	gm/cm^2
w_b	width of fuel bed	cm
w_o	weight per unit area of solid	gm/cm^2
x,y,z	spatial distance	cm

Greek Letters

α	thermal conductivity	cal/cm-sec-°C
$\overline{\alpha}$	integrated average absorptance factor	dimensionless
δ	thickness of solid samples	cm
ε	effective heating number	dimensionless
κ	thermal diffusivity of solid	cm^2/sec
ρ	density of solid	gm/cm^3
ρ_f, ρ_g	density of fuel and gas, respectively	gm/cm^3

ρ_w	density of water at 20°C	gm/cm^3
ρ_{be}	bulk density	gm/cm^3
σ	particle surface to volume ratio	cm^{-1}
σ	standard deviation	dimensions of number for which calculated
η	dimensionless variable	dimensionless
θ	dimensionless temperature	dimensionless
θ_r	burning time	sec
ϕ_w	wind coefficient	dimensionless
ϕ_s	slope coefficient	dimensionless

BIBLIOGRAPHY

1. Blackshear, P. L., and Kanury, A. M. "On the Combustion of Wood. I: A Scale Effect in the Pyrolysis of Solids." Combustion Science and Technology, 2 (1970), 1-4.

2. Bowles, R. L., et al. "Control Chart Manual." Unpublished Report. B. F. Goodrich Chemical Company (March 1962).

3. Bowles, R. L., et al. "Multiple Correlation." 1st. ed. Unpublished Report. B. F. Goodrich Chemical Company (November 1962).

4. Brown, C. R. "Determination of the Ignition Temperatures of Solid Materials." Fuel, 14 (1935), 14.

5. Brown, L. E. "An Experimental and Analytic Study of Wood Pyrolysis." Ph.D. dissertation. University of Oklahoma, Norman, Oklahoma, 1972.

6. "Flammability of Automotive Interior Trim Materials--Horizontal Test Method--SAE J369." Society of Automotive Engineers Technical Report J369 (1969).

7. Fons, W. L. "Heating and Ignition of Small Wood Cylinders." Industrial and Engineering Chemistry, 4L (1950), 21-30.

8. Fons W. L.; Bruce, H. D.; and Pong, W. Y. "A Steady State Technique for Studying the Properties of Free-Burning Wood Fires." International Symposium on the Use of Models in Fire Research, Publication No. 786 (1961).

9. Fons, W. L.; Clements, H. B.; and George, P. M. "Scale Effects of Propagation Rate of Laboratory Crib Fires." Ninth Symposium (International) on Combustion, The Combustion Institute (1963), 860-866.

10. Frandsen, W. H. "Fire Spread Through Porous Fuels from the Conservation of Energy." Combustion and Flame, 16 (1971), 9-16.

11. Frandsen, W. H. "A Proposed Measurement of the Heat of Preignition of Fine Forest Fuels." Paper presented at Combustion Institute, Western States Section, Los Angeles (Spring 1968).

12. Frandsen, W. H., and Rothermel, R. C. "Measuring the Energy-Release Rate of a Spreading Fire." Combustion and Flame, 19 (1972), 17-24.

13. Goldsmith, A. "Flammability Characteristics of Vehicle Interior Materials." Final Report, Project J6152, IIT Research Institute, NHSB Contract No. FH-11-6892, Chicago (May 1969).

14. Havens, J. A. "Thermal Decomposition of Wood." Ph.D. dissertation. University of Oklahoma, Norman, Oklahoma, 1969.

15. Havens, J. A.; Welker, J. R.; and Sliepcevich, C. M. "Pyrolysis of Wood: A Thermoanalytical Study." Journal of Fire and Flammability, 2 (October 1971), 321-333.

16. Hilado, C. J. "Flammability Characteristics of Cellular Plastics." Industrial and Engineering Chemistry, 6, 3 (1967), 154-166.

17. Hilado, C. J. Flammability Handbook for Plastics. Stamford, Conn.: Technomic Publishing Co., 1969.

18. Hottel, H. C., and Williams, G. C. "The Modeling of Firespread Through a Fuel Bed." Tenth Symposium (International) on Combustion, The Combustion Institute (1965), 997-1007.

19. Kanury, A. M., and Blackshear, P. L. "On the Combustion of Wood. II: The Influence of Internal Convection on the Transient Pyrolysis of Cellulose." Combustion Science and Technology, 2 (1970), 5-9.

20. Kanury, A. M., and Blackshear, P. L. "Some Considerations Pertaining to the Problem of Wood-Burning." Combustion Science and Technology, 1 (1970), 339-355.

21. Koohyar, A. "The Ignition of Wood by Flame Radiation." Ph.D. dissertation. University of Oklahoma, Norman, Oklahoma, 1967.

22. MacLean, J. D. "Thermal Conductivity of Wood." Heating, Piping and Air Conditioning (July 1940), 459-464.

23. Magee, R. S., and McAlevy, R. F. "The Mechanism of Flame Spread." Journal of Fire and Flammability, 2 (October 1971), 271-297.

24. Murty, K. A., and Blackshear, P. L. "Pyrolysis Effects in the Transfer of Heat and Mass in Thermally Decomposing Organic Solids." Eleventh Symposium (International) on Combustion, The Combustion Institute (1966), 517-523

25. Rangaprasad, N. "The Piloted Ignition of Thin Materials." Ph.D. dissertation. Univeristy of Oklahoma, Norman, Oklahoma, 1972.

26. Robertson, A. F.; Gross, D.; and Loftus, D. "A Method for Measuring Surface Flammability of Materials Using a Radiant Energy Soruce." American Society for Testing Materials. Proceedings, 56 (1956), 1437-1453.

27. Rothermel, R. C. "An Examination of Radiation's Role in Rate of Fire Spread in Wildland Fuels." M. S. thesis. Colorado State University, Fort Collins, Colorado, 1971.

28. Rothermel, R. C. "A Mathematical Model for Predicting Fire Spread in Wildland Fuels." U.S. Dept. of Agriculture, Forest Service Research Paper INT-115, Ogden, Utah (1972).

29. Rothermel, R. C., and Anderson, H. E. "Fire Spread Characteristics Determined in the Laboratory." U.S. Department of Agriculture, Forest Service Research Paper INT-30, Ogden, Utah (1966).

30. Rothermel, R. C.; Frandsen, W. H.; and Philpot, C. W. "Recent Advances on the Fire Spread Model." Paper presented at Combustion Institute, Missoula, Montana (April 1971).

31. Simms, D. L. "The Correlation of Ignition Time with the Physical Properties of Material, Part I. Spontaneous Ignition of Cellulosic Materials." Fire Research Note No. 319, Joint Fire Research Organization, England (1958).

32. Simms, D. L. "Experiments on the Ignition of Cellulosic Materials by Thermal Radiation." Combustion and Flame, 5 (1961), 369-375.

33. Simms, D. L. "Ignition of Cellulosic Materials by Radiation." Combustion and Flame, 4, 4 (1960), 293-300.

34. Simms, D. L. "On Pilot Ignition of Wood by Radiation." Combustion and Flame, 7 (1963), 253-261.

35. Sliepcevich, C. M., et al. Escape Worthiness of Vehicles and Occupant Survival." Report No. DOT HS-800 428, Contract FH-11-7303, University of Oklahoma Research Institute, Norman (1970), Part I, Chapter 4.

36. Sliepcevich, C. M., et al. "Escape Worthiness of Vehicles for Occupancy Survivals and Crashes, Part One, Research Programs." Final Report, Dept. of Transportation Report No. 1770-FR-1-1, Contract No. FH-11-7512, University of Oklahoma, Norman (July 1972).

37. Snedecor, G. W. Statistical Methods. Ames, Iowa: Iowa State College Press, 1946.

38. Vogel, M., and Williams, F. A. "Flame Propagation Along Matchstick Arrays." Combustion Science and Technology, 1 (1970), 429-436.

39. Wesson, H. R. "The Piloted Ignition of Wood by Radiant Heat." D. Engr. dissertation. University of Oklahoma, Norman, Oklahoma, 1970.

APPENDICES

APPENDIX A

TABLES OF DATA

TABLE A-1

DATA

Material	Sample No.	Density g/cm^3	Thickness cm	Weight / Area g/cm^2	Experimental Burning Rate (R_o) inches/minute			Average Burning Rate cm/sec
I. Nylon Fabrics								
Sea blue	N-1	0.447	0.079	0.0353	1.37	1.61	1.58	0.0644
Dark blue	N-2	0.530	0.066	0.0350	1.51	1.58	1.58	--
Beige	N-3	0.448	0.086	0.0387	2.26	1.84	1.70	--
Black	N-4	0.407	0.099	0.0404	2.41	2.48	2.62	0.1060
Gray on black	N-5	0.375	0.102	0.0383	1.14	1.04	1.06	0.0457
Blue on blue	N-6	0.447	0.0915	0.0409	1.07	1.06	1.07	--
Blue/green	N-7	0.357	0.113	0.0404	1.10	1.13	1.01	0.0457
Smooth maroon	N-8	0.607	0.061	0.0370	1.32	0.73	1.04	0.0436
Smooth lt. blue	N-9	0.531	0.074	0.0393	1.36	1.33	1.58	0.0601
Smooth black	N-10	0.540	0.064	0.0346	1.08	1.11	1.18	0.0474
Smooth beige	N-11	0.573	0.071	0.0407	1.17	1.04	1.01	0.0453
Smooth pat. beige	N-12	0.551	0.061	0.0356	1.21	1.12	1.22	0.0500
Blue w/ metal	N-13	0.391	0.119	0.0465	1.93	2.18	2.11	0.0876
Beige w/ metal	N-14	0.408	0.114	0.0465	1.94	1.86	1.95	0.0813
II. Vinyl Fabrics								
Black w/ dents	V-1	0.700	0.142	0.0994	2.27	2.07	2.05	0.0902
Red w/ dents	V-2	0.668	0.130	0.0868	3.68	3.42	3.39	0.1482
Beige w/ dents	V-3	0.680	0.142	0.0966	2.81	2.54	2.38	0.1092
Beige w/ perf.	V-4	0.828	0.122	0.1011	2.08	2.00	1.90	0.0843
Black w/ perf.	V-5	0.782	0.119	0.0929	4.19	4.53	4.10	0.1808
Red (cockle)	V-6	0.880	0.076	0.0668	2.71	3.81	3.78	0.1452
Black	V-7	0.884	0.089	0.0787	3.14	3.16	--	0.1334
Beige	V-8	0.871	0.058	0.0505	4.14	4.00	4.77	0.1820
Med. blue	V-9	0.836	0.084	0.0702	2.50	3.33	--	0.1230

TABLE A-1--Continued

Material	Sample No.	Density g/cm^3	Thickness cm	Weight / Area g/cm^2	Experimental Burning Rate (R_o) inches/minute					Average Burning Rate cm/sec
Dark blue	V-10	0.887	0.086	0.0763	2.71	--	--			0.1143
Metallic blue	V-11	0.797	0.074	0.0590	4.20	4.55	--			0.1854
Light blue	V-12	0.807	0.058	0.0468	4.03	--	--			0.1706
Red (cockle)	V-13	0.903	0.071	0.0641	See Table					0.1550
Gray	V-15	1.05	0.051	0.0536	See Table					0.256
III. Cotton Cloth										
Thread count:										
48 x 28	CT-1	0.535	0.066	0.0353	See Table					0.155
48 x 40	CT-3	0.561	0.046	0.0258	4.54	5.13	4.56			0.204
48 x 44	CT-4	0.558	0.043	0.0241	5.55	5.13	5.00			0.223
48 x 50	CT-5	0.529	0.041	0.0217	6.14	5.81	6.10			0.262
48 x 56	CT-6	0.564	0.036	0.0203	5.65	6.29	5.81	5.59		0.249
48 x 60	CT-7	0.536	0.036	0.0193	5.70	5.92	5.84			0.264
IV. Filter Paper										
Whatman #1	FP-1	0.460	0.020	0.0092	See Table					0.361
Whatman #3	FP-2	0.463	0.038	0.01763	6.52	6.45	6.32	6.52	6.45	0.273
Whatman #4	FP-3	0.460	0.020	0.0092	6.85	7.25	6.66	6.75	7.35	0.294
Whatman #6	FP-4	0.576	0.0178	0.0102	8.82	8.10	7.69	8.95	8.11	0.358
Whatman #40	FP-5	0.470	0.020	0.0095	9.09	7.70	8.93	7.70	7.94	0.350
Whatman #54	FP-6	0.496	0.0178	0.0088	10.71	10.53	10.71	10.00	10.53	0.444
Whatman #115	FP-7	0.735	0.0102	0.0075	11.76	11.54	11.32	11.54	11.32	0.487
V. Nylon Carpeting										
Blue carpet	C-1	0.174	0.394	0.0685	0.54	0.40	0.63			0.0224
Brown carpet	C-3	0.211	0.343	0.0726	0.34	0.45	--			0.017
Black carpet	C-4	0.230	0.442	0.1017	0.55	0.34	--			0.019
Dark ginger carpet	C-6	0.188	0.338	0.0638	0.73	0.48	0.49			0.020

TABLE A-1--Continued

Material	Sample No.	Density g/cm^3	Thickness cm	Weight / Area g/cm^2	Experimental Burning Rate (R_o) inches/minute			Average Burning Rate cm/sec
Black carpet	C-7	0.208	0.318	0.0661	--	0.42	--	0.018
Dark turquoise cpt	C-8	0.268	0.394	0.1055	--	0.52	0.52	0.022
Med. nugget carpet	C-9	0.182	0.467	0.0617	0.57	0.55	0.48	0.029
VI. Woods								
A. Balsa								
3/32"	B3/32-1	0.197	0.239	0.0471		5.587		0.2365
	B3/32-2	0.174	0.238	0.0415		5.917		0.2505
	B3/32-3	0.139	0.2385	0.0332		7.143		0.3024
	B3/32-4	0.132	0.2384	0.0314		7.194		0.3046
	B3/32-5	0.126	0.239	0.0300		7.752		0.3282
	B3/32-6	0.1193	0.239	0.0285		7.752		0.3282
	B3/32-7	0.1319	0.240	0.0319		8.000		0.3390
	B3/32-8	0.130	0.239	0.0310		6.803		0.288
	B3/32-9	0.1856	0.236	0.0438		5.814		0.246
	B3/32-10	0.2045	0.237	0.0485		4.608		0.195
	B3/32-11	0.2111	0.236	0.0498		4.762		0.202
	B3/32-12	0.1882	0.2365	0.0445		5.128		0.217
1/16"	B1/16-1	0.170	0.1621	0.0275		7.143		0.3024
	B1/16-2	0.145	0.162	0.0235		7.752		0.3282
	B1/16-3	0.100	0.1626	0.0163		12.500		0.5292
	B1/16-4	0.0994	0.162	0.0161		10.101		0.4276
	B1/16-5	0.1055	0.1615	0.0170		11.236		0.4757
	B1/16-6	0.104	0.162	0.01685		10.989		0.4652
	B1/16-7	0.1686	0.147	0.0248		7.752		0.328
	B1/16-8	0.1503	0.149	0.0224		7.937		0.336
	B1/16-9	0.1823	0.147	0.0268		7.143		0.302
	B1/16-10	0.1821	0.147	0.0267		7.463		0.316
	B1/16-11	0.1783	0.149	0.0266		7.194		0.305
	B1/16-12	0.1852	0.1475	0.0273		7.519		0.318

TABLE A-1--Continued

Material	Sample No.	Density g/cm^3	Thickness cm	Weight Area g/cm^2	Experimental Burning Rate (R_o) inches/minute	Average Burning Rate cm/sec
B. Redgum	G-1	0.390	0.152	0.0592	4.464	0.1890
	G-2	0.381	0.1902	0.0726	5.025	0.2128
	G-3	0.383	0.176	0.0674	6.173	0.2613
	G-4	0.374	0.188	0.0704	3.972	0.1660
	G-5	0.378	0.2065	0.0780	3.937	0.1667
	G-6	0.371	0.1695	0.0629	4.425	0.1873
C. Ash	A-1	0.591	0 344	0.2033	1.361	0.0576
	A-2	0.597	0.245	0.1462	1.424	0.0603
	A-3	0.581	0.2495	0.1450	2.193	0.0928
	A-4	0.590	0.281	0.1657	1.414	0.0599
	A-5	0.577	0.296	0.1708	1.721	0.0729
	A-6	0.570	0.244	0.1392	1.645	0.0696
D. Oak	O-1	0.648	0.269	0.1744	1.326	0.0562
	O-2	0.711	0.270	0.1919	1.486	0.0629
	O-3	0.720	0.2455	0.1767	1.350	0.0571
	O-4	0.655	0.281	0.1841	2.358	0.0998
	O-5	0.700	0.2445	0.1706	2.336	0.0989
	O-6	0.677	0.2405	0.1628	2.257	0.0956
E. Balsa						
1/32"	Bl/32-1	0.127	0.1016	0.0129	15.152	0.6415
	Bl/32-2	0.127	0.1008	0.0128	13.699	0.580
	Bl/32-3	0.134	0.1006	0.0135	15.873	0.672
	Bl/32-4	0.1173	0.1001	0.01174	14.925	0.6319
	Bl/32-5	0.0994	0.1006	0.0100	18.868	0.7988
	Bl/32-6	0.1164	0.1006	0.0117	17.241	0.730

TABLE A-1--Continued

Material	Sample No.	Density g/cm^3	Thickness cm	Weight / Area g/cm^2	Experimental Burning Rate (R_o) inches/minute				Average Burning Rate cm/sec
#1 Whatman Filter paper	F-1	0.460	0.020	0.0092	8.20	8.62	8.47	9.26	0.361
					8.47	8.62	8.93	8.93	
					8.77	8.47	8.40	9.01	
					8.33	9.26	8.48	8.40	
					8.33	8.33	9.26	8.06	
					8.06	7.94	8.00	8.00	
					8.07	8.48	9.09	8.62	
Two sheets #1 Whatman Filter paper	F-1	0.460	0.020	0.0092	5.27	5.22	5.31	6.32	0.220
					5.89	5.77	5.13	4.96	
					5.13	4.62	4.58	5.18	
					4.69	5.13	5.31	5.18	
					4.48	4.80	4.77	5.56	
					4.69	4.77	5.05	5.18	
					4.32	5.66	6.25	5.09	
					5.83	5.61			
Vinyl fabric	V-13	0.903	0.071	0.0641	3.75	4.19	3.82	4.33	0.1550
					3.98	4.10	3.27	3.64	
					3.89	3.68	3.66	3.64	
					3.91	2.40	3.73	3.94	
					3.92	3.83	3.23	3.58	
					3.63	3.23	4.08	3.97	
					3.73	2.72	3.33	3.56	
					3.74	3.69			
Vinyl fabric	V-15	1.05	0.051	0.0536	5.36	5.71	5.77	6.19	0.256
					5.66	6.00	6.00	6.59	
					6.19	5.41	6.67	6.59	
					6.00	6.25	6.00	6.59	
					6.06	5.56	7.06	5.41	

TABLE A-1--Continued

Material	Sample No.	Density g/cm^3	Thickness cm	Weight / Area g/cm^2	Experimental Burning Rate (R_o) inches/minute				Average Burning Rate cm/sec
Cotton fabric parallel to warp	CT-1	0.535	0.066	0.0353	2.68	2.57	2.86	2.68	0.155
					3.09	2.92	2.89	2.52	
					2.54	3.07	3.15	3.05	
					2.84	3.52	3.07	3.01	
					2.82	3.18	2.69	3.39	
					3.23	3.20	3.45	3.27	
					2.68	3.28	2.81	3.35	
					3.51	2.92	2.88	3.07	
					3.01	3.52			
Nylon fabric	N-25	0.494	0.0686	0.0339	2.66	2.18	2.76	2.56	0.108
					2.64	2.53	2.58	2.51	
					2.39	2.57	2.67	2.57	
					2.49	2.33	2.54	2.64	
					2.49	2.51	2.58	2.56	
					2.49	2.56	2.60	2.55	
					2.65	2.60	2.51	2.72	
					2.49	2.53			
Nylon fabric	N-27	0.528	0.0508	0.0268	3.39	3.20	4.44	8.00	0.145
					9.33	2.80	4.00	2.97	
					5.45	3.33	1.58	2.78	
					3.17	3.24	3.01	4.15	
					2.02	1.52	1.36	3.65	
					1.89	3.29	4.64	3.02	
					3.00	2.97	2.31	2.56	
					1.62	3.76	1.93	2.65	
					4.09	6.67	2.23		

TABLE A-2

PHYSICAL AND THERMAL PROPERTY DATA USED TO CALCULATE EQUATIONS IV-32

Material Sample No.	Thickness δ cm	Weight/Area w_o g/cm^2	Density ρ g/cm^3	Heat Capacity c_p cal/g-°C	Thermal Conduc. $k \times 10^4$ cal/cm-s-°C	Thermal Diffus. $\kappa \times 10^3$ cm^2/sec	Slope s cal/cm^2-sec$^{1/2}$	Burning Rate R_o cm/sec
I. Nylon Fabrics								
N-1	0.079	0.0353	0.447	0.40	2.575	1.46	4.45	0.0644
N-4	0.099	0.0404	0.407	0.40	2.42	1.49	4.45	0.1060
N-5	0.102	0.0383	0.375	0.40	2.30	1.51	4.45	0.0457
N-7	0.113	0.0404	0.357	0.40	2.18	1.53	3.33	0.0457
N-8	0.061	0.0370	0.607	0.40	3.31	1.38	4.27	0.0436
N-9	0.074	0.0393	0.531	0.40	2.98	1.41	4.05	0.0601
N-10	0.064	0.0346	0.540	0.40	3.03	1.40	3.90	0.0474
N-11	0.071	0.0407	0.573	0.40	3.22	1.39	4.70	0.0453
N-12	0.061	0.0356	0.551	0.40	3.08	1.40	3.90	0.0500
N-13	0.119	0.0465	0.391	0.40	2.35	1.51	4.05	0.0876
N-14	0.114	0.0465	0.408	0.40	2.43	1.48	5.00	0.0813
II. Vinyl Fabrics								
V-1	0.142	0.0994	0.700	0.40	1.92	0.696	2.83	0.0902
V-2	0.130	0.0868	0.668	0.40	1.875	0.700	3.75	0.1482
V-3	0.142	0.0966	0.680	0.40	1.89	0.695	2.33	0.1092
V-4	0.122	0.1011	0.828	0.40	2.17	0.662	3.37	0.0843
V-5	0.119	0.0929	0.782	0.40	2.08	0.667	2.83	0.1808
V-6	0.076	0.0668	0.880	0.40	2.29	0.651	4.37	0.1452
V-7	0.089	0.0787	0.884	0.40	2.29	0.651	3.75	0.1334
V-8	0.058	0.0505	0.871	0.40	2.235	0.654	3.47	0.1820
V-9	0.084	0.0702	0.836	0.40	2.235	0.654	4.15	0.1230
V-10	0.086	0.0763	0.887	0.40	2.29	0.651	3.47	0.1143
V-11	0.074	0.0590	0.797	0.40	2.11	0.700	3.75	0.1854
V-12	0.058	0.0468	0.807	0.40	2.125	0.664	3.33	0.1706
V-13	0.071	0.0641	0.903	0.40	2.325	0.646	3.90	0.1550
V-15	0.051	0.0536	1.05	0.40	2.67	0.636	3.30	0.2560

TABLE A-2

PHYSICAL AND THERMAL PROPERTY DATA USED TO CALCULATE EQUATIONS IV-32

Material Sample No.	Thickness δ cm	Weight / Area w_o g/cm^2	Density ρ g/cm^3	Heat Capacity c_p cal/g-°C	Thermal Conduc. $k \times 10^4$ cal/cm-s-°C	Thermal Diffus. $\kappa \times 10^3$ cm^2/sec	Slope s cal/cm^2-sec$^{1/2}$	Burning Rate R_o cm/sec
I. Nylon Fabrics								
N-1	0.079	0.0353	0.447	0.40	2.575	1.46	4.45	0.0644
N-4	0.099	0.0404	0.407	0.40	2.42	1.49	4.45	0.1060
N-5	0.102	0.0383	0.375	0.40	2.30	1.51	4.45	0.0457
N-7	0.113	0.0404	0.357	0.40	2.18	1.53	3.33	0.0457
N-8	0.061	0.0370	0.607	0.40	3.31	1.38	4.27	0.0436
N-9	0.074	0.0393	0.531	0.40	2.98	1.41	4.05	0.0601
N-10	0.064	0.0346	0.540	0.40	3.03	1.40	3.90	0.0474
N-11	0.071	0.0407	0.573	0.40	3.22	1.39	4.70	0.0453
N-12	0.061	0.0356	0.551	0.40	3.08	1.40	3.90	0.0500
N-13	0.119	0.0465	0.391	0.40	2.35	1.51	4.05	0.0876
N-14	0.114	0.0465	0.408	0.40	2.43	1.48	5.00	0.0813
II. Vinyl Fabrics								
V-1	0.142	0.0994	0.700	0.40	1.92	0.696	2.83	0.0902
V-2	0.130	0.0868	0.668	0.40	1.875	0.700	3.75	0.1482
V-3	0.142	0.0966	0.680	0.40	1.89	0.695	2.33	0.1092
V-4	0.122	0.1011	0.828	0.40	2.17	0.662	3.37	0.0843
V-5	0.119	0.0929	0.782	0.40	2.08	0.667	2.83	0.1808
V-6	0.076	0.0668	0.880	0.40	2.29	0.651	4.37	0.1452
V-7	0.089	0.0787	0.884	0.40	2.29	0.651	3.75	0.1334
V-8	0.058	0.0505	0.871	0.40	2.235	0.654	3.47	0.1820
V-9	0.084	0.0702	0.836	0.40	2.235	0.654	4.15	0.1230
V-10	0.086	0.0763	0.887	0.40	2.29	0.651	3.47	0.1143
V-11	0.074	0.0590	0.797	0.40	2.11	0.700	3.75	0.1854
V-12	0.058	0.0468	0.807	0.40	2.125	0.664	3.33	0.1706
V-13	0.071	0.0641	0.903	0.40	2.325	0.646	3.90	0.1550
V-15	0.051	0.0536	1.05	0.40	2.67	0.636	3.30	0.2560

TABLE A-2--Continued

Material Sample No.	Thickness δ cm	Weight Area w_o g/cm^2	Density ρ g/cm^3	Heat Capacity c_p cal/g-°C	Thermal Conduc. $k \times 10^4$ $\frac{cal}{cm\text{-}s\text{-}°C}$	Thermal Diffus. $\kappa \times 10^3$ cm^2/sec	Slope s $\frac{cal}{cm^2\text{-}sec^{1/2}}$	Burning Rate R_o cm/sec
III. Cotton Fabrics								
CT-1	0.066	0.0353	0.535	0.34	1.75	0.953	3.37	0.155
CT-3	0.046	0.0258	0.561	0.34	1.79	0.940	2.83	0.204
CT-4	0.043	0.0241	0.558	0.34	1.79	0.940	2.90	0.223
CT-5	0.041	0.0217	0.529	0.34	1.76	0.941	3.08	0.262
CT-6	0.036	0.0203	0.564	0.34	1.79	0.940	2.72	0.249
CT-7	0.036	0.0193	0.536	0.34	1.79	0.940	2.50	0.264
IV. Filter Papers								
FP-1	0.020	0.0092	0.460	0.34	1.586	1.06	1.97	0.361
FP-2	0.038	0.01763	0.463	0.34	1.694	1.06	2.86	0.273
FP-3	0.020	0.0092	0.460	0.34	1.586	1.06	2.13	0.294
FP-4	0.0178	0.0102	0.576	0.34	2.054	1.06	2.22	0.358
FP-5	0.020	0.0095	0.470	0.34	1.694	1.06	2.47	0.350
FP-6	0.0178	0.0088	0.496	0.34	1.766	1.06	2.07	0.444
FP-7	0.0102	0.0075	0.735	0.34	2.667	1.06	2.22	0.487
V. Nylon Carpets								
C-1	0.394	0.0685	0.174	0.40	1.35	1.94	5.71	0.0224
C-3	0.343	0.0726	0.211	0.40	1.525	1.81	3.33	0.017
C-4	0.442	0.1017	0.230	0.40	1.60	1.75	5.71	0.019
C-6	0.338	0.0638	0.188	0.40	1.425	1.90	6.25	0.020
C-7	0.318	0.0661	0.208	0.40	1.525	1.83	5.00	0.018
C-8	0.394	0.1055	0.268	0.40	1.80	1.68	3.42	0.022
C-9	0.467	0.0617	0.132	0.40	1.40	1.90	6.00	0.029

TABLE A-2--Continued

Material Sample No.	Thickness δ cm	Weight Area w_o g/cm^2	Density ρ g/cm^3	Heat Capacity c_p cal/g-°C	Thermal Conduc. $k \times 10^4$ $\frac{cal}{cm\text{-}s\text{-}°C}$	Thermal Diffus. $\kappa \times 10^3$ cm^2/sec	Slope s $\frac{cal}{cm^2\text{-}sec^{1/2}}$	Burning Rate R_o cm/sec
VI. Woods								
A. Balsa, 3/32"								
B3/32-1	0.239	0.0471	0.197	0.34	1.51	2.25	2.61	0.236
B3/32-2	0.238	0.0415	0.174	0.34	1.40	2.37	2.50	0.251
B3/32-3	0.2385	0.0332	0.139	0.34	1.23	2.60	2.32	0.302
B3/32-4	0.2384	0.0314	0.132	0.34	1.20	2.67	2.29	0.305
B3/32-5	0.239	0.0300	0.126	0.34	1.17	2.73	2.25	0.328
B3/32-6	0.239	0.0285	0.1193	0.34	1.14	2.81	2.21	0.328
B3/32-7	0.240	0.0319	0.1319	0.34	1.20	2.68	2.28	0.339
B3/32-8	0.239	0.0310	0.130	0.34	1.19	2.69	2.28	0.288
B3/32-9	0.236	0.0438	0.1856	0.34	1.46	2.31	2.55	0.246
B3/32-10	0.237	0.0485	0.2045	0.34	1.55	2.23	2.63	0.195
B3/32-11	0.236	0.0498	0.2111	0.34	1.58	2.20	2.66	0.202
B3/32-12	0.2365	0.0445	0.1882	0.34	1.47	2.30	2.55	0.217
Balsa, 1/16"								
B1/16-1	0.1621	0.0275	0.170	0.34	1.38	2.39	1.94	0.302
B1/16-2	0.162	0.0235	0.145	0.34	1.26	2.56	2.02	0.328
B1/16-3	0.1626	0.0163	0.100	0.34	1.05	3.09	1.79	0.529
B1/16-4	0.162	0.0161	0.0994	0.34	1.04	3.08	1.79	0.428
B1/16-5	0.1615	0.0170	0.1055	0.34	1.07	2.98	1.82	0.476
B1/16-6	0.162	0.01685	0.104	0.34	1.07	3.03	1.82	0.465
B1/16-7	0.147	0.0248	0.1686	0.34	1.37	2.39	2.02	0.328
B1/16-8	0.149	0.0224	0.1503	0.34	1.29	2.52	1.96	0.336
B1/16-9	0.147	0.0268	0.1823	0.34	1.44	2.32	2.08	0.302
B1/16-10	0.147	0.0267	0.1821	0.34	1.44	2.33	2.08	0.316
B1/16-11	0.149	0.0266	0.1783	0.34	1.42	2.34	2.08	0.305
B1/16-12	0.1475	0.0273	0.1852	0.34	1.45	2.30	2.08	0.318

TABLE A-2--Continued

Material Sample No.	Thickness δ cm	Weight Area w_o g/cm^2	Density ρ g/cm^3	Heat Capacity c_p cal/g-°C	Thermal Conduc. $kx10^4$ $\frac{cal}{cm\text{-}s\text{-}°C}$	Thermal Diffus. $\kappa x10^3$ cm^2/sec	Slope s $\frac{cal}{cm^2\text{-}sec^{1/2}}$	Burning Rate R_o cm/sec
B. Redgum								
G-1	0.152	0.0592	0.390	0.34	2.43	1.83	2.63	0.189
G-2	0.1902	0.0726	0.381	0.34	2.39	1.84	2.90	0.213
G-3	0.176	0.0674	0.383	0.34	2.40	1.84	2.81	0.261
G-4	0.188	0.0704	0.374	0.34	2.36	1.86	2.87	0.166
G-5	0.2065	0.0780	0.378	0.34	2.73	1.84	2.98	0.167
G-6	0.1695	0.0629	0.371	0.34	2.34	1.86	2.74	0.187
C. Ash								
A-1	0.344	0.2033	0.591	0.34	3.39	1.69	4.10	0.0576
A-2	0.245	0.1462	0.597	0.34	3.42	1.68	3.87	0.0603
A-3	0.2495	0.1450	0.581	0.34	3.35	1.70	3.85	0.0928
A-4	0.281	0.1657	0.590	0.34	3.39	1.69	3.96	0.0599
A-5	0.296	0.1708	0.577	0.34	3.33	1.70	3.96	0.0729
A-6	0.244	0.1392	0.570	0.34	3.29	1.70	3.81	0.0696
D. Oak								
O-1	0.269	0.1744	0.648	0.34	3.67	1.67	3.54	0.0562
O-2	0.270	0.1919	0.711	0.34	3.97	1.64	3.66	0.0629
O-3	0.2455	0.1767	0.720	0.34	4.01	1.64	3.60	0.0571
O-4	0.281	0.1841	0.655	0.34	3.70	1.66	3.58	0.0998
O-5	0.2445	0.1706	0.700	0.34	3.91	1.64	3.56	0.0989
O-6	0.2405	0.1628	0.677	0.34	3.80	1.65	3.50	0.0956

TABLE A-3

BURNING RATE CALCULATIONS, SLIEPCEVICH MODEL (36)

Material Sample No.	w_o g/cm^2	slope (s) cal/cm^2-sec$^{1/2}$	R_o cm/sec	t* sec	H_a^* cal/cm^2-sec	$R_o\sqrt{t^*}$	$R_o\sqrt{t^*}_{ave}$
Nylon							Average =
N-1	0.0353	4.45	0.0644	0.63	5.54	0.0511	0.0527
N-4	0.0404	4.45	0.1060	0.36	7.42	0.0636	
N-5	0.0383	4.45	0.0457	1.01	4.14	0.0460	
N-7	0.0404	3.33	0.0457	1.35	2.87	0.0531	
N-8	0.0370	4.27	0.0436	1.20	3.84	0.0477	
N-9	0.0393	4.05	0.0601	0.81	4.44	0.0541	
N-10	0.0346	3.90	0.0474	1.00	3.99	0.0475	
N-11	0.0407	4.70	0.0453	1.07	4.54	0.0468	
N-12	0.0356	3.90	0.0500	0.91	4.19	0.0477	
N-13	0.0465	4.05	0.0876	0.54	5.46	0.0640	
N-14	0.0465	5.00	0.0813	0.52	6.91	0.0589	
Vinyl							Average =
V-1	0.0994	2.83	0.0902	0.86	3.10	0.0837	0.0824
V-2	0.0868	3.75	0.1482	0.32	7.07	0.0839	
V-3	0.0966	2.33	0.1092	0.69	2.83	0.0907	
V-4	0.1011	3.37	0.0843	0.88	3.55	0.0791	
V-5	0.0929	2.83	0.1808	0.27	5.50	0.0940	
V-6	0.0668	4.37	0.1452	0.28	8.31	0.0775	
V-7	0.0787	3.75	0.1334	0.37	6.60	0.0808	
V-8	0.0505	3.47	0.1820	0.18	8.47	0.0783	
V-9	0.0702	4.15	0.1230	0.39	6.64	0.0768	
V-10	0.0763	3.47	0.1143	0.48	5.25	0.0792	
V-11	0.0590	3.75	0.1854	0.19	9.13	0.0812	
V-12	0.0468	3.33	0.1706	0.22	7.18	0.0792	
V-13	0.0641	3.90	0.1550	0.27	7.53	0.0803	
V-15	0.0536	3.30	0.256	0.11	10.14	0.0896	

TABLE A-3--Continued

Material Sample No.	w_o g/cm^2	Slope (s) cal/cm^2-sec$^{1/2}$	R_o cm/sec	t* sec	H_a^* cal/cm^2-sec	$R_o\sqrt{t^*}$	$R_o\sqrt{t^*_{ave}}$
Cottons							Average =
CT-1	0.0353	3.37	0.155	0.24	6.87	0.0686	0.0720
CT-3	0.0258	2.83	0.204	0.12	8.19	0.0724	
CT-4	0.0241	2.90	0.223	0.10	8.78	0.0724	
CT-5	0.0217	3.08	0.262	0.08	11.16	0.0724	
CT-6	0.0203	2.72	0.249	0.08	9.77	0.0711	
CT-7	0.0193	2.50	0.264	0.09	8.20	0.0745	
Filter Paper							Average =
FP-1	0.0092	1.97	0.361	0.0375	10.12	0.0699	0.0689
FP-2	0.01763	2.86	0.273	0.0665	11.09	0.0704	
FP-3	0.0092	2.13	0.294	0.0480	9.73	0.0644	
FP-4	0.0102	2.22	0.358	0.0395	11.17	0.0702	
FP-5	0.0095	2.47	0.350	0.0355	13.10	0.0658	
FP-6	0.0088	2.07	0.444	0.0260	13.08	0.0716	
FP-7	0.0075	2.22	0.487	0.0205	15.58	0.0697	
Carpet							Average =
C-1	0.0685	5.71	0.0224	3.15	3.22	0.0398	0.0438
C-3	0.0726	3.33	0.017	7.20	1.24	0.0456	
C-4	0.1017	5.71	0.019	5.33	2.47	0.0439	
C-6	0.0638	6.25	0.020	3.05	3.58	0.0350	
C-7	0.0661	5.00	0.018	4.38	2.39	0.0376	
C-8	0.1055	3.42	0.022	6.65	1.33	0.0568	
C-9	0.0617	6.00	0.029	2.71	3.64	0.0478	

TABLE A-3--Continued

Material Sample No.	w_o g/cm^2	Slope (s) cal/cm^2-sec$^{1/2}$	R_o cm/sec	t* sec	H_a* cal/cm^2-sec	$R_o\sqrt{t^*}$	$R_o\sqrt{t^*_{ave}}$
Wood - Balsa							Average = 0.108
B3/32-1	0.0471	2.61	0.2365	0.213	4.82	0.109	
B3/32-2	0.0415	2.50	0.2505	0.188	4.92	0.1085	
B3/32-3	0.0332	2.32	0.3024	0.130	5.49	0.1091	
B3/32-4	0.0314	2.29	0.3046	0.1265	5.48	0.1084	
B3/32-5	0.0300	2.25	0.3282	0.111	5.76	0.1094	
B3/32-6	0.0285	2.21	0.3282	0.110	5.67	0.1087	
B3/32-7	0.0319	2.28	0.3390	0.107	5.96	0.1109	
B3/32-8	0.0310	2.28	0.288	0.1385	5.21	0.1072	
B3/32-9	0.0438	2.55	0.246	0.195	4.91	0.1086	
B3/32-10	0.0485	2.63	0.195	0.291	4.15	0.1052	
B3/32-11	0.0498	2.66	0.202	0.277	4.31	0.1063	
B3/32-12	0.0445	2.55	0.217	0.240	4.45	0.1063	
							Average = 0.1085
B1/16-1	0.0275	1.94	0.302	0.129	4.68	0.1086	
B1/16-2	0.0235	2.02	0.328	0.106	5.23	0.1067	
B1/16-3	0.0163	1.79	0.529	0.0446	7.10	0.1118	
B1/16-4	0.0161	1.79	0.428	0.0626	6.00	0.1069	
B1/16-5	0.0170	1.82	0.476	0.0535	6.62	0.1100	
B1/16-6	0.01685	1.82	0.465	0.0554	6.46	0.1095	
B1/16-7	0.0248	2.02	0.328	0.108	5.17	0.108	
B1/16-8	0.0224	1.96	0.336	0.101	5.19	0.1068	
B1/16-9	0.0268	2.08	0.302	0.126	4.90	0.1073	
B1/16-10	0.0267	2.08	0.316	0.117	5.08	0.1082	
B1/16-11	0.0266	2.08	0.305	0.124	4.94	0.1074	
B1/16-12	0.0273	2.08	0.318	0.117	5.12	0.1088	

TABLE A-3--Continued

Material Sample No.	w_o g/cm^2	Slope (s) cal/cm^2-sec$^{1/2}$	R_o cm/sec	t* sec	H_a^* cal/cm^2-sec	$R_o\sqrt{t^*}$	$R_o\sqrt{t^*_{ave}}$
Wood - Ash							Average =
A-1	0.2033	4.10	0.0576	2.39	2.65	0.0891	0.0884
A-2	0.1462	3.87	0.0603	1.96	2.76	0.0844	
A-3	0.1450	3.85	0.0928	1.005	3.84	0.0930	
A-4	0.1657	3.96	0.0599	2.08	2.75	0.0864	
A-5	0.1708	3.96	0.0729	1.56	3.17	0.0909	
A-6	0.1392	3.81	0.0696	1.55	3.06	0.0867	
Wood - Gum							Average =
G-1	0.0592	2.63	0.189	0.258	5.18	0.0960	0.0980
G-2	0.0726	2.90	0.213	0.222	6.15	0.1003	
G-3	0.0674	2.81	0.261	0.1565	7.10	0.1033	
G-4	0.0704	2.87	0.166	0.330	5.00	0.0954	
G-5	0.0780	2.98	0.167	0.336	5.15	0.0966	
G-6	0.0629	2.74	0.187	0.264	5.33	0.0963	
Wood - Oak							Average =
O-1	0.1744	3.54	0.0562	2.64	2.18	0.0913	0.0976
O-2	0.1919	3.66	0.0629	2.28	2.42	0.0950	
O-3	0.1767	3.60	0.0571	2.58	2.24	0.0917	
O-4	0.1841	3.58	0.0998	1.09	3.44	0.1040	
O-5	0.1706	3.56	0.0989	1.07	3.44	0.1025	
O-6	0.1628	3.50	0.0956	1.12	3.31	0.1011	

TABLE A-4

IGNITION DATA FROM WESSON'S RESEARCH (39)

δ cm	ρ g/cc	H_i	t_{ig}	$\kappa \times 10^3$ cm/s^2	$\bar{\alpha}$	$\bar{\bar{\alpha}}$	$H_i\bar{\alpha} = H_a$	$H_i\bar{\bar{\alpha}} = \bar{H}_a$	$\frac{H_a}{\rho^{1/3}}$	$\frac{H_R}{\rho^{1/3}}$	$H_R = \bar{H}_a$-Cor.
Ash											
2.54	0.686	0.36	465.0	1.473	0.765	0.825	0.275	0.297	0.330	0.357	0.122
		0.60	120.0				0.458	0.495	0.550	0.594	0.334
	$\rho^{1/3}$=	1.06	23.0				0.811	0.875	0.975	1.051	0.730
	0.883	1.12	19.5				0.856	0.924	1.028	1.110	0.782
		1.52	11.0				1.162	1.253	1.397	1.505	1.118
		1.99	8.7				1.522	1.641	1.830	1.971	1.511
		2.72	3.25				2.080	2.245	2.497	2.700	2.118
		2.90	2.40				2.216	2.392	2.660	2.810	2.266
		2.30	5.5				1.760	1.898	2.114	2.280	1.770
		2.05	6.6				1.568	1.692	1.880	2.030	1.562
		1.45	18.5				1.108	1.196	1.330	1.435	1.061
		1.00	54.0				0.765	0.825	0.918	0.991	0.679
		0.82	98.0				0.627	0.676	0.752	0.812	0.524
Oak											
2.54	0.709	0.76	67.0	1.555	0.773	0.810	0.587	0.615	0.657	0.688	0.460
		1.01	29.0				0.780	0.817	0.873	0.915	0.670
	$\rho^{1/3}$=	1.50	14.0				1.159	1.213	1.297	1.360	1.078
	0.893	2.06	4.4				1.592	1.668	1.785	1.868	1.538
		2.56	2.0				1.977	2.073	2.210	2.320	1.946
		2.60	2.5				2.007	2.104	2.250	2.360	1.977
		2.85	2.2				2.200	2.305	2.465	2.575	2.180
		2.20	3.50				1.700	1.781	1.905	1.997	1.651
		2.00	6.0				1.546	1.620	1.730	1.515	1.490
		1.42	26.0				1.097	1.150	1.228	1.289	1.013
		0.51	512.0				0.394	0.413	0.441	0.462	0.246
		1.15	418.0				0.888	0.931	0.995	1.042	0.787

TABLE A-4--Continued

δ cm	ρ g/cc	H_i	t_{ig}	$\kappa \times 10^3$ cm/s^2	$\bar{\alpha}$	$\bar{\bar{\alpha}}$	$H_i\bar{\alpha} = H_a$	$H_i\bar{\bar{\alpha}} = \bar{H}_a$	$\frac{H_a}{\rho^{1/3}}$	$\frac{H_R}{\rho^{1/3}}$	$H_R = \bar{H}_a$-Cor.
Gum -- benzene flames											
2.54	0.624	0.80	78.0	1.398	0.766	0.825	0.613	0.660	0.716	0.771	0.507
		1.01	28.0				0.774	0.833	0.904	0.972	0.687
	$\rho^{1/3}$=	1.50	6.5				1.150	1.238	1.343	1.445	1.103
	0.856	2.22	2.6				1.700	1.831	1.985	2.140	1.701
		2.68	1.6				2.055	2.210	2.400	2.580	2.084
		0.76	122.0				0.582	0.626	0.680	0.731	0.471
		0.98	48.0				0.751	0.808	0.877	0.944	0.661
		1.43	18.0				1.095	1.180	1.280	1.378	1.044
		2.03	8.0				1.555	1.674	1.818	1.955	1.544
		2.30	4.8				1.762	1.895	2.060	2.215	1.767
Balsa -- 1000 w lamps											
1.97	0.0901	3.25	2.0	1.765	0.408	0.551	1.325	1.791	2.930	3.960	1.663
		3.20	2.0				1.305	1.765	2.890	3.905	1.637
	$\rho^{1/3}$ =	2.75	3.4				1.122	1.516	2.485	3.350	1.386
	0.452	2.35	4.6				0.960	1.295	2.123	2.865	
		1.80	8.3				0.735	0.993	1.625	2.195	
		1.38	15.0				0.564	0.761	1.246	1.684	
		2.03	4.0				0.829	1.119	1.834	2.470	
		1.48	9.4				0.605	0.816	1.339	1.805	
		1.00	20.8				0.408	0.551	0.904	1.220	

TABLE A-4--Continued

ρ	$\rho^{1/3}$	H_i	t_{ig}	$\bar{\alpha}$	$\bar{\bar{\alpha}}$	H_a	$\bar{H}_a$	$\frac{H_a}{\rho^{1/3}}$	correct	$H_R = \bar{H}_a - c.$	$\frac{H_R}{\rho^{1/3}}$
Balsa -- benzene flames											
0.074	0.420	2.22	1.3	0.753	0.810	1.67	1.798	3.98	0.130	1.668	3.97
0.089	0.447	1.70	1.8			1.28	1.38	2.86	0.138	1.142	2.55
0.086	0.442	1.02	11.2			0.768	0.826	1.74	0.146	0.680	1.54
0.070	0.412	0.83	26.0			0.625	0.672	1.52	0.153	0.519	1.26
0.103	0.469	0.88	20.0			0.663	0.713	1.41	0.151	0.562	1.20
0.112	0.482	1.05	9.10			0.791	0.850	1.64	0.145	0.705	1.46
0.103	0.469	1.29	6.0			0.971	1.045	2.07	0.140	0.905	1.93
0.099	0.463	1.56	2.5			1.175	1.264	2.54	0.135	1.129	2.44
0.106	0.474	1.58	2.5			1.190	1.280	2.51	0.134	1.146	2.42
0.100	0.464	2.12	1.0			1.596	1.717	3.45	0.130	1.587	3.42

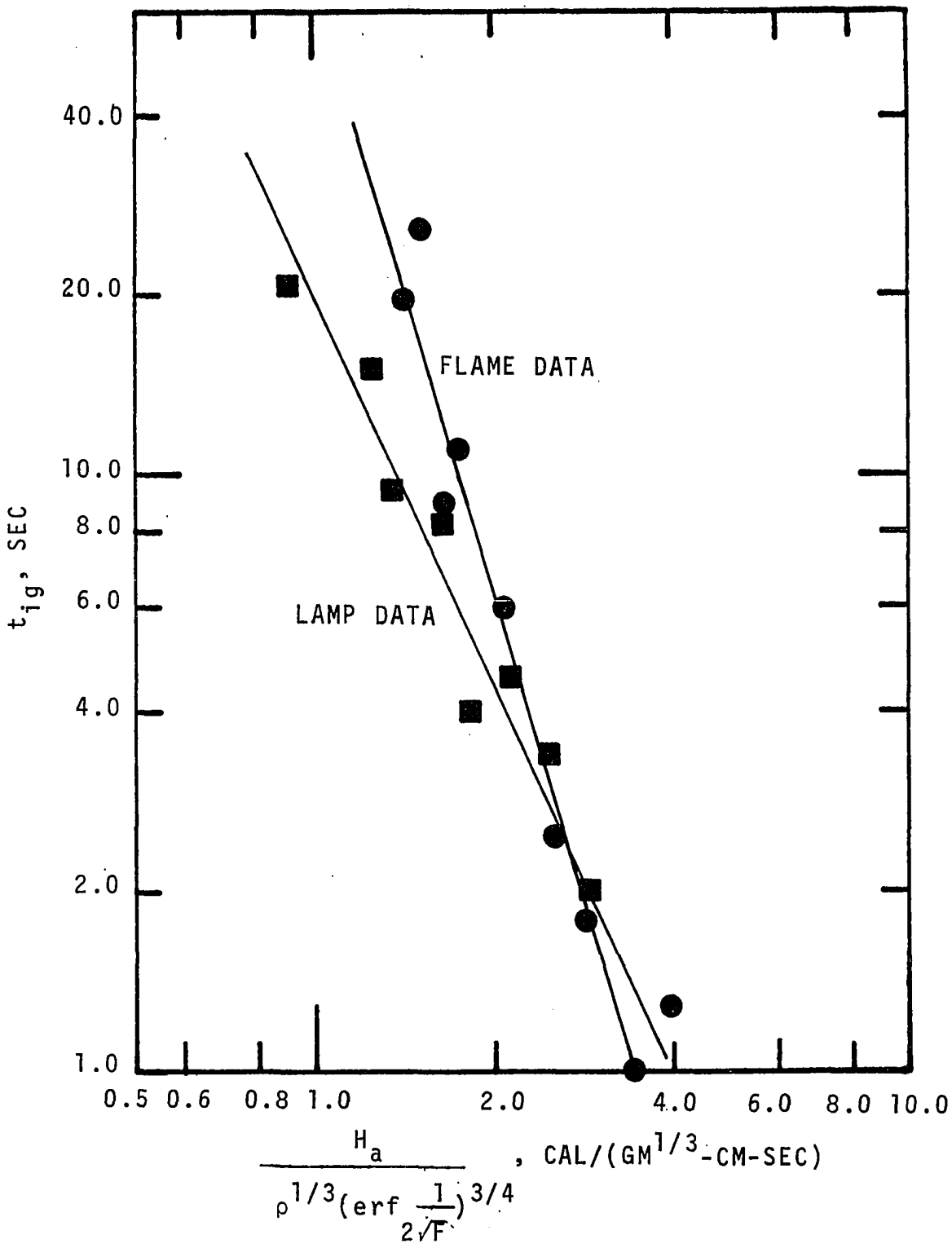

Figure A-1. The Variation of the Ignition Time with the Initially Absorbed Irradiance Corrected for Density and Thickness Effects for Balsa (39).

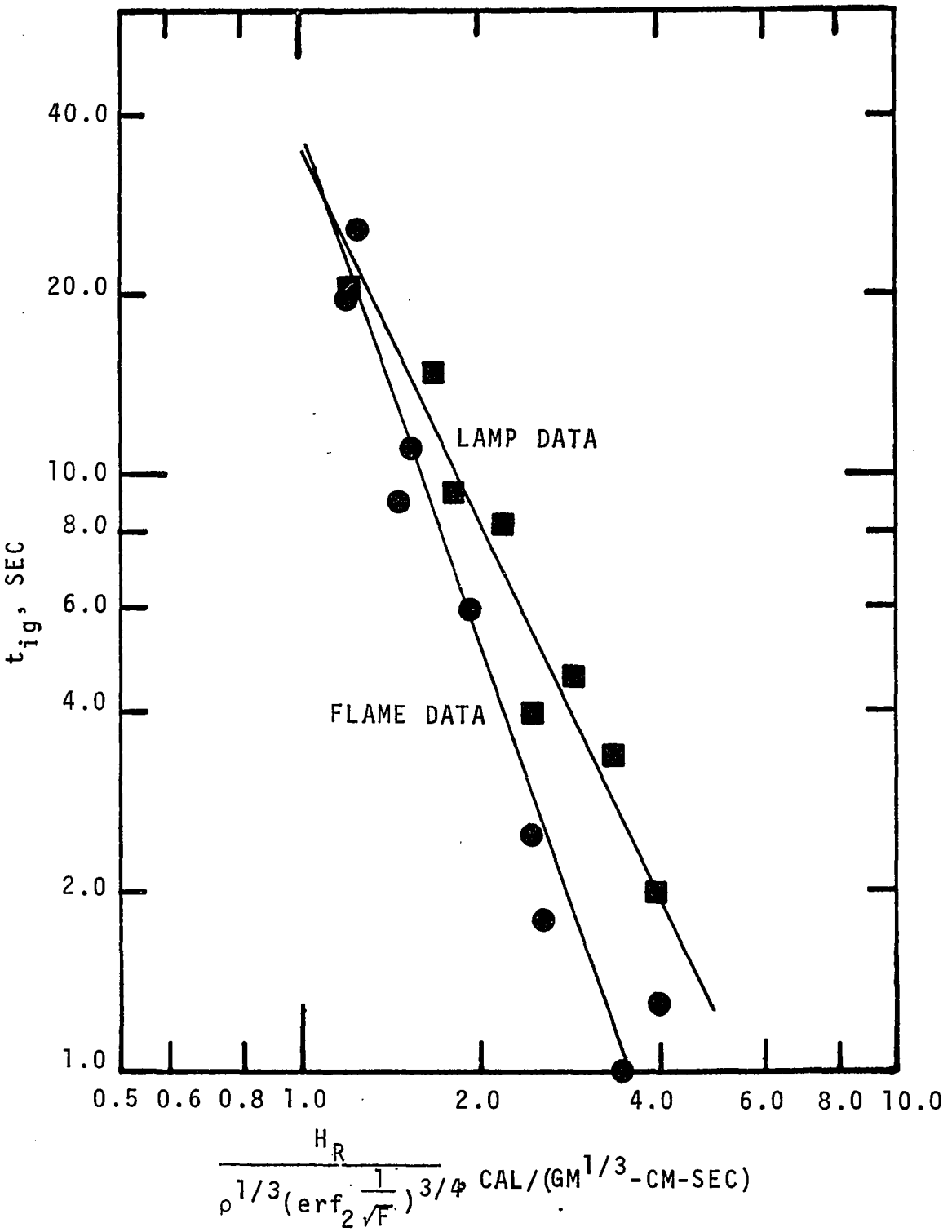

Figure A-2. The Variation of Ignition Time with Retained Energy Corrected for Density and Thickness Effects for Balsa (39).

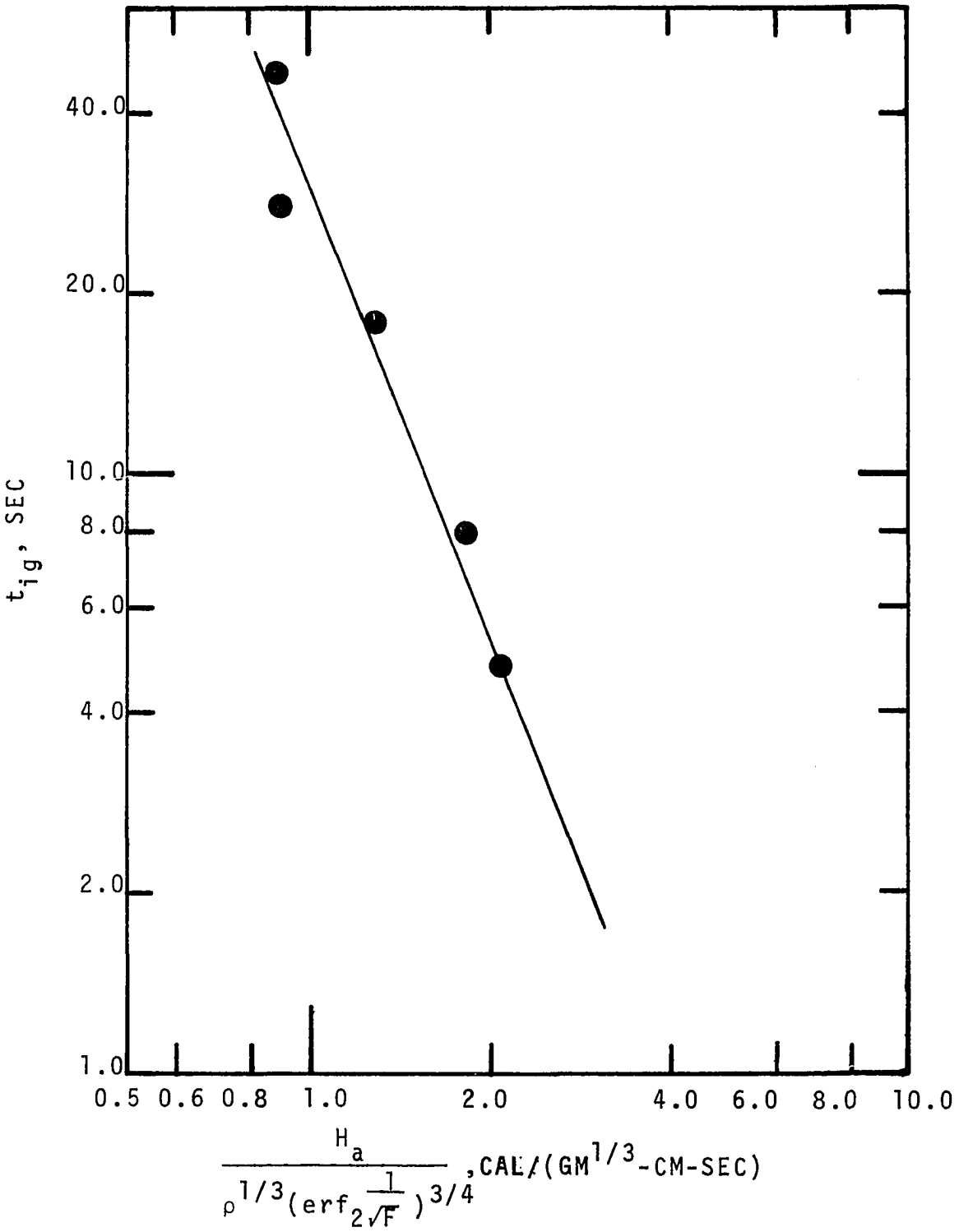

Figure A-3. The Variation of Ignition Time with Initially Absorbed Irradiance Corrected for Density and Thickness Effects for Redgum (39).

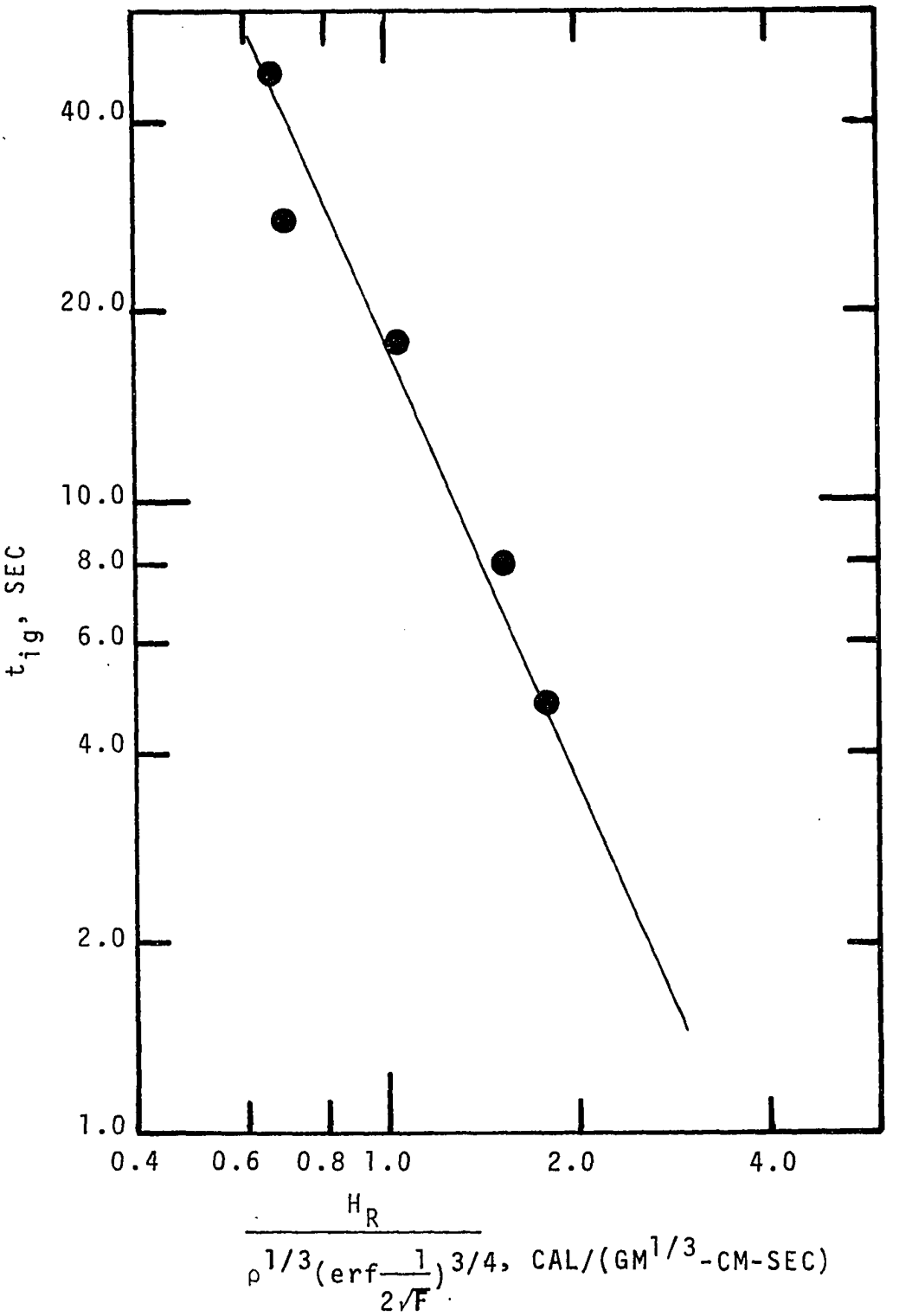

Figure A-4. The Variation of Ignition Time with Retained Energy Corrected for Density and Thickness Effects for Redgum (39).

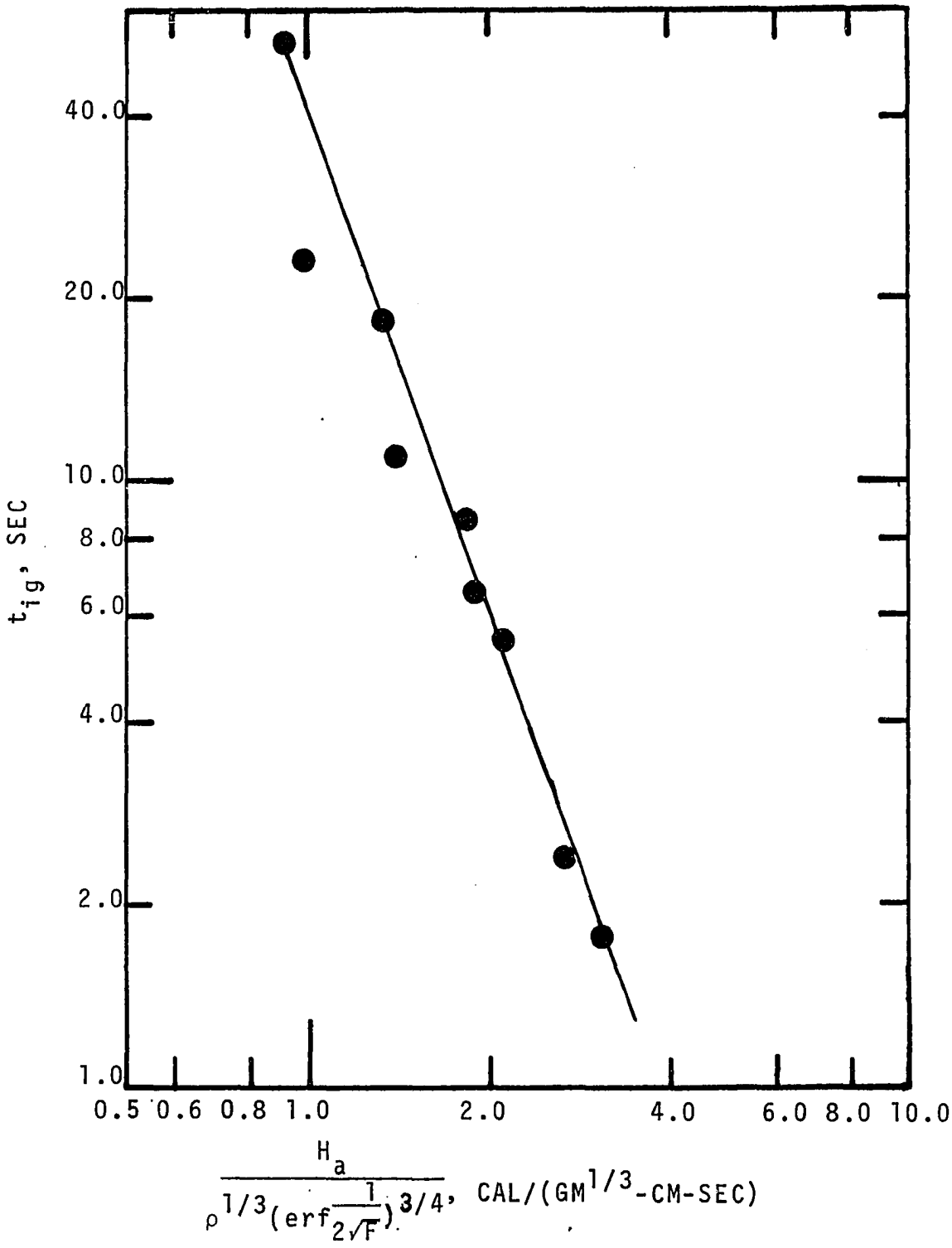

Figure A-5. The Variation of Ignition Time with Initially Absorbed Irradiance Corrected for Density and Thickness Effects for Ash (39).

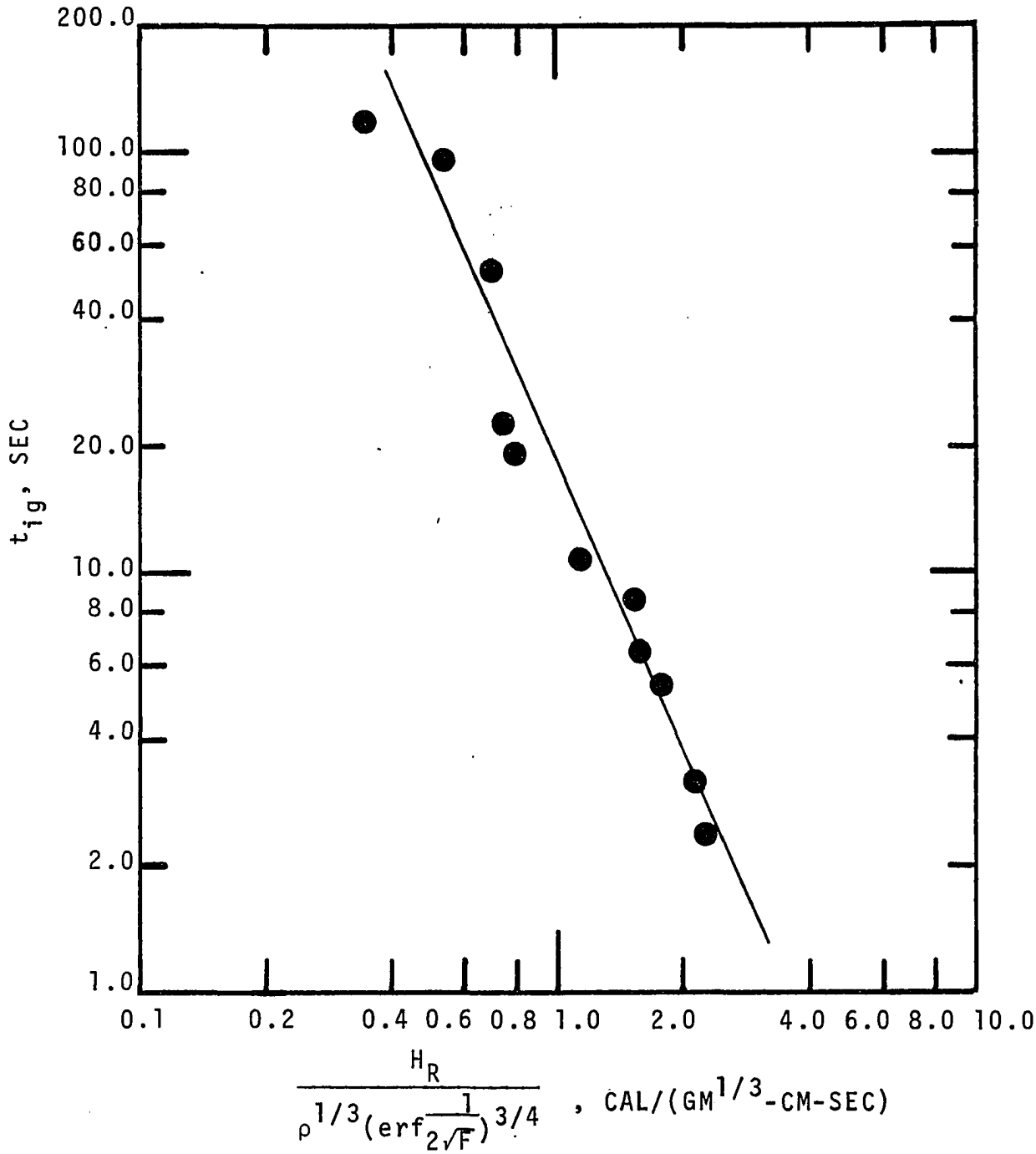

Figure A-6. The Variation of Ignition Time with Initially Absorbed Irradiance Corrected for Density and Thickness Effects for Ash (39).

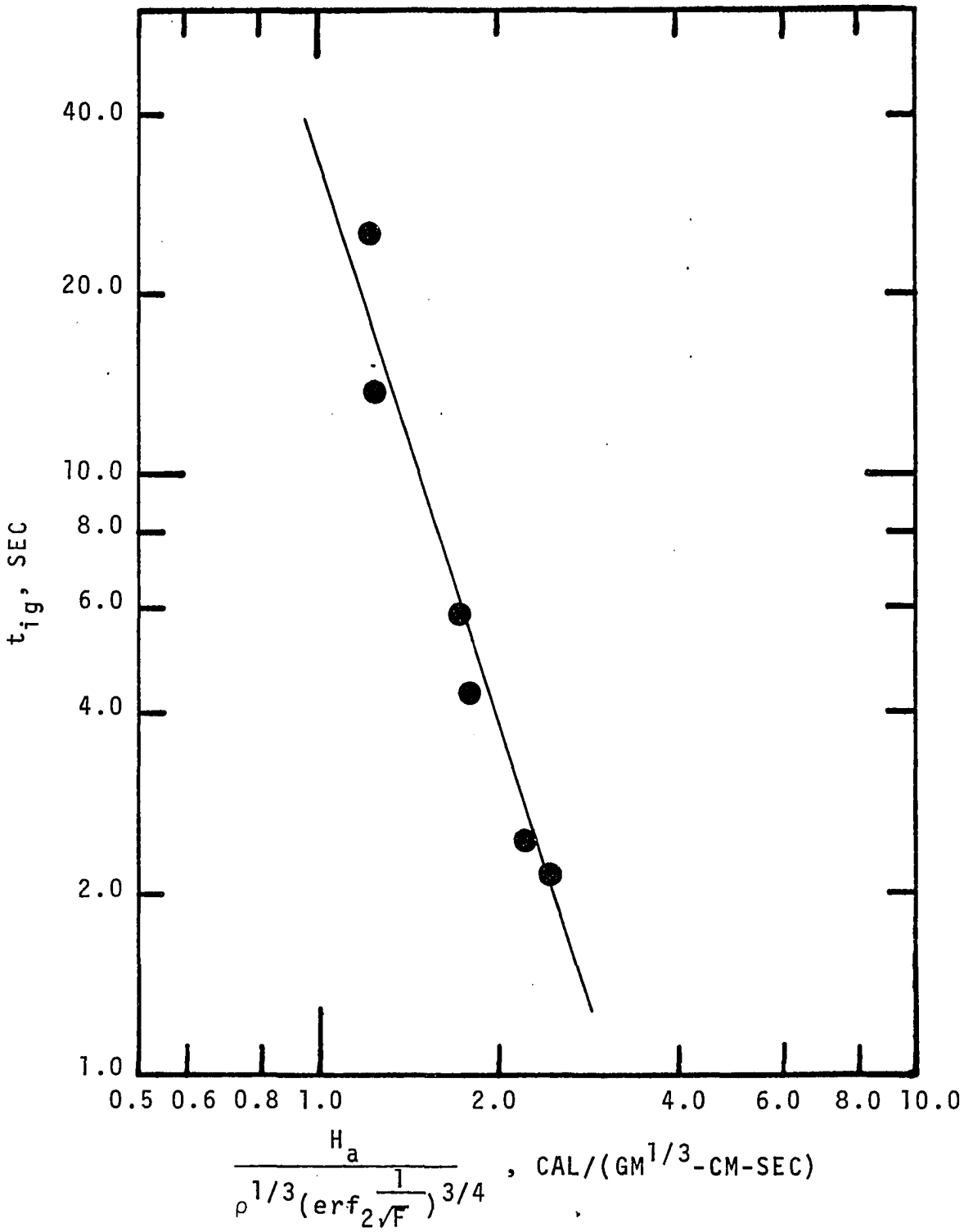

Figure A-7. The Variation of Ignition Time with Initially Absorbed Irradiance Corrected for Density and Thickness Effects for Oak (39).

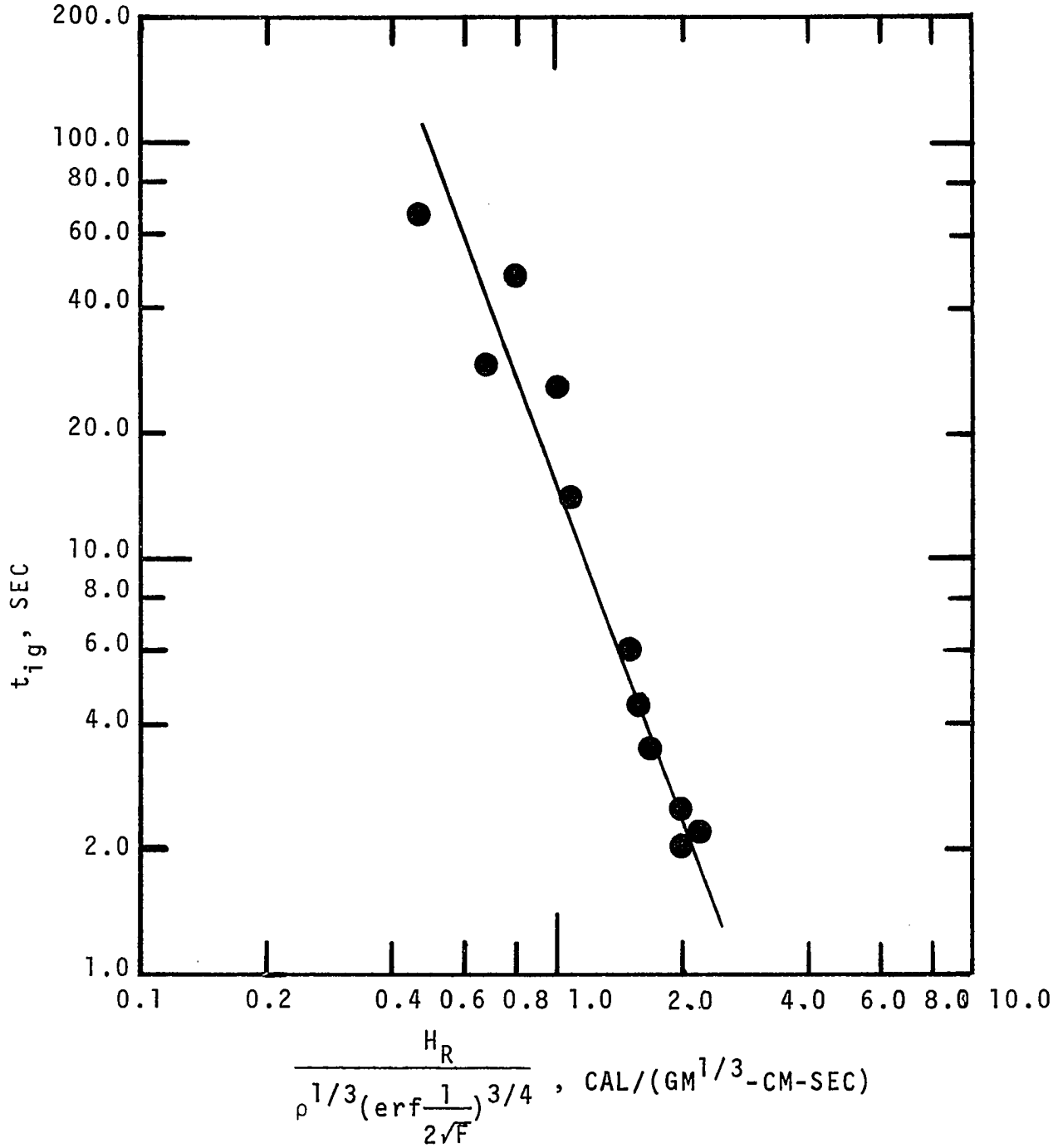

Figure A-8. The Variation of Ignition Time with Retained Energy Corrected for Density and Thickness Effects (39).

TABLE A-5

CORRECTIONS ON WESSON'S IGNITION DATA TO ACCOUNT FOR THICKNESS DIFFERENCES

Material	δ	$\alpha x 10^3$	ρ	$2\sqrt{\alpha t}$	$\frac{\delta}{2\sqrt{\alpha t}}$	erf $\frac{\delta}{2\sqrt{\alpha t}}$	erf 3/4	t_{ig}	H_a
B3/32-1	0.2388	1.765	0.197	0.084	2.85	1.0	1.0	1	2.00
				0.1188	2.01	1.0	1.0	2	1.63
	slope = 2.61		$\rho^{1/3}$=	0.1880	1.271	0.9275	0.945	5	1.18
			0.582	0.2056	1.161	0.8991	0.9236	6	1.09
				0.2378	1.005	0.8447	0.881	8	0.949
				0.2656	0.901	0.7969	0.8437	10	0.854
B3/32-2	0.2380		0.174		2.835	1.0	1.0	1	1.93
					2.005	1	1	2	1.56
			$^{1/3}$=		1.265	0.9275	0.945	5	1.13
			0.558		1.159	0.8991	0.9236	6	1.04
					1.001	0.8447	0.881	8	0.909
					0.897	0.7969	0.8437	10	0.819
B3/32-3	0.2385		0.139		2.84	1	1	1	1.79
					2.010	1	1	2	1.45
	slope = 2.32		$\rho^{1/3}$=		1.27	0.9275	0.945	5	1.05
			0.518		1.161	0.8991	0.9236	6	0.966
					1.005	0.8447	0.881	8	0.844
					0.900	0.7969	0.8437	10	0.760
B3/32-4	0.2384	1.765	0.132		2.84	1	1	1	1.76
					2.01	1	1	2	1.43
	slope = 2.21		$\rho^{1/3}$=		1.27	0.9275	0.945	5	1.03
			0.510		1.161	0.8991	0.9236	6	0.951
					1.005	0.8447	0.881	8	0.831
					0.900	0.7969	0.8437	10	0.749

TABLE A-5--Continued

Material	δ	$\alpha x 10^3$	ρ	$2\sqrt{\alpha t}$	$\frac{\delta}{2\sqrt{\alpha t}}$	erf $\frac{\delta}{2\sqrt{\alpha t}}$	erf 3/4	t_{ig}	H_a
B3/32-5	0.2388		0.132		2.85	1	1	1	1.73
					2.01	1	1	2	1.41
	slope = 2.25		$\rho^{1/3}$=		1.271	0.9275	0.945	5	1.02
			0.502		1.161	0.8991	0.9236	6	0.937
					1.005	0.8447	0.881	8	0.818
					0.901	0.7969	0.8437	10	0.737
B3/32-6	0.2385		0.1193		2.84	1	1	1	1.70
					2.01	1	1	2	1.38
	slope = 2.21		$\rho^{1/3}$=		1.27	0.9275	0.945	5	0.995
			0.492		1.161	0.8991	0.9236	6	0.918
					1.005	0.8447	0.881	8	0.802
					0.900	0.7969	0.8437	10	0.722
B1/16-1	0.1621	1.765	0.170	0.084	1.93	0.9937	0.9953	1	1.73
				0.1188	1.363	0.9462	0.9594	2	1.35
			$\rho^{1/3}$=	0.1880	0.862	0.7772	0.828	5	0.893
	slope = 1.94		0.504	0.2056	0.788	0.7348	0.792	6	0.806
				0.2378	0.682	0.6652	0.736	8	0.686
				0.2656	0.610	0.6117	0.692	10	0.607
B1/16-2	0.1620		0.145		1.93	0.9937	0.9953	1	1.81
					1.363	0.9462	0.9594	2	1.41
	slope = 2.02		$\rho^{1/3}$=		0.862	0.7772	0.828	5	0.932
			0.526		0.788	0.7348	0.792	6	0.842
					0.682	0.6652	0.736	8	0.716
					0.610	0.6117	0.692	10	0.633

TABLE A-5--Continued

Material	δ	$\alpha x 10^3$	ρ	$2\sqrt{\alpha t}$	$\frac{\delta}{2\sqrt{\kappa t}}$	erf $\frac{\delta}{2\sqrt{\alpha t}}$	erf 3/4	t_{ig}	H_a
B1/16-3	0.1626		0.100		1.935	0.9938	0.99534	1	1.59
					1.370	0.9473	0.9592	2	1.25
	slope = 1.79		$\rho^{1/3}$=		0.865	0.7787	0.829	5	0.823
			0.464		0.791	0.7367	0.796	6	0.746
					0.684	0.6666	0.738	8	0.633
					0.613	0.6139	0.694	10	0.560
B1/16-4	0.1618	1.765	0.0994	0.084	1.93	0.9937	0.9953	1	1.59
				0.1188	1.363	0.9462	0.9594	2	1.25
	slope = 1.79		$\rho^{1/3}$=	0.1880	0.862	0.7772	0.828	5	0.822
			0.464	0.2056	0.788	0.7348	0.792	6	0.742
				0.2378	0.682	0.6652	0.736	8	0.632
				0.2656	0.610	0.6117	0.692	10	0.559
B1/16-5	0.1615		0.1055		1.923	0.9934	0.9950	1	1.62
					1.360	0.9456	0.9590	2	1.27
	slope = 1.82		$\rho^{1/3}$=		0.860	0.7761	0.827	5	0.837
			0.473		0.786	0.7336	0.792	6	0.757
					0.680	0.6638	0.735	8	0.643
					0.608	0.6101	0.690	10	0.568
B1/16-6	0.1620		0.104		1.93	0.9937	0.9953	1	1.61
					1.363	0.9462	0.9594	2	1.26
	slope = 1.82		$\rho^{1/3}$=		0.862	0.7772	0.828	5	0.833
			0.470		0.788	0.7348	0.792	6	0.752
					0.682	0.6652	0.736	8	0.640
					0.610	0.6117	0.692	10	0.566

TABLE A-5--Continued

Material	δ	$\alpha x 10^3$	ρ	$2\sqrt{\alpha t}$	$\frac{\delta}{2\sqrt{\alpha t}}$	erf $\frac{\delta}{2\sqrt{\alpha t}}$	erf 3/4	t_{ig}	H_a
A-1	0.344	1.473	0.591	0.0768	4.48	1.0	1.0	1	3.19
				0.1086	3.17	1.0	1.0	2	2.23
			$\rho^{1/3}$=	0.1716	2.01	1.0	1.0	5	1.49
			0.8395	0.2428	1.415	0.9545	0.9656	10	1.05
				0.3435	1.00	0.8427	0.8795	20	0.709
				0.4204	0.82	0.7538	0.8090	30	0.764
				0.4856	0.71	0.6847	0.7530	40	0.449
				0.5944	0.58	0.5879	0.6695	60	0.332
A-2	0.245	1.473	0.597	0.0768	3.19	1.0	1.0	1	3.20
				0.1086	2.26	1.0	1.0	2	2.24
			$\rho^{1/3}$=	0.1716	1.43	0.9569	0.9675	5	1.44
			0.8423	0.2428	1.01	0.8468	0.8830	10	0.967
				0.3435	0.71	0.6847	0.7530	20	0.609
				0.4204	0.58	0.5879	0.6715	30	0.636
				0.4856	0.50	0.5205	0.6130	40	0.367
				0.5944	0.41	0.4380	0.5381	60	0.267
A-3	0.2495	1.473	0.581	0.0768	3.25	1.0	1.0	1	3.170
				0.1086	2.30	1.0	1.0	2	2.22
			$\rho^{1/3}$=	0.1716	1.455	0.9604	0.9702	5	1.43
			0.835	0.2428	1.027	0.8576	0.891	10	0.967
				0.3435	0.73	0.6981	0.764	20	0.612
				0.4204	0.59	0.5959	0.678	30	0.637
				0.4856	0.51	0.5292	0.620	40	0.368
				0.5944	0.42	0.4475	0.5470	60	0.269

TABLE A-5--Continued

Material	δ	$\alpha x 10^3$	ρ	$2\sqrt{\alpha t}$	$\frac{\delta}{2\sqrt{\alpha t}}$	erf $\frac{\delta}{2\sqrt{\alpha t}}$	erf 3/4	t_{ig}	H_a
A-4	0.281	1.473	0.590	0.0768	3.66	1.0	1.0	1	3.185
				0.1086	2.59	1.0	1.0	2	2.490
			$\rho^{1/3}$=	0.1716	1.64	0.9796	0.9834	5	1.46
			0.839	0.2428	1.155	0.8976	0.9220	10	1.010
				0.3435	0.82	0.7538	0.8090	20	0.652
				0.4204	0.67	0.6566	0.7296	30	0.689
				0.4856	0.58	0.5879	0.6715	40	0.400
				0.5944	0.47	0.4937	0.5890	60	0.292
A-5	0.296	1.473	0.577	0.0768	3.85	1.0	1.0	1	3.165
				0.1086	2.73	1.0	1.0	2	2.22
			$\rho^{1/3}$=	0.1716	1.725	0.9853	0.9895	5	1.46
			0.833	0.2428	1.22	0.9155	0.9360	10	1.01
				0.3435	0.86	0.7761	0.8268	20	0.661
				0.4204	0.70	0.6778	0.7465	30	0.700
				0.4856	0.61	0.6117	0.6917	40	0.409
				0.5944	0.50	0.5205	0.6125	60	0.301
A-6	0.244	1.473	0.570	0.0768	3.19	1.0	1.0	1	3.153
				0.1086	2.26	1.0	1.0	2	2.21
			$\rho^{1/3}$=	0.1716	1.43	0.9569	0.9675	5	1.42
			0.8296	0.2428	1.01	0.8468	0.8830	10	0.952
				0.3435	0.71	0.6847	0.7530	20	0.600
				0.4204	0.58	0.5879	0.6715	30	0.627
				0.4856	0.50	0.5205	0.6130	40	0.361
				0.5944	0.41	0.4380	0.5381	60	0.263

TABLE A-5--Continued

Material	δ	$\alpha x 10^3$	ρ	$2\sqrt{\alpha t}$	$\frac{\delta}{2\sqrt{\alpha t}}$	erf $\frac{\delta}{2\sqrt{\alpha t}}$	erf 3/4	t_{ig}	H_a
G-1	0.1517	1.398	0.390	0.0748	2.03	1.0	1.0	1	1
				0.1057	1.435	0.9576	0.968	2	1.84
			$\rho^{1/3}$=	0.1672	0.907	0.8004	0.846	5	1.08
			0.731	0.2364	0.642	0.6210	0.700	10	0.655
				0.3348	0.45	0.4755	0.5725	20	0.398
				0.4096	0.37	0.3992	0.5020	30	0.294
				0.4730	0.32	0.3491	0.4540	40	0.232
G-2	0.1904	1.398	0.381	0.0748	2.55	1.0	1.0	1	1
				0.1057	1.801	0.9891	0.9917	2	1.87
			$\rho^{1/2}$=	0.1672	1.139	0.8927	0.9183	5	1.16
			0.7250	0.2364	0.805	0.7450	0.802	10	0.744
				0.3348	0.570	0.5798	0.665	20	0.458
				0.4096	0.465	0.4892	0.585	30	0.339
				0.4730	0.40	0.4284	0.530	40	0.269
G-3	0.1757	1.398	0.383	0.0748	2.35	1.0	1.0	1	2.775
				0.1057	1.662	0.9812	0.9859	2	1.86
			$\rho^{1/2}$=	0.1672	1.051	0.8628	0.890	5	1.13
			0.7265	0.2364	0.743	0.7066	0.771	10	0.717
				0.3348	0.525	0.5421	0.632	20	0.436
				0.4096	0.43	0.4569	0.556	30	0.323
				0.4730	0.37	0.3992	0.5020	40	0.255
G-4	0.1880	1.398	0.374	0.0748	2.51	1.0	1.0	1	2.752
				0.1057	1.779	0.9881	0.991	2	1.86
			$\rho^{1/2}$=	0.1672	1.124	0.8880	0.9194	5	1.15
			0.7205	0.2364	0.795	0.7391	0.797	10	0.735
				0.3348	0.56	0.5716	0.6574	20	0.450
				0.4096	0.46	0.4847	0.581	30	0.335
				0.4730	0.40	0.4284	0.530	40	0.267

TABLE A-5--Continued

Material	δ	$\alpha x 10^3$	ρ	$2\sqrt{\alpha t}$	$\frac{\delta}{2\sqrt{\alpha t}}$	erf $\frac{\delta}{2\sqrt{\alpha t}}$	erf 3/4	t_{ig}	H_a
G-5	0.2065	1.398	0.378	0.0748	2.76	1.0	1.0	1	2.762
				0.1057	1.954	0.9942	0.99565	2	1.87
			$\rho^{1/3}$=	0.1672	1.235	0.9192	0.9388	5	1.18
			0.723	0.2364	0.874	0.7834	0.833	10	0.771
				0.3348	0.62	0.6194	0.698	20	0.479
				0.4096	0.504	0.5250	0.6165	30	0.357
				0.4730	0.440	0.4662	0.564	40	0.285
G-6	0.1695	1.398	0.371	0.0748	2.27	1.0	1.0	1	2.747
				0.1057	1.604	0.9767	0.9825	2	1.84
			$\rho^{1/3}$=	0.1672	1.014	0.8484	0.884	5	1.11
			0.719	0.2364	0.717	0.6894	0.756	10	0.696
				0.3348	0.51	0.5292	0.620	20	0.423
				0.4096	0.41	0.4380	0.5385	30	0.310
				0.4730	0.36	0.3893	0.4925	40	0.248
O-1	0.2690	1.555	0.648	0.0789	3.42	1.0	1.0	1	2.718
				0.1116	2.41	1.0	1.0	2	2.164
			$\rho^{1/3}$=	0.1764	1.528	0.9692	0.9768	55	1.581
			0.8655	0.2494	1.081	0.8737	0.9036	10	1.173
				0.3528	0.76	0.7175	0.7795	20	0.810
				0.4320	0.62	0.6194	0.6980	30	0.634
				0.4988	0.54	0.5549	0.6430	40	0.531
O-2	0.270	1.555	0.711	0.0789	3.42	1.0	1.0	1	2.803
				0.1116	2.41	1.0	1.0	2	2.232
			$\rho^{1/3}$=	0.1764	1.528	0.9692	0.9768	5	1.631
			0.8928	0.2494	1.081	0.8737	0.9036	10	1.210
				0.3528	0.76	0.7175	0.7795	20	0.835
				0.4320	0.625	0.6242	0.7020	30	0.658
				0.4988	0.54	0.5549	0.6430	40	0.548

TABLE A-5--Continued

Material	δ	$\alpha x 10^3$	ρ	$2\sqrt{\alpha t}$	$\frac{\delta}{2\sqrt{\alpha t}}$	erf $\frac{\delta}{2\sqrt{\alpha t}}$	erf 3/4	t_{ig}	H_a
O-3	0.2455	1.555	0.720	0.0789	3.11	1.0	100	1	2.815
				0.1116	2.20	1.0	1.0	2	2.241
			$\rho^{1/3}$=	0.1764	1.392	0.9510	0.963	5	1.614
			0.8965	0.2494	0.984	0.8360	0.8743	10	1.176
				0.3528	0.696	0.6750	0.7447	20	0.801
				0.4320	0.57	0.5798	0.6643	30	0.625
				0.4988	0.49	0.5117	0.6045	40	0.518
O-4	0.2810	1.555	0.655	0.0789	3.56	1.0	1.0	1	2.727
				0.1116	2.52	1.0	1.0	2	2.172
			$\rho^{1/3}$=	0.1764	1.593	0.9759	0.974	5	1.582
			0.8686	0.2494	1.127	0.8889	0.9155	10	1.193
				0.3528	0.80	0.7421	0.8159	20	0.850
				0.4320	0.65	0.6420	0.7175	30	0.652
				0.4988	0.56	0.5716	0.6570	40	0.545
O-5	0.2445	1.555	0.700	0.0789	3.10	1.0	1.0	1	2.788
				0.1116	2.19	1.0	1.0	2	2.220
			$\rho^{1/3}$=	0.1764	1.386	0.9500	0.9623	5	1.598
			0.888	0.2494	0.980	0.8342	0.873	10	1.163
				0.3528	0.693	0.6729	0.743	20	0.792
				0.4320	0.566	0.5765	0.6620	30	0.617
				0.4988	0.49	0.5117	0.6050	40	0.513
O-6	0.2405	1.555	0.677	0.0789	3.05	1.0	1.0	1	2.758
				0.1116	2.16	1.0	1.0	2	2.200
			$\rho^{1/3}$=	0.1764	1.363	0.9461	0.9593	5	1.576
			0.8783	0.2494	0.964	0.8272	0.8636	10	1.138
				0.3528	0.68	0.6638	0.7353	20	0.775
				0.4320	0.557	0.5691	0.6550	30	0.604
				0.4988	0.482	0.5045	0.5990	40	0.475

TABLE A-5--Continued

Material	δ	$\alpha x 10^3$	ρ	$2\sqrt{\alpha t}$	$\frac{\delta}{2\sqrt{\alpha t}}$	erf $\frac{\delta}{2\sqrt{\alpha t}}$	erf 3/4	t_{ig}	H_a
B1/16-7	0.1468	1.765	0.1686	0.084	1.748	0.9865	0.9899	1	1.889
				0.1188	1.236	0.9195	0.9390	2	1.454
	slope = 2.02		$1/3_=$	0.1880	0.781	0.7306	0.7902	5	0.935
			0.553	0.2056	0.714	0.6872	0.7548	6	0.843
				0.2378	0.617	0.6172	0.6963	8	0.712
				0.2656	0.553	0.5658	0.6524	10	0.628
B1/16-8	0.1490	1.765	0.1503	0.084	1.774	0.9879	0.9909	1	1.819
				0.1188	1.254	0.9239	0.9424	2	1.404
	slope = 1.96		$1/3_=$	0.1880	0.793	0.7379	0.7962	5	0.906
			0.532	0.2056	0.725	0.6948	0.7610	6	0.818
				0.2378	0.627	0.6247	0.7027	8	0.692
				0.2656	0.561	0.5734	0.6589	10	0.610
B1/16-9	0.1470	1.765	0.1823	0.084	1.750	0.9867	0.9900	1	1.937
				0.1188	1.237	0.9198	0.9392	2	1.491
	slope = 2.08		$1/3_=$	0.1880	0.782	0.7312	0.7907	5	0.959
			0.567	0.2056	0.715	0.6881	0.7555	6	0.865
				0.2378	0. 8	0.6179	0.6969	8	0.731
				0.2656	0.553	0.5658	0.6524	10	0.644
B1/16-10	0.1468	1.765	0.1821	0.084	1.748	0.9865	0.9899	1	1.936
				0.1188	1.236	0.9195	0.9390	2	1.491
	slope = 2.08		$1/3_=$	0.1880	.781	0.7306	0.7902	5	0.959
			0.567	0.2056	0.714	0.6872	0.7548	6	0.864
				0.2378	0.617	0.6171	0. 963	8	0.730
				0.2656	0.553	0.5688	0.6524	10	0.644

TABLE A-5--Continued

Material	δ	$\alpha x 10^3$	ρ	$2\sqrt{\alpha t}$	$\frac{\delta}{2\sqrt{\alpha t}}$	erf $\frac{\delta}{2\sqrt{\alpha t}}$	erf 3/4	t_{ig}	H_a
B1/16-11	0.1490	1.765	0.1783		1.774	0.9879	0.9909	1	1.925
					1.254	0.9239	0.9424	2	1.486
	slope = 2.08		$\rho^{1/3}$=		0.793	0.7379	0.7962	5	0.959
			0.563		0.725	0.6948	0.7610	6	0.865
					0.627	0.6247	0.7027	8	0.732
					0.561	0.5734	0.6589	10	0.645
B1/16-12	0.1475	1.765	0.1852		1.756	0.9870	0.9902	1	1.947
					1.242	0.9210	0.9401	2	1.500
	slope = 2.08		$\rho^{1/3}$=		0.785	0.7330	0.7922	5	0.966
			0.570		0.717	0.6894	0.7566	6	0.871
					0.620	0.6194	0.6982	8	0.736
					0.555	0.5674	0.6538	10	0.648
B3/32-7	0.2395	1.765	0.1319	0.084	2.85	1.0	1.0	1	1.756
				0.1188	2.02	1.0	1.0	2	1.425
	slope = 2.28		$\rho^{1/3}$=	0.1880	1.274	0.9284	0.9458	5	1.030
			0.509	0.2056	1.165	0.9005	0.9244	6	0.950
				0.2378	1.007	0.8455	0.8817	8	0.830
				0.2656	0.902	0.7979	0.8442	10	0.748
B3/32-8	0.2390	1.765	0.1300		2.85	1.0	1.0	1	1.749
					2.01	1.0	1.0	2	1.420
	slope = 2.28		$\rho^{1/3}$=		1.271	0.9277	0.9453	5	1.026
			0.507		1.162	0.8996	0.9237	6	0.946
					1.005	0.8447	0.8811	8	0.826
					0.900	0.7969	0.8434	10	0.744

TABLE A-5--Continued

Material	δ	$\alpha x 10^3$	ρ	$2\sqrt{\alpha t}$	$\frac{\delta}{2\sqrt{\alpha t}}$	erf $\frac{\delta}{2\sqrt{\alpha t}}$	erf 3/4	t_{ig}	H_a
B3/32-9	0.2360	1.765	0.1856		2.81	1.0	1.0	1	1.970
					1.987	0.9951	0.9963	2	1.593
	slope = 2.55		$\rho^{1/3}$=		1.255	0.9241	0.9425	5	1.152
			0.571		1.148	0.8955	0.9206	6	1.062
					0.992	0.8393	0.8769	8	0.926
					0.889	0.7912	0.8389	10	0.833
B3/32-10	0.2370	1.765	0.2045	0.084	2.82	1.0	1.0	1	2.032
				0.1188	1.995	0.9952	0.9964	2	1.643
	slope = 2.63		$\rho^{1/2}$=	0.1880	1.261	0.9254	0.9435	5	1.189
			0.589	0.2056	1.153	0.8970	0.9217	6	1.097
				0.2378	0.997	0.8414	0.8785	8	0.957
				0.2656	0.892	0.7928	0.8402	10	0.861
B3/32-11	0.2360	1.765	0.2111		2.81	1.0	1.0	1	2.056
					1.987	0.9951	0.9963	2	1.663
	slope = 2.66		$\rho^{1/3}$=		1.255	0.9241	0.9425	5	1.202
			0.596		1.148	0.8955	0.9206	6	1.108
					0.992	0.8373	0.8769	8	0.967
					0.889	0.7912	0.8389	10	0.870
B3/32-12	0.2365	1.765	0.1882		2.82	1.0	1.0	1	1.977
					1.991	0.9951	0.9963	2	1.598
	slope = 2.55		$\rho^{1/3}$=		1.258	0.9247	0.9430	5	1.156
			0.573		1.150	0.8961	0.9210	6	1.066
					0.995	0.8406	0.8779	8	0.931
					0.890	0.7918	0.8394	10	0.837

APPENDIX B

TABLE OF FLAMMABILITY TESTS

Identification and Title	Sponsoring Organization	Date	Intended Application	Number of Specimens	Selection of Specimen	Size of Specimen	Exposed Area of Specimen	Pretest Treatment and Conditioning	Size of Test Enclosure	Ventilation or Air Supply
Method 5900 Fed. Spec. CCC-T-191b, "Flame Resistance of Cloth; Horizontal".	Gen. Servs. Admin.	15 May, 1951	Flame proofed & fire resistant fabrics & some untreated fabrics with very open weave	2;(1 ea. from warp & filling directions).	Length parallel to warp or filling directions.	7x10-in.	6 x 9-in.	Circulating air at 140 to 145°F for 4 ± ⅛ hr.	An enclosure to protect from draft.	Room atmosphere.
Method 5902 Fed. Spec. CCC-T-191b, "Flame Resistance of Cloth; Vertical".	Gen. Servs. Admin.	15 May, 1951	Flame proofed & fire resistant fabrics other than pile fabrics.	10;(5 ea. from warp & filling directions).	Length parallel to warp or filling directions.	2¾x12-in.	2 x 12-in.	70 ± 2°F, 65 ± 12% RH for 4 hrs. min.	Sheet-metal cabinet 12 to 14-in. wide, 12 to 14-in. deep 30-in. high.	Approx. ½-in. dia. holes at top and bottom.
Method 5904 Fed. Spec. CCC-T-191b, "Flame Resistance of Cloth; Vertical, Field".	Gen. Servs. Admin.	15 May, 1951	Flame proofed and fire resistant fabrics other than pile fabrics.	3	None	Any size with exposed edge.	2 x 5-in.	None specified.	No enclosure.	Room atmosphere.
Method 5903T Fed. Spec. CCC-T-191b, "Flame Resistance of Cloth; Modified".	Gen. Servs. Admin.	15 Jan, 1959	Flame proofed and fire-resistant fabrics other than pile fabrics.	10;(5 ea. from warp & filling directions).	Length parallel to warp or filling directions.	2¾x12-in.	2 x 12-in.	70 + 2°F, 65 ± 2% RH for 16 hrs. min.	Sheet-metal cabinet, 12 to 14-in. wide, 12 to 14-in. deep 30-in. high.	Approx. ½-in. dia. holes at top and bottom.
Method 5906 Fed. Spec. CCC-T-191b, "Burning Rate of Cloth; Horizontal".	Gen. Servs. Admin.	15 May, 1951 •	Cloth that has not been flame proofed, including pile and napped cloth.	5, provided difference between results for any 2 is less than 40% from average of those tested; otherwise 10.	Length parallel to the more hazardous direction.	4½x12½-in.	2 x 12½-in.	Circulating air at 140 to 145°F for 4 ± ½ hr.	Metal cabinet 8-in. wide, 15-in. long, 14-in. high, kept at 140°F by heaters.	½-in. clearance all around top; 5 equidistant ¾-in. holes along each side at bottom.
Method 5908 Fed. Spec. CCC-T-191b, "Burning Rate of Cloth; 45° Angle."	Gen. Servs. Admin.	15 May, 1951	Cloth that has not been flame proofed.	5	Length parallel to more hazardous direction.	2x6-in.	1½ x 6-in.	Circulating air at 140 to 145°F for 4 ± ½ hr.	Metal hood or cabinet (unspecified size).	Cabinet permits free ventilation.
Method 5910 Fed. Spec. CCC-T-191b, "Burning Rate of Cloth; 30° Angle".	Gen. Servs. Admin.	15 May, 1951	Cloth that has not been flame proofed and does not contain fibers or finishes which melt and cling.	6;(3 ea. from warp and filling directions). One only if material does not support combustion.	Length parallel to warp or filling directions.	1x6-in.	1 x 6-in.	Circulating air at 140 to 145°F for 4 ± ½ hr.	No enclosure.	Room atmosphere.
Method 2021 Fed. Test Method Std. No. 406 "Flammability of Plastics Over 0.050 Inch in Thickness".	Gen. Servs. Admin.	5 Oct. 1961	Rigid plastics in the form of sheets or molded bars over 0.050 in. thick.	10	At random (per Gen. Req.)	0.5x5-in.; actual thickness.	All exposed except area under clamp.	23 + 1.1°C (73.5 + 2°F) 50 ± 4% RH for 48 hrs. if less than ½-in. thick; 96 hrs. if thicker. (Per Gen. Req.)	Completely enclosed laboratory hood.	Exhaust fan is used only after test.
Method 2022 Fed. Test Method Std. No. 406 "Flammability of Plastics 0.050-in. and Under in Thickness".	Gen. Servs. Admin.	5 Oct, 1961	Plastics in the form of sheets or films 0.050-in. or less in thickness.	5 minimum	At random (per Gen. Req.)	1x18-in.	1 x 12-in.; (12-in. length is exposed below clamp).	23 + 1.1°C (73.5 + 2°F)50 + 4% RH for 48 hrs. (per Gen. Req.) 2 hr. at 23 + 3°C after fuse is attached.	Sheet-metal or other fire-resistant enclosure 12-in. wide; 12-in. deep; 30-in. high.	Open at top; 1-in. high opening around bottom.
Method 2023 Fed. Test Method Std. No. 406 "Flame Resistance".	Gen. Servs. Admin.	5 Oct, 1961	Plastics difficult to ignite; primarily those that are self-extinguishing by meth. 2021 & 2022.	5 (per Gen. Req.)	At random (per Gen. Req.)	0.5x0.5 x5.0-in.	Unsupported span not less than 4-in.	23+1.1°C (73.5± 2°F) 50+4% RH, for 48 hrs, if less than ½-in. thick; 96 hrs. if thicker (per Gen. Req.).	Enclosure of sufficient size to contain apparatus, and without draft.	Vent holes around sides near base and exhaust fan at top operating at min. suction.

COMPARISON OF FLAMMAB

	Size of Test Enclosure	Ventilation or Air Supply	Specimen Holder	Orientation of Specimen	Ignition Source	Location of Ignition Source	Time of Exposure	Method of Timing	Requirements for Validation	Criteria or Levels of Acceptability	It
ir °F	An enclosure to protect from draft.	Room atmosphere.	Metal frame mounted on corner legs.	Horizontal	0.3 ml. ethyl alcohol in specified cup; spark ignited.	3 in. below center of specimen.	Till alcohol fuel has burned.	None	None	None	Greatest burned h of char.
rs.	Sheet-metal cabinet 12 to 14-in. wide, 12 to 14-in. deep 30-in. high.	Approx. ¼-in. dia. holes at top and bottom.	Metal frame clamps long edges.	Vertical	Bunsen or Tirrill burner with 1½-in. high flame.	Top of burner 3/4-in. below end of specimen.	12 sec.	Stop-watch or other device (to 1/5 sec.).	None	None	Flaming t Char leng sample, a
	No enclosure.	Room atmosphere.	Two U-shaped matched plates of 1/16-in. sheet metal.	Vertical	Paraffin candle of 3/4-in. dia.	Candle vertical with top of wick 1/10-in. below edge of specimen.	12 sec.	Stop-watch or other device (to 1/5 sec.).	None	None	Average f Char leng
	Sheet-metal cabinet, 12 to 14-in. wide, 18 to 14-in. deep 30-in. high.	Approx. ¼-in. dia. holes at top and bottom.	Metal frame clamps long edges.	Vertical	Bunsen or Tirrill burner with 1½-in. high flame, using a specified gas.	Top of burner ¾-in. below end of specimen.	12 sec.	Stop-watch or other device (to 1/5 sec.).	None	None	Flaming ti Char lengt sample, an
	Metal cabinet 8-in. wide, 15-in. long, 14-in. high, kept at 140°F by heaters.	¼-in. clearance all around top; 5 equidistant ¾-in. holes along each side at bottom.	Two matched rectangular frames, 15½ by 4-in. outside dimensions.	Horizontal	Bunsen or Tirrill burner with 1½-in. high flame.	Top of burner 3/4-in. below end of specimen.	Continuously	Stop-watch or other device (to 1/5 sec.).	Timing begins after 1½-in. length of specimen has burned.	None	Time for fl 10-in. gage of 5 highes
	Metal hood or cabinet (unspecified size).	Cabinet permits free ventilation.	Metal frame, 7x4-in., with wires strung across width.	At 45°	Metered gas jet from 36-gage hypodermic needle; butane fuel; 3/8-in. flame.	Gas jet nozzle is 3/16-in. from face of specimen.	One second	Timer actuated by falling weight when thread burns through.	None	None	Average tim cation of f thread burn time for fl fixed dista
	No enclosure.	Room atmosphere.	Metal frame, 8x1½-in., with wires strung across width.	At 30° to horizontal except lowest ¼-in. which is vertical, and free from frame.	Safety-book match	At exposed edge of bent-down (vertical portion of specimen.)	5 sec.	Stop-watch or other device (to 1/5 sec.)	None	None	Time from ap of flame and burned. (Ave in each dire
	Completely enclosed laboratory hood.	Exhaust fan is used only after test.	Laboratory ring-stand and clamp.	Length horizontal; width at 45° to horiz. Piece of gauze, horiz., ⅜-in. below specimen.	Bunsen burner with blue flame 1-in. high.	Tip of flame contacts end of specimen.	30 sec. if burning does not continue, another 30 sec. exposure to flame is provided immediately after burning ceases.	Stop-watch	Timing begins when burning reaches 1-in. mark (on lower edge) & stops on reaching 4-in. mark.	"Non-burning" if no ignition on 2 attempts "Burning" if burning reaches 4-in. from end. "Self-extinguishing" if burning does not reach 4-in. mark.	Length burne mark and tim
	heet-metal r other ire-resistng enclosure 12-in. ide; 12-in. eep; 30-in. igh.	Open at top; 1-in. high opening around bottom.	Spring type paper clamp.	Vertical	1x1x0.010 piece of specified fuse material ignited by safety match; or single drop of benzene ignited by safety match or spark.	Fuse attached to lower end of specimen with overlap of ¼-in.; or benzene applied ¼-in. above lower edge & allowed to run down.	Till fuel has burned out.	Stop-watch or timer.	Timing begins with ignition of fuse.	None	Time to burn completely or until flame i guished, and ed or charred.
	closure of fficient e to con- n appara- , and hout ift.	Vent holes around sides near base and exhaust fan at top operating at min. suction.	Support "Suitable" for holding specimen vertical.	Vertical	Specified resistance coil heats specimen to generate gases; spark plugs used for ignition.	Axes of horiz. spark plugs ¼-in. above top of coil & electrodes 1/8-in. from specimen.	Coil "on" until 30 sec. after ignition or 600 sec. max. Plugs spark continuously, but are moved away after ignition.	Stop-Watch	None	None	Time to ignite Distance of fla from top of coi ing time after shut-off.

I OF FLAMMABILITY TEST METHODS

Identification and Title	Sponsoring Organization	Date	Intended Application	Number of Specimens	Selection of Specimen	Size of Specimen	Exposed Area of Specimen	Pretest Treatment and Conditioning	Size of Test Enclosure	Ventilation or Air Supply
Method DDD-C-95, Fed.Spec. DDD-C-95, "Carpets and Rugs, Wool, Nylon, Acrylic, Modacrylic".	Gen. Servs. Admin.	16 Apr. 1965	Carpets and rugs intended for use as floor coverings.	2	Not specified.	6x6-in.	6 x 6-in.	To equilibrium at 94°F, 30%RH	Chamber 12-in. wide, 12-in. deep, 9-in. high.	Chamber is open at top
Nbl 8019b (CCN-NBS) Material Fed. St'd. "Flame Spread Properties of Materials".	Nat. Bureau of Std's.	26 Dec. 1962	Wide variaty of structural and finish materials. (Intended as alternate to ASTM Desig. E84).	4 minimum	Arrangement that yields the highest flame spread.	6x18-in.	Approx. 5½ x 17½-in. (not given explicitly).	Predried 24 hrs. at 140°F then to equilibrium at 73 + 5°F, 50± 5% RH	No enclosure.	Apparatus is below exhaust hood with induced draft.
Method FSS 453, "Flame Resistant Material", "Flight Standards Service Release No. 453".	Fed. Aviation Agency	9 Nov. 1961	Flame-resistent materials for airframe applications.	3	For fabrics, length is parallel to more hazardous direction.	Approx. 4 x14-in.	2 x 13-in.	None specified.	None specified.	Draft-free conditions.
Method 191-53 Commercial Standard (Rev.) "Flammability of Clothing Textiles".	Dept. of Commerce	30 Jan. 1953	Clothing textiles.	5;(10 if flame spread time for first 5 is less than 2½-sec; or if some don't burn).	Preliminary tests to determine direction of fastest burning.	2x6-in.	1½ x 6-in.	Dried at 105°C (221°F) for 30 min and cooled in dessicator Laundering & dry cleaning for flame-retarding finish; brushing for raised fiber.	Cabinet 14½-in. wide, 8½-in. deep, 14-in. high.	Twelve ½-in. dia. holes equidistant at rear of top & ventilating strip at front bottom.
Method ASTM Desig: C209-55(1964) "Testing Structural Insulating Board Made from Vegetable Fibers".	ASTM	1960; reapproved, 1966.	Structural insulating board made from vegetable fibers.	3	Selecteddat random.	12x12-in.	12 x 12-in.	To equilibrium at 70+2°F 50±5% RH.	No enclosure	Room atmosphere.
Method ASTM D469; D626-55T, "Fire Retardant Properties of Treated Textile Fabrics".	ASTM	1955	Treated textile fabrics used in-aide structures.	10;(5 ea. from warp and filling directions).	Length parallel to warp or filling directions; specimens taken from at least 3 widely spaced sections of 2 sq.yd. sample (min.).	2x12½-in.	2 x 12;(½-in. length is covered by clamp).	70 + 2°F, 65 + 2% RH, for 16 hrs.	Sheet-metal shield 12-in. wide; 12-in. deep; 30-in. high.	Open at top; opening at bottom 1-in. high and 5-in. long.
Method ASTM Desig: D635-63, "Flammability of Rigid Plastics Over 0.127 cm (0.050-in.) in Thickness".	ASTM	1963	Rigid plastics in the form of sheets or molded bars over 0.050-in. thick.	10 minimum; however, testing is discontinued when 3 burning specimens are found.	Not specified.	0.5x5-in. actual thickness.	All exposed except area under clamp.	None; tested "as received".	Completely enclosed laboratory hood.	Exhaust fan is used only after test.
Method ASTM Desig: D757-65, "Flammability of Plastics Self-Extinguishing Type".	ASTM	1965	Rigid plastics thicker than 0.050-in. that are "self-extinguishing" by Meth. D635.	3 of each thickness (minimum).	Thickness as uniform as possible and smooth surfaces.	0.50x4¾ x½-in. thick; or actual thickness if over 0.050-in.	0.5 x 4-in.	None; tested "as received".	Completely enclosed laboratory hood.	Exhaust fan "off" during test, or at very low speed.

	Ventilation or Air Supply	Specimen Holder	Orientation of Specimen	Ignition Source	Location of Ignition Source	Time of Exposure	Method of Timing	Requirements for Validation	Criteria or Levels of Acceptability	Items Measured and/or Reported
in.	Chamber is open at top	Specimen lies on floor of chamber.	Horizontal	Methenamine timed burning tablet.	Burning tablet is placed in center of specimen and is ignited with match.	Burning tablet burns to completion.	None	None	Longest diameter of charred area must not exceed 2-in.	Longest diameter of charred area to nearest 0.1-in.
e.	Apparatus is below exhaust hood with induced draft.	Several mounting techniques are prescribed depending on specimen thickness, opacity, tendency, to delaminate, etc.	Length at 30° from vertical, burning from top downward on lower surface.	12x18-in. vertical panel with radiant output of black body at 1238± 7°F; also ½-in. I.D. pilot burner with 2-in. flame.	Pilot burner flame contacts or within ¼-in. of contacting top center of specimen. Radiant panel at 4½-in. from specimen at top.	15 min.; or until flame has progressed full length of specimen if it occurs sooner.	Timer calibrated to 0.01 min.	None	Flame spread index is calculated by equation based on rate of progress of flame front and a factor related to rate of heat liberation.	Time of arrival of flame front at successive 3-in. gage marks. (Also provides for meas. temp. & smoke density.)
	Draft-free conditions.	Metal frame that clamps 2 long edges and one end of specimen.	Horizontal, facing down.	Bunsen or Tirrill burner.	Not specified.	15 sec.	Not specified	Timing begins after 1½-in. length has burned, and stops when burning front is at least 1-in. from end.	Average burn rate of 3 specimens must not exceed 4 in./min.	Time and distance after flame front passes 1½-in. gage mark (Avg. for 3 specimens).
½- 4-	Twelve ½-in. dia. holes equidistant at rear of top & ventilating strip at front bottom.	Two matched 1/16-in. metal plates with clamps along sides.	At 45°	Metered gas jet from 26-gage hypodermic needle; butane fuel with ⅜-in. flame.	Flame is applied to surface near the lower end.	One second.	Timer actuated by falling weight when thread burns through.	None	Class 1 - Flame spread time of 3½ sec or more (for raised fiber more than 7 sec or if surface flash does not ignite or fuse base). Class 2 - Four to 7 sec (incl.) for raised fiber with base ignited or fused. Class 3 - Less than 3½ sec; less than 4 sec; for raised fiber with base fabric ignited or fused.	Time for flame to traverse 5-in. length; avg. value for samples that burn.
e	Room atmosphere.	Four vertical 3/16-in. dia. steel posts with pointed ends on 7x11-in. centers; one pair 4-in. high, the other 11-in.	At 45°; specimen rests on posts.	1 ml absolute ethyl alcohol in specified cup.	Center of base of cup is 1-in. below a point on lower surface of specimen 3-in. from lower edge and midway from side edges.	Until alcohol is burned out. Flame and glow are extinguished 1 min. after fuel is exhausted.	Not specified	None	None	Major & minor axes of charred region; area is calculated as that of true ellipse; avg. for all specimens.
l in. n. a.	Open at top; opening at bottom 1-in. high and 5-in. long.	A "suitable" clamp (not otherwise specified).	Vertical	Bunsen or Tirrill burner using specified gas and gas pressure.	Top of burner ¾-in. below end of specimen.	12 sec.	Not specified	None	Flaming not to exceed 2 sec. after removal of burner for any specimen; avg. length of char for 10 specimens not to exceed 3½-in., & max. not to exceed 4½-in.	Flaming time; char length as caused by tear using specified hooks and weights.
	Exhaust fan is used only after test.	Laboratory ring-stand with adjustable clamps.	Length horizontal; width at 45° to horizontal. Piece of 20-mesh gauze, horiz., ⅜-in. below specimen.	Bunsen burner with blue flame 1-in. high.	Tip of flame contacts end of specimen.	30 sec. If burning does not continue another 30 sec. exposure to flame is provided immediately after burning ceases.	Stop-watch	Timing begins when burning reaches 1-in. mark (on lower edge) & stops on reaching 4-in. mark.	"Non-burning" if no ignition in 2 attempts "Burning" if burning reaches 4-in. from end. "Self-extinguishing" if burning does not reach 4-in. mark.	Length burned from 1-in. mark, and time.
	Exhaust fan "off" during test, or at very low speed.	Clamp on arm that rotates about horizontal axis.	Length horizontal; width vertical.	Silicon carbide rod of 5/16-in. dia. at 950±10°C (1742±18°F).	End of specimen is pressed against middle of hot SiC rod with force of approx. 1 oz. Axes of rod & specimen are perpendicular.	3 min±3sec. from contact of specimen with heated rod until it is removed and flame is extinguished by inert gas jets	Stop-watch or timer clock.	Method applies only to specimens that burn.	None	Length burned (to 0.04-in.) at center of ½-in. side to point where no charring or melting are visible; burning time if less than 3 min.

Identification and Title	Sponsoring Organization	Date	Intended Application	Number of Specimens	Selection of Specimen	Size of Specimen	Exposed Area of Specimen	Pretest Treatment and Conditioning	Size of Test Enclosure	Ventilation or Air Supply
Method ASTM Desig: D1230-61; "Flammability of Clothing Textiles".	ASTM	1961	Clothing textiles.	5;(10 if flame spread time for first 5 is less than 3½ sec, or if some don't burn).	Preliminary tests to determine direction of fastest burning.	2x6-in.	1½ x 6-in.	Dried at 105°C (221°F) for 30 min. and cooled in dessicator. Laundering, & dry cleaning for flame-retarding finish; brushing for raised fiber.	Cabinet 14½-in. wide; 8½-in. deep; 14-in. high.	Twelve ½-in. dia. holes equidistant at rear of top, and ventilating strip at front bottom.
Method ASTM Desig: D1433-58(1966), "Flammability of Flexible Thin Plastic Sheeting".	ASTM	1958; reapproved 1966.	Flexible plastics in form of film or thin sheeting.	10;(5 ea. from machine and transverse directions).	Free of folds or wrinkles.	3x9-in.	1½x6-in. (6-in. gage length is all on 45° inclined section).	23±2°C (73.4±3.6°F) 50±5%RH for 40 hrs.	An enclsoure to protect from drafts.	Holes at top and bottom of cabinet.
Method ASTM Desig: D1692-67T, "Flammability of Plastic Sheeting and Cellular Plastics".	ASTM	1967	Plastic sheeting and cellular plastics that do not shrink, curl, or melt away. Material must flame.	3 that burn past 5-in. gage mark; otherwise up to 10.	Cut from section of uniform density.	2x6-in. of actual thickness if less than ½-in.; otherwise cut to ½-in. with skin removed.	2 x 6-in.	23±2°C(73.4±3.6°F) 50±5%RH until successive 24-hr. weighings are within 1%.	Recommended cabinet 24-in. wide; 12-in. deep; 30-in. high; (or any large enclosure).	Open at top; approx. 1-in. high opening around bottom.
Method ASTM Desig: E 84-61, "Surface Burning Characteristics of Building Materials".	ASTM	1961	Wide variety of building materials.	Single specimen.	Truly representative specimen.	20-in. wide 25 ft. long.	17½-in. wide, 25 ft. long.	To equilibrium at: 70±5°F, 35 to 40% RH.	Horizontal duct with inside dimensions of 17½-in. wide, 12±½-in. high, 25 ft. long.	Induced draft of 0.075-in. water downstream of test section; air supply at 70±5°F & 35-40% RH.
Method ASTM Desig: E162-67,"Surface Flammability of Materials Using a Radiant Heat Energy Source".	ASTM	1967	Materials not specified. Intended for R & D, and not for building code ratings.	4 minimum.	Arrangement that yields the highest flame spread.	6x18-in.	Approx. 5½ x 17⅝-in. (not given explicity).	Predried 24 hrs. at 140°F, then to equilibrium at 73±5°F, 50±5% RH.	No enclosure.	Apparatus is below exhaust hood with induced draft.
Method ASTM Desig: E286-65T, "Surface Flammability of Building Materials Using an 8-ft. Tunnel Furnace".	ASTM	1965	Materials that can be mounted in 14-in. by 8 ft. frame Intended for R & D and not for building code ratings.	Single specimen.	None	13.75 in. wide, 8 ft. long.	Exposed length is 94.5-in.	To equilibrium at 75±5°F, 35 to 40% RH.	Horiz. furnace with stack located below (but not connected to) exhaust hood.	Natural draft through air inlets spaced along lower wall of furnace.

COMPARISON OF FLAMMABIL

tilation r Air upply	Specimen Holder	Orientation of Specimen	Ignition Source	Location of Ignition Source	Time of Exposure	Method of Timing	Requirements for Validation	Criteria or Levels of Acceptability	Items Measured and/or Reported
lve ½-in. . holes idistant rear of , and vea- ating ip at front tom.	Two matched 1/16-in. metal plates with clamps along sides.	At 45°.	Metered gas jet from 26-gage hypodermic needle; butane fuel.	Flame is applied to surface near the lower end.	One second	Timer actuated by falling weight when thread burns through.	None	Class 1 - Flame spread time of 3½ sec or more (more than 7 sec for raised fiber) Class 2 - Four to 7 sec (incl.) for raised fiber with base ignited or fused. Class 3 - Less than 3½ sec; (less than 4 sec for raised fiber with base ignited or fused).	Time for flame to traverse 5-in. length.
es at top bottom cabinet.	Two matched U-shaped plates held together by 2 spring-type paper clamps.	At 45° to horizontal except lowest 1-in. which is vertical.	Gas jet from 22-gage hypodermic needle; butane fuel with ½-in. horiz. flame.	Tip of needle ½-in. from middle of vertical piece of specimen (cut tip of needle facing up).	Continuously	Electric timer actuated by microswitches that are tripped by burning through strings 6-in. apart.	None	"Self-extinguishing" if first string burns but second does not; "Non-burning" if specimen extinguishes before 1st string burns. (Burning rate is avg. of only those specimens that burn).	Time for flame to traverse 6-in. gage length.
n at top; rox. 1-in. h opening und bottom.	3x8½-in. screen (of 1/16-in. wire & ½-in. mesh) with end bent up 90° to leave horiz. place 3x8-in.	Horizontal with end abutting bent-up portion of screen.	Bunsen or Tirrill burner with 1 7/32+1/16-in. wing top; propane fuel; 1½-in. flame.	Burner wing top ½-in. below screen with outer edge of flame tangent to outer edge of screen.	60 sec.	Timer accurate to ±1 sec.	Test stops when 3 specimens burn to 5-in. gage mark.	"Self-extinguishing" if none of 10 specimens burn to gage mark.	Time from first application until flame reaches 5-in. gage mark, or time to extinguishment & dist. to extreme evidence of flame front.
duced draft 0.075-in. ter down- ream of st section; r supply at +5°F & 35- F RH.	Specimen rests on ledge of chamber walls.	Horizontal	Two gas burners with output determine by calibration tests (approx. 5000 Btu/ min.)	Burners 12-in. upstream from "fire end" of specimen, 7½± ½-in. below its lower surface & 4-in. on each side of longitudinal centerline.	10 min; or complete combustion of specimen if it occurs sooner. Burners "on" continuously.	Not specified.	Equipment is calibrated using asbestos cement board and red oak flooring.	Flame spread classification is calculated in prescribed manner, based on comparison with standards of redoak and asbestos cement board.	Time for flame to spread 19½ ft, if less than 10 min.; or max. distance that flame reaches. (Also provides for mass temp. & smoke density.)
paratus is low exhaust od with duced draft.	Several mounting techniques are prescribed depending on specimen thickness, opacity, tendency to delaminate, etc.	Length at 30° from vertical, burning from top downward on lower surface.	12x18-in. vertical panel with radiant output of black body at 1238± 7°F; also ½-in. I.D. pilot burner with 2 to 3-in. flame.	Pilot burner flame contacts, or within ½-in. of top center of specimen. Radiant panel is 4¾ in. from specimen at closest point (top).	15 min.; or until flame has progressed full length of specimen if it occurs s sooner.	Timer calibrated to 0.01 min.	Time begins when specimen holder is placed on frame.	Flame spread index is calculated by equation based on rate of progress of flame front and a factor related to rate of heat liberation.	Time of arrival of flame front at successive gage marks at 3-in. intervals. (Also provides for mass. temp. & smoke density.)
ıtural draft ırough air ılets spac- l along ear wall of rnace.	A frame of angle iron 14-in. wide 8 ft. long.	Length at 6° to horiz.; width at 30° to horiz.	Gas burners with output determined by calibration tests (approx. 3400 Btu/ min.))separate igniting burner.	Igniting burner at one end of specimen. Firebox of main burners runs full length beneath specimen chamber.	Continuously for test period of 19± 1 min. depending on calibration test.	Not specified.	Time begins when burners are lighted.	Flame spread index is calculated in prescribed manner based on comparison with standards of red oak and asbestos millboard.	Time for flame to travel 87-in.; if less than 19 min. (which is time for red oak); otherwise max. distance that flame reaches in 19 min. (Also provides for mass. temp. & smoke density.)

AMMABILITY TEST METHODS

Identification and Title	Sponsoring Organization	Date	Intended Application	Number of Specimens	Selection of Specimen	Size of Specimen	Exposed Area of Specimen	Pretest Treatment and Conditioning	Size of Test Envlosure	Ventilation or Air Supply	Spec Ho
BS 2963, Method b, British Standard Methods of Test for the Flammability of Fabrics.	British Standards Institution	1958	Fabrics of all constructions that may be cut to form flat sheets.	6	Preliminary tests to determine direction of fastest burning.	2x6-in.	1½ x 5¾-in.	Dried at 105± 2°C for 30 min. and cooled in dessicator or airtight container. Tested at 59 to 86°F and 20 to 80% RH. Brushing for raised fiber.	Cabinet 14½-in. wide, 8½-in. deep, 14-in. high.	Twelve ½-in. dia. holes equidistant near top of rear wall, and 12x½-in. slit at front bottom.	Two st plate grip men a sides top.
Method DIN 53382, Testing of Plastic Foils and Artificial Leather. Effect of Flame Test on One Side, Swivel Burner Method of Testing.	German Standard	Oct. 1957	Effect of flame on one side of plastic sheet and artificial leather used on a support of some kind.	3	Taken uniformly from width of material.	200x170 min. (7.87x 6.69-in.)	Entire specimen is exposed.	16 hrs. at 20±2°C, 65± 5% RH. Tested at room temp.	No enclosure.	Room atmospheres (draft-free).	Specim stenter over a curved of ply with dimens horiz
Method NFPA 701, "Fire Tests, Flame Resistant Textiles, Films".	National Fire Protection Assn.	1968	Flame resistant materials for interior furnishings, protective clothing, and outdoor coverings.	10; (5 ea. from warp & filling directions).	Each lot of 5 cut from at least 4 separate places to indicate uniformity.	2¾x10-in.	2 x 10-in.	Circulating air at 140 to 145°F for 1 to 1½ hrs; other procedures are prescribed.	Enclosure 12-in. wide; 12-in. deep; 30-in. high.	Open at top; vent holes along bottom of at least 2 sides total 6 sq. in. min.	Metal clamps edges.
Method NFPA 702, "Wearing Apparel Flammability".	National Fire Protection Assn.	1968	Textile and other products for clothing use.	5	Length parallel to more hazardous direction.	2x6-in.	1½ x 6-in.	Dried at 221°F for 30 min. and cooled in dessicator. Laundering and dry cleaning for flame retarding finish; brushing for raised fiber.	Cabinet 14½-in. wide; 8½-in. deep; 14-in. high.	Twelve ½-in. dia. holes equidistant at rear of top & ventilating strip at front bottom.	Two m 1/16-i plate
SAE J639, "Flammability of Automotive Interior Trim."	Society of Automotive Engineers, Inc.	Not dated.	Materials used in automotive interiors.	3	Preliminary tests to determine direction of fastest burning.	4x14-in. or actual thickness if less than ½-in. otherwise cut to ½-in., but include primary surface.	2 x 13-in.	70±2°F, 65±5% RH for 24-hr. min.; combing for napped or tufted material.	Draft-free cabinet.	Blower "off" during test.	Two ma shaped each thick.
Ford, MTMH, MN24-1; Ford, "Flammability Test for Trim Materials".	Ford Motor Co.	30 Oct. 1962	Textile trim materials.	Not given in test description.	Not given in test description.	6x6-in.	All exposed except area under clamp.	Not given in test description.	Hood to eliminate strong air currents and carry off fumes.	Hood to eliminate strong air currents and carry off fumes.	Ring-s and or Labora clamp.
Am. Motors, Method 34, "Ignition and Burning of Upholstery Materials."	American Motors Corp.	19 July, 1966.	Combustible properties of upholstery materials.	One or more as needed.	To cover all variations in pattern, composition, and construction.	4x4-in.	4 x 4-in.	16 hrs. minimum at 70°F, 65% RH.	Laboratory hood or other well-ventilated area.	Draft-free conditions.	Specim pleased 6 x 6- piece uretha foam, min. t ness.
Am. Motors, Method 101, "Flame Retardant Property".	American Motors Corp.	15 Mar. 1962	Sealer or like material which may be subjected to flame or heat in production.	1 to 4 depending on results obtained.	None	1x12x¼-in. high.	1x12x¼-in. high.	5-min. flash time before flame is applied; 77 ± 3°F.	Open bench.	Room atmosphere.	Cast o panel, ±0.03
Auto.Mfrs. Assn., Method S121, "Fire Retardant Materials for Interiors -- Passenger Cars, Multipurpose Passenger Vehicles, Trucks and Buses.	Automobile Manufacturers Assn, Inc. (comments on Docket 3-3).	4 Dec. 1967	Exposed interior trim materials for use in passenger cars, multipurpose passenger vehicles, trucks, and buses.	3	Length parallel to more hazardous direction.	4x14-in.	2 x 13-in. min. with free end ½-in. from end of frame.	To equilibrium at: 70 + 5°F 65 ± 5% RH.	No enclosure specified.	Draft-free conditions.	Metal that c 2 long and on of spe

COMPARISON OF FLAMMABILI

ion	Specimen Holder	Orientation of Specimen	Ignition Source	Location of Ignition Source	Time of Exposure	Method of Timing	Requirements for Validation	Criteria or Levels of Acceptability	Items Measured and/or Reported
-in. les ant of 1, -in. front	Two metal U-plates that grip specimen along sides and at top.	At 45°; raised fibers facing up; others to give highest burning rate.	Metered gas jet from 26-gage hypodermic needle (0.010 I.D.) butane fuel; ⅜-in. flame.	Burner tube perpendicular to fabric surface 5/16-in. from it, ¼-in. above bottom edge, on centerline.	Flame is applied to duration of test.	Time to 0.1 sec. End time indicated by burning of thread 5-in. from point of ignition.	None	"Flame resistance rating" given as 2.5xavg. burn time in seconds; "Flame resistance less than 100" if none of 6 specimens burn.	Time for flame to traverse 5-in. length; average for specimens that burn.
nos- isaft-	Specimen is stretched over slightly-curved piece of plywood, with short dimension horizontal.	Vertical, with slight curvature about vertical axis.	165 min. (6.5 in.) burner tube rotates from vertical to horiz. Uses coal gas with 40 min. (1.57-in.) flame when vertical.	Burner moves from vertical to horiz. When horiz. burner tip is 20 min. (0.79-in.) from specimen.	Burner traverses final 30° of swing in 10 sec. and returns at same rate with no delay.	Not specified.	None	None	Time that specimen burns or glows; or if it does. Also length of burn mark.
top; les ottom east sq.	Metal holder clamps long edges.	Vertical.	Bunsen or Tirrill burner with 1½-in. high flame.	Top of burner ¾-in. below end of specimen. Burner inclined at 25° from vertical.	12 sec.	Not specified.	None	Flaming not to exceed 2 sec. after removal of burner; vertical spread of flame and afterglow not to exceed specified limits based on fabric weight.	Flaming time & distance; char length as caused by tear made in prescribed manner.
½-in. les tant of antila- rip at ottom.	Two matched 1/16-in metal plates.	At 45°	Metered gas jet from 26-gage hypodermic needle; butane fuel; ⅜-in. flame.	Flame impinges on bottom edge; in case of raised fiber, 1 sec. only.	Until ignition occurs; in case of raised fiber, 1 sec. only.	Timer actuated by falling weight when thread burns through.	For raised fiber if base fabric does not ignite or fuse, or timer thread doesn't burn, Specimen is processed again as ordinary material.	Textiles: Class 1 - time of flame spread 20 sec. or more. Class 2 - time of flame spread 8-19 sec. Class 3 - time of flame spread 3-7 sec. Class 4 - time of flame spread less than 3 sec.	Time for flame to traverse 5-in. gage length (avg. of 5 specimens).
off" est.	Two matched U-shaped frames, each ⅜-in. thick.	Horizontal facing down.	Bunsen or Tirrill burner with 1½-in. flame using a specified gas.	Center of burner barrel directly below center of open end of specimen (no dist. given).	15 sec.	Stop-watch (to 1/5 sec.).	Timing begins after 1½-in. length has burned.	DNI-does not ignite -- if no flame in 15 sec. SE/NBR-self-extinguishing but no burning rate -- if extinguishes in 1½-in. or less. SE/BR -- self-extinguishes beyond initial 1½-in. Burning rate based on distance burned beyond 1½-in.	Time and distance after flame front passes 1½-in. gage mark (avg. for 3 specimens).
alimin- ng air and ff	Ring-stand and ordinary laboratory clamp.	Vertical.	Hypodermic needle (3-in., BD-22); natural gas; ½-in. flame.	Tip of needle is 1½-in. from surface of specimen.	Not given in test description.	Stop-watch calibrated in seconds.	Not given in test description.	Not given in test description.	Observation of whether material ignites and supports combustion, and whether it burns or smolders after removal of flame.
ree ons.	Specimen is placed on 6 x 6-in. piece of urethane foam ½-in. min. thickness.	Horizontal, facing up.	A lit, untipped cigarette.	Cigarette is placed on center of specimen and adjusted to make good contact.	Until cigarette is consumed.	Not required.	None	No ignition or flame; No reactions after cigarette is consumed. No damage over area ⅜-in. by length of cigarette. No crevice in foam deeper than ⅛-in. nor wider than ¼-in.	Size of damaged region.
nos-	Cast on steel panel, 4x12 x0.036-in.	Length is vertical	Bunsen burner; natural gas; 2½-in. flame.	Tip of flame is applied to center of ribbon.	30 to 60 sec. in 10-sec. steps, depending on results.	Stop-watch.	None	No flame for more than 3 sec., and self-extinguishment. Material must not run, drip, sag, expand, or crinkle deeper than 1/16-in.	Time of flame exposure and results.
ree ons.	Metal frame that clamps 2 long edges and one end of specimen.	Horizontal, facing down.	A match or similar means.	Not specified (presumably at free end of specimen).	15 sec.	Not specified.	Minimum 10-in. length used for timing. Timing begins after approx. 1½-in. of burn and stops at least 1-in. from end.	No spontaneous combustion up to 250°F; if specimen does not support combustion after 15-sec. flame exposure; if avg. burn rate of 3 specimens does not exceed 15 in./min.	Time for flame to traverse 10-in. length.

MMABILITY TEST METHODS

APPENDIX C

STATISTICAL TECHNIQUES

Several statistical techniques have been employed in the calculation of the regression line representing Equations IV-32. These include analysis of the burning rate data for bad data points, a t-distribution test to determine important variables, and calculation of the standard error of estimate and the multiple regression correlation coefficient (2, 3).

The following calculational scheme was incorporated into the multi-regression program to check for bad data. This technique calculates an unbiased centerline through the data and then checks to see if any point is more than 3 standard deviations away from the line. If it is, the point is deleted. The technique consists of the following steps:

1. Add all the individual observations and divide by the number of observations ($[\Sigma x_i]/N$).
2. Add and subtract to the average calculated in (1), 3 times the standard deviation ($\sigma = \sqrt{[\Sigma (x_i-\bar{x})^2]/[N-1]}$).
3. Delete all values of x_i which fall outside the range calculated in (2).
4. Calculate a new average with the data remaining after applying (3).

5. Repeat Steps (1), (2), and (3).
6. Replace any data that was previously deleted but now falls between the presently calculated $\bar{x} \pm 3\sigma$.
7. Calculate a new average.
8. Repeat Steps (2) through (7) until no more data are deleted or put back in.
9. The final $\bar{x}$ is the center line.

The coefficient of correlation was calculated as follows:

1. The average value of R_o (burning rate) was calculated by

$$\bar{R}_o = (\Sigma R_{o_i})/(N-1) \qquad \text{(C-1)}$$

2. The sum of the squares of the deviation of R_{o_i} from R_o was calculated by:

$$S = \Sigma\ (R_{o_i} - \bar{R}_o)^2 \qquad \text{(C-2)}$$

3. The sum of the squares of the deviation of the calculated value from the experimental was calculated by:

$$z = \Sigma[R_{o_i} - K(\rho c_p)_i^a\ (s_i)^b\ (\delta_i)^c\ (\kappa_i)^d]^2 \qquad \text{(C-3)}$$

where the i's represent the i^{th} value of the variable.

4. Then the multiple correlation coefficient (R) is:

$$R = \sqrt{1 - (2/s)} \qquad \text{(C-4)}$$

The standard error of estimate was calculated

$$S_{R_o,x} = \text{Error of } x \text{ on } R_o$$

$$= \sqrt{\frac{(1-R^2)(n-1)(\Sigma R_{o_i})^2}{n - m - 1}} \qquad \text{(C-5)}$$

where R = multiple correlation coefficient

n = number of data points

m = number of variables being used (4)

R_{o_i} = i^{th} value of R_o

The last statistical technique which was incorporated into the computer program used in the multi-regression analysis was a t-test. This proved very useful, in that it allowed variables to be discarded as being negligible in correlating the data. This test was performed as follows:

1. The multiple correlation using all variables was calculated according to Equations C-1 through C-4.
2. Each variable was then correlated against the burning rate, R_o, using a least squares fit as:

$$\ln R_o = b_x \ln x_i \qquad \text{(C-6)}$$

the value of b_x being

$$b_x = \frac{\Sigma (x_i - \bar{x})(R_{o_i} - \bar{R}_o)}{\Sigma (x_i - \bar{x})^2} \qquad \text{(C-7)}$$

where x_i = the i^{th} value of the variable x

$\bar{x}$ = the average value of x

$\bar{R}_o$ = the average burning rate

R_{o_i} = the i^{th} value of R_o

3. The standard deviation, s_{b_x}, of the regression coefficients calculated in Step (2) was then calculated by:

$$s_{b_x} = \sqrt{\frac{(s_{R_o,x})^2}{\Sigma\, x_i^2}} \qquad \text{(C-8)}$$

or:

$$s_{b_x} = \sqrt{\frac{(1-R^2)\,(n-1)\,(\Sigma R_{o_i})^2}{\Sigma\, x_i^2\,(n-m-1)}} \qquad \text{(C-9)}$$

4. A value for t was then calculated for each of the sets of b_x and s_{b_x} by:

$$t_x = b_x / s_{b_x} \qquad \text{(C-10)}$$

where the subscript x refers to the variables ρc_p, s^*, δ, and κ.

5. To be of significance, a variable must have $t \geq 2$.

6. The t values were examined for condition (5). If there were more than two variables with $t < 2$, the variable with the lowest t value was deleted, and Steps (1) through (5) repeated. This was continued until all variables left in the multiple regression analysis program had a $t \geq 2$.

This technique of examining the t values of each variable proved to be a very powerful tool in analyzing the data. It was the use of this technique which resulted in Equation IV-32c having only the slope based on ignition data, s*, as a correlating variable.

APPENDIX D

APPLICATION OF THE BUCKINGHAM PI METHOD OF DIMENSIONAL ANALYSIS USED IN THE DERIVATION OF EQUATIONS IV-23 AND IV-24

The Buckingham Pi method was applied to the variables which were found to be important in describing the burning process in order to derive the dimensionless equation, Equation IV-25. As previously stated, these variables were found to be the density, ρ; heat capacity, c_p; thermal diffusivity, κ; thickness, δ; temperature rise to ignition, ΔT_{ig}; the product $H_a^* \sqrt{t_i^*} = s^*$, the slope; and the burning rate, R_o.

The above variables have dimensions of:

R_o:	length/time	$= L/t$
ρ :	mass/volume	$= M/L^3$
c_p:	energy/mass-temperature	$= E/M\text{-}T$
ΔT_{ig}:	temperature	$= T$
κ :	area/time	$= L^2/t$
s*:	energy/area-time$^{1/2}$	$= E/L^2\text{-}t^{1/2}$
δ :	length	$= L$

The maximum number of independent groups, n, that can be obtained from application of this method is equal to the

number of independent variables, m, minus the number of primary dimensions, r (in this case, n = 7 - 5 = 2). Hence, a maximum of two dimensionless groups, Π_1 and Π_2, can be found for the present case. Since there are seven variables and five dimensions, in order to apply the Buckingham Pi method, two of the variables must be held constant. The variables chosen to be fixed were the burning rate, R_o, and the slope, s*. The analysis is then performed as follows:

$$\Pi_1 = (\rho)^a \ (\delta)^b \ (c_p)^c \ (\kappa)^d \ (\Delta T_{ig})^e \ R_o \qquad \text{(D-1)}$$

or in dimensional form:

$$\Pi_1 = (M/L^3)^a \ (L)^b \ (E/M\text{-}T)^c \ (L^2/t)^d \ (T)^e \ L/t \qquad \text{(D-2)}$$

from which

$$\Sigma M = 0 = a - c \qquad \text{(D-3a)}$$

$$\Sigma L = 0 = -3a + b + 2d + 1 \qquad \text{(D-3b)}$$

$$\Sigma T = 0 = -c + e \qquad \text{(D-3c)}$$

$$\Sigma E = 0 = c \qquad \text{(D-3d)}$$

$$\Sigma t = 0 = -d - 1 \qquad \text{(D-3e)}$$

Simultaneous solution of Equations D-3 yields values of the constants of a = c = e = 0, b = 1, and d = -1.

Therefore Equation D-1 becomes

$$\Pi_1 = R_o \delta/\kappa \qquad \text{(D-4)}$$

The second group is obtained by

$$\Pi_2 = (\rho)^a \ (\delta)^b \ (c_p)^c \ (\kappa)^d \ (\Delta T_{ig})^e \ s^* \qquad \text{(D-5)}$$

or in dimensional form:

$$\Pi_2 = (M/L^3)^a \ (L)^b \ (E/M\text{-}T)^c \ (L^2/t)^d \ (T)^e \ E/L^2\text{-}t^{1/2} \tag{D-6}$$

from which

$$M = 0 = a - c \tag{D-7a}$$

$$L = 0 = -3a + b + 2d - 2 \tag{D-7b}$$

$$T = 0 = -c + e \tag{D-7c}$$

$$E = 0 = c + 1 \tag{D-7d}$$

$$t = 0 = -d - 1/2 \tag{D-7e}$$

Simultaneous solution of Equations D-7 yields values of the constants of $a = c = e = -1$, $b = 0$ and $d = -1/2$. Therefore Equation D-5 becomes

$$\Pi_2 = \frac{s^*}{\sqrt{\kappa}\rho c_p \Delta T_{ig}} \tag{D-8}$$